Quantum Field Theory

A New Approach, Compatible with Gravity

Peter Gerwinski

May 2021

Contact: theo-phys@peter.gerwinski.de

Abstract

This is an introduction to a new approach to quantum field theory. It works in the Schrödinger picture without using time-ordered perturbation theory (Feynman diagrams) and without producing singularities, thus removing the obstacles that prevent us from unifying quantum field theory with general relativity. It explains how to set up and to solve, numerically, the Schrödinger equation for a system where particles and anti-particles can be created and annihilated, and it sketches how to proceed from there to quantum gravity, in particular to the quantisation of noncommutative geometry.

This is a self-contained introduction to quantum field theory, starting with relativistic quantum theory (Dirac equation). Readers are assumed to be already familiar with non-relativistic quantum theory (Schrödinger equation) and with special relativity.

Contents

List of Figures

Chapter 1

Introduction

As of 2021, the most precise description of nature provided by theoretical physics consists of two parts,

- *quantum field theory* with its *Standard Model* of elementary particles (*quarks* and *leptons*, *electromagnetic*, *weak* and *strong interaction*, the *Higgs boson*), and
- *general relativity*, the theory of *gravity*.

It is well-known that these two theories don't go well together. But what's the problem?

The usual answer reads: "We haven't yet succeeded to quantise gravity."

The term "quantisation" is ambiguous. Applied to a force – electromagnetic, weak or strong force, or gravity – its usual meaning is to describe the force by particles which "carry" it from one of the interacting partners to the other one. To visualise how this could work one can imagine two astronauts in space bandying a ball. The recoils from throwing and catching the ball would drive them apart.

Now imagine that the astronauts can absorb and create the balls as needed and that the recoil can also be negative, pulling the astronauts together. That's how *photons*, the electromagnetic interaction particles, are usually imagined to work. Likewise, there are *weakons* for the weak interaction and *gluons* for the strong interaction. (I'm using "strong interaction" as a synonym for "colour interaction".)

Now what about gravitons for gravity?

Photons, weakons and gluons are described by *Feynman diagrams*. Applying the same tool to gravity leads to diverging integrals. Taken by itself that isn't unusual; similar problems emerge for the other interactions, too. There is a method called *renormalisation* which extracts useful information from the diverging integrals – except for gravity, where it doesn't work.

There are ongoing attempts to overcome these problems. The most prominent ones are loop quantum gravity and supersymmetric approaches, including string theory. However there is, as of 2021, no experimental evidence in support of any of these approaches. On the contrary, so far all predictions beyond the Standard Model and general relativity have been refuted by experiments [1, § 2C].

Okay, when we cannot quantise gravity, then what about gravitising quantum field theory?

Gravity is described by general relativity, whose main tool is geometry. Thus to "gravitise" something means to use geometry to describe it.

In fact this approach already exists: *noncommutative geometry* [2]. By attaching discrete extra dimensions to the curved spacetime of general relativity and by studying geometry on that space, noncommutative geometry derives the full Standard Model of elementary particles, coupled to gravity, from an astonishingly small input.

Doesn't that mean that noncommutative geometry is the long-sought unification of quantum field theory and general relativity?

Many scientists say "no" because noncommutative geometry "cannot be quantised". Yes, noncommutative geometry derives general relativity and quantum field theory from a common input, but it doesn't tell us how to apply Feynman diagrams to gravity.

But are Feynman diagrams really the only valid meaning of "quantisation"? What about a new quantisation method, which doesn't use Feynman diagrams and avoids the problems which arise from applying them to gravity?

Feynman diagrams are extremely successful. In fact they represent the most successful theory ever developed in physics. This doesn't exactly make it attractive to replace them by something which isn't even known to work at all.

But there is an even more important reason. Quantum field theory is a many-particle theory, which includes effects like pair annihilation and creation which can alter the number of particles in a system. To describe these many-particle effects, Feynman graphs (and other theories such as lattice gauge theory) rely on time-ordered perturbation theory. It is this perturbation theory which causes the known incompatibilities to gravity.

So the problem of combining general relativity with quantum field theory is the choice of the tools to apply to the combined theory. When we apply time-ordered perturbation theory we have to overcome its incompatibility to gravity. That's what string theory aims at. When we don't apply time-ordered perturbation theory we must find some other way to describe many-particle effects such as pair annihilation and creation.

That's what this paper does.

Instead of trying to apply a method which is known to work for quantum field theory to gravity, we apply a method which is known to work for gravity to quantum electrodynamics, the simplest case of quantum field theory. We trade the problem of applying time-ordered perturbation theory to gravity for the problem of a non-perturbative description of pair annihilation and creation, and we solve it (see section 4.4).

So this paper removes the main obstacle on our way to quantum gravity. The way itself is still there, and it is a long one, but it appears to be passable now. (See chapter 5 for details.)

In this paper we will rebuild quantum electrodynamics, starting from the non-relativistic Schrödinger equation, then going relativistic with the Dirac equation and the Maxwell equations. We will give the concept of "quantisation" a precise meaning and develop a new, non-perturbative quantisation method which doesn't use Feynman diagrams. We'll use creation and annihilation operators in their mathematical sense, which doesn't always coincide with what their names suggest. We'll make use of the computer to solve hyperbolic partial differential equations for us, watch beautiful visualisations of simulations, including annihilation and creation of electron-positron pairs, and maybe we'll get a tiny insight in how nature really looks like, beyond the limited scope of our senses.

Enjoy!

Chapter 2

One Particle

Before we address annihilation and creation of particles, we must understand how a single particle works. In this chapter we'll review quantum physics for single particles in the non-relativistic and the relativistic case. At the same time we'll develop the numeric methods which allow us to study quantum physics in the Schrödinger picture by simulating it on a computer.

2.1 Nonrelativistic Quantum Mechanics

We all know the time-dependent *Schrödinger equation*,

$$i\hbar\frac{\partial}{\partial t}\psi(x,t) = H\psi(x,t). \tag{2.1}$$

[You don't? Then – I'm really sorry – the remaining parts of this publication probably won't make much sense for you, maybe except for the results and the outlook towards the end. I hope you enjoyed the introduction, though. :–]

This equation means: We have a wave function $\psi(x,t)$ in position representation, and we are interested in its time development. We get it by solving a differential equation: We apply a linear operator, the *Hamiltonian* H, to the wave function, and we get its derivative with respect to time, multiplied by a factor $i\hbar$.

The term "Hamiltonian" is ambiguous. In this case, the Hamiltonian H is a *Hamiltonian operator*. It is generated from the classical *Hamiltonian function* by substituting the *momentum operator* $-i\hbar\frac{\partial}{\partial x}$ for the momentum $p(t)$ and the multiplication operator x for the coordinate $x(t)$, both of which are vector-valued functions of the time t. This procedure is called *quantisation* – or *first quantisation* to distinguish it from *second quantisation*, which we will encounter in chapter 3.

In classical mechanics, a physical system is described by the Hamiltonian function $H(p,q,t)$ and its state by the coordinate $x(t)$ and the momentum $p(t)$. In the *Schrödinger picture* of quantum mechanics, the system is described by the Hamiltonian operator H and its state by the wave function $\psi(x,t)$.

Mathematically, the wave function $\psi(x,t)$ maps the three-dimensional position vector x and the time t – four real numbers – to a complex number,

$$\psi : \mathbb{R}^3 \times \mathbb{R} \to \mathbb{C} : (x,t) \mapsto \psi(x,t). \tag{2.2}$$

We view the wave function as an element of a Hilbert space. This implies that we treat the function itself as an infinite-dimensional vector, where $(x,t) \in \mathbb{R}^3 \times \mathbb{R}$ is the index, and the

components are complex-valued. In fact its dimension is not only infinite, but uncountably infinite, since the index doesn't come from a countable set like $\mathbb{N}$, but from the uncountable set $\mathbb{R}^3 \times \mathbb{R}$.

In the same sense the Hamiltonian is an uncountably infinite-dimensional matrix. The same holds for other operators such as the position operator, multiplication by x, which has the position x on the diagonal of the matrix and zero everywhere else, and it holds for the momentum operator $p = -i\hbar\frac{\partial}{\partial x}$, which is, as we will see later, a fully-occupied matrix in position representation (and a diagonal matrix in momentum representation).

The usual path from here would be to introduce bra vectors and ket vectors and to compute eigenvalues, eigenstates, and expectation values of the operators involved (H, x, and p so far). You have done all this when you studied non-relativistic quantum mechanics.

Instead, let's ask the computer to solve this differential equation for us.

2.1.1 The Quantum Euler Method

To make things simple, let's take just one spatial dimension. We store $\psi(x,t)$ for $t = 0$ as a big array of complex numbers, thus preparing an initial state for our quantum system.

As an example, let's prepare a Gaussian wave packet at the (mean) position x_0, with the (mean) momentum p_0, and with a position uncertainty Δx,

$$\psi(x,0) := e^{\frac{i}{\hbar}p_0 x - \left(\frac{x-x_0}{\Delta x}\right)^2}. \tag{2.3}$$

(Since we don't need it now, we ignore the norm of the wave function.)

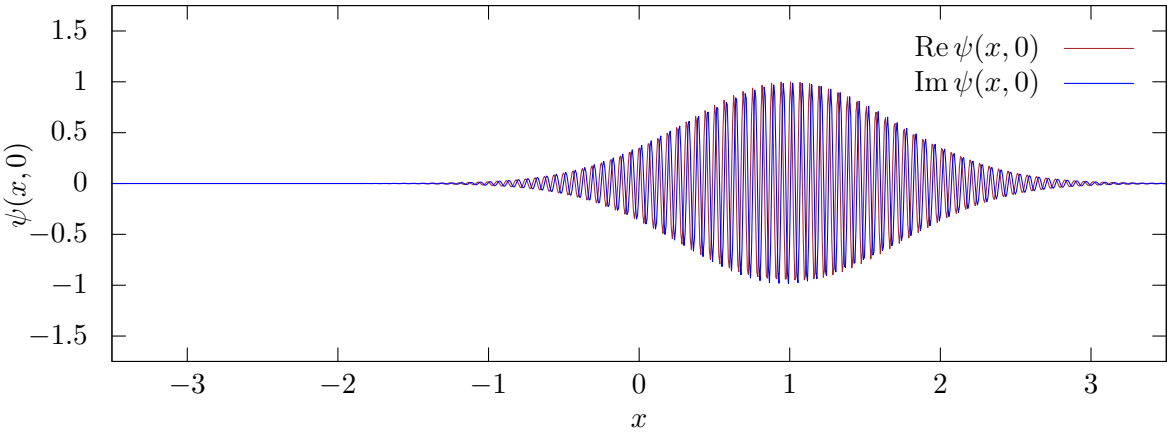

Figure 2.1: Gaussian wave packet with $x_0 = 1$, $p_0 = 1$, $\Delta x = 1$, $\hbar = 0.01$ in position representation

Figure 2.1 shows this type of initial state for $x_0 = 1$, $p_0 = 1$, and $\Delta x = 1$, with the units scaled in such a way that $\hbar$ takes the numerical value of 0.01. (For a detailed discussion of the units see subsection 2.1.5.) We see the wave packet centred around $x_0 = 1$. In the distance of $\Delta x = 1$ from x_0 the amplitude goes down to $\frac{1}{e}$ of its maximum. The initial momentum p_0 becomes visible in the shape of rapid oscillations.

Now we want to see what happens to this wave fucntion, its time development. This means to solve its Schrödinger equation.

To set up the Schrödinger equation in the first place we need a Hamiltonian. Again we make things simple and choose

$$H := \tfrac{p^2}{2m} + V(x), \tag{2.4}$$

i. e. the Hamiltonian of a one-dimensional particle of mass m in a potential $V(x)$. $p = -i\hbar\frac{\partial}{\partial x}$ is the momentum operator, and $\frac{p^2}{2m}$ is the kinetic energy of the particle.

To solve a differential equation numerically we take a small time interval Δt and hope that the conditions don't change too much during that time interval. Then we let the system evolve under these conditions and calculate the new conditions at the end of our time interval. This is the simplest method to solve a differential equation numerically, the *explicit Euler method*.

How can we apply the Euler method, or something similar, to the Schrödinger equation?

Let's forget about $V(x)$ for the moment. Then our Schrödinger equation reads

$$\tfrac{\partial}{\partial t}\psi(x,t) = -\tfrac{i}{\hbar}\tfrac{p^2}{2m}\psi(x,t) = \tfrac{i\hbar}{2m}\tfrac{\partial^2}{\partial x^2}\psi(x,t). \tag{2.5}$$

This is a so-called hyperbolic partial differential equation. When we write it with a zero on one side of the equal sign, the derivatives with respect to t and x have opposite signs. This makes it intricate to solve, even with a computer. However let's try.

How to compute the second spatial derivative of $\psi(x,t)$? Numerical analysis teaches us that it is usually a bad idea to approximate the spatial derivative of a function stored in an array by dividing the difference of two adjacent points in the array through the difference in x represented by their positions in the array. Often they will have almost the same value. When we compute their difference, all except a few of their significant digits will annihilate each other, which implies that our calculated derivative will have a very poor precision.

Fortunately there is a much better method. When we take the Fourier transform $\mathcal{F}\big(f(x)\big)(k)$ of a function $f(x)$,

$$\mathcal{F}\big(f(x)\big)(k) := \tfrac{1}{\sqrt{2\pi}}\int_{-\infty}^{\infty} f(x)\, e^{-ikx}\, dx, \tag{2.6}$$

then we get its derivative by multiplying by ik,

$$\mathcal{F}\left(\tfrac{\partial f}{\partial x}(x)\right)(k) = ik\,\mathcal{F}\big(f(x)\big)(k). \tag{2.7}$$

In our case, $\hbar k = p$. The Fourier transform

$$\tilde{\psi}(p,t) := \mathcal{F}\big(\psi(x,t)\big)\big(\tfrac{p}{\hbar}, t\big) \tag{2.8}$$

is in fact the momentum representation of our wave function $\psi(x,t)$. So all we need to do is to transform our wave function to momentum representation. Then our Schrödinger equation reads

$$\tfrac{\partial}{\partial t}\tilde{\psi}(p,t) = -\tfrac{i}{\hbar}\tfrac{p^2}{2m}\,\tilde{\psi}(p,t). \tag{2.9}$$

The Fourier transform has turned our hyperbolical partial differential equation into an ordinary differential equation.

Now we can write down its solution

$$\tilde{\psi}(p, t+\Delta t) = e^{-\frac{i}{\hbar}\frac{p^2}{2m}\Delta t}\,\tilde{\psi}(p,t). \tag{2.10}$$

As long as $V(x) = 0$, this solution is even exact.

Of course this result is the Fourier transform of the function we are acutally interested in. But this is not a problem, since we can apply a reverse Fourier transform,

$$\mathcal{F}^{-1}\big(\tilde{f}(k)\big)(x) := \tfrac{1}{\sqrt{2\pi}} \int_{-\infty}^{\infty} \tilde{f}(k)\, e^{ikx}\, dk. \tag{2.11}$$

In fact a Fourier transform and a reverse Fourier transform only differ by a sign.

Again fortunately, it is reasonably easy for a computer to compute the Fourier transform of a wave function stored in an array. There are even high-quality libraries for this purpose such as FFTW [3] readily available as Free Software (Open Source).

So if we want to see the free time development of a given initial state $\psi(x,t)$, we just let our computer Fourier transform it to momentum representation $\tilde{\psi}(p,t)$, then multiply it point-wise by $e^{-\frac{i}{\hbar}\frac{p^2}{2m}\Delta t}$. After that we transform it back to position representation and obtain the free time development $\psi(x, t+\Delta t)$.

Now that we know what $\frac{p^2}{2m}$ does, let's switch it off and study just $V(x)$ instead,

$$\tfrac{\partial}{\partial t}\psi(x,t) = -\tfrac{i}{\hbar} V(x)\psi(x,t). \tag{2.12}$$

At each position x this is already an ordinary differential equation. We can immediately write down its solution

$$\psi(x, t+\Delta t) = e^{-\frac{i}{\hbar}V(x)\Delta t}\, \psi(x,t) \tag{2.13}$$

which is again exact as long as $\frac{p^2}{2m}$ is absent.

Unfortunately both parts of the Hamiltonian are there, which forces us to use an approximation. When Δt is small, there is hope that it doesn't hurt too much that we cannot apply $\frac{p^2}{2m}$ and $V(x)$ simultaneously, but only in sequence,

$$\psi(x, t+\Delta t) = \mathcal{F}^{-1}\left(e^{-\frac{i}{\hbar}\frac{p^2}{2m}\Delta t}\, \mathcal{F}\left(e^{-\frac{i}{\hbar}V(x)\Delta t}\, \psi(x,t)\right)\left(\tfrac{p}{\hbar}, t\right)\right)(x,t) + \mathcal{O}(\Delta t^2). \tag{2.14}$$

This means: To simulate a quantum particle in an arbitrary potential, the computer needs

- to multiply the wave function, stored in an array in position representation, pointwise by $e^{-\frac{i}{\hbar}V(x)\Delta t}$,
- to Fourier transform the wave function to momentum representation,
- to multiply it pointwise by $e^{-\frac{i}{\hbar}\frac{p^2}{2m}\Delta t}$,
- and to Fourier transform the wave function back to position representation

in a loop.

See the program qpendulum.cpp for an implementation [4].

In the initialisation in the main program you can choose one of multiple templates for $V(x)$, or you can write your own one. For comparison, the program also simulates a classical particle under the influence of the same potential. To make this work for your own potential you have to provide the matching force

$$F(x) = -\tfrac{\partial}{\partial x} V(x). \tag{2.15}$$

In the case of the harmonic oscillator, $V(x) = \frac{1}{2}\frac{mg}{l}x^2$ (corresponding to $F(x) = -\frac{mg}{l}x$), the Gaussian wave packet changes its form, but it stays a wave packet whose mean position follows precisely the path of the classical particle.

The source file qpendulum.cpp is written for you to play with, for instance by trying out different shapes of the potential $V(x)$. Even a slight change to the potential, e. g. using the simple pendulum $V(x) = 1 - \frac{mg}{l}\cos x$ (corresponding to $F(x) = -\frac{mg}{l}\sin x$) instead of an ideal harmonic oscillator, causes the wave packet to change its form drastically until it fills the entire potential well. (Since our array has a finite size our system is finite-dimensional, thus the wave packet will recover after some while. However this can take quite long, depending on the potential.)

Although we have applied this method to a one-dimensional particle in a constant potential, it is by no means restricted to that. This method works well in arbitrary dimensions, and it has no problem with an explicitly time dependent potential, $V(x, t)$.

▶ **Exercise 2.1:** Write a program that simulates a two-dimensional non-relativistic hydrogen atom, i. e. a quantum particle in an external attractive Coulomb potential.

Solution: Figure 2.2 shows how the result can look like. The yellow and cyan colours visualise the real and imaginary part of the wave function. The initial state (left) is a Gaussian wave packet located below the (invisible) centre, travelling right. It travels to the right and upwards, circles around the centre, and interferes with itself.

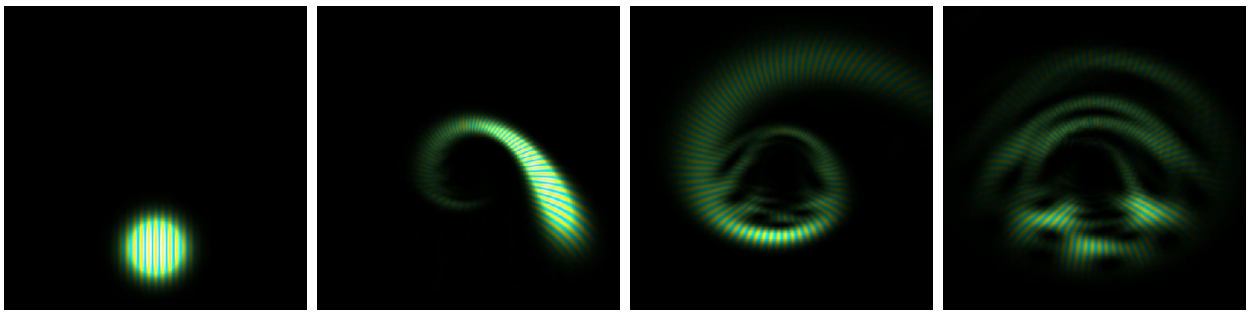

Figure 2.2: Simulation of non-relativistic, two-dimensional hydrogen

▶ **Exercise 2.2:** Write a "quantum pong" game, a program that simulates a two-dimensional non-relativistic quantum particle between an upper and a lower potential wall, where two players can move "rackets" of peaks of the potential up and down, trying not to let the quantum particle escape.

Solution: See [5].

2.1.2 Wave Functions

Figure 2.3 shows four screenshots from qpendulum. In the upper half of each screenshot we see a classical simple pendulum, which visualises an ideal classical harmonic oscillator. Below that we see the wave function of the corresponding quantum particle. In the left column the particle is close to the centre; in the right column it is close to the right reversal point. In the upper row the particle is moving to the right, and in the lower row to the left. We can see this from the phase difference between the real part (yellow) and the imaginary part (blue) of the wave function: In the pair of graphs of the real and imaginary part of the wave function, the imaginary part indicates the direction of motion. This also holds for the initial state, fig. 2.1, where the imaginary part is plotted in blue as well, and the particle is moving to the right.

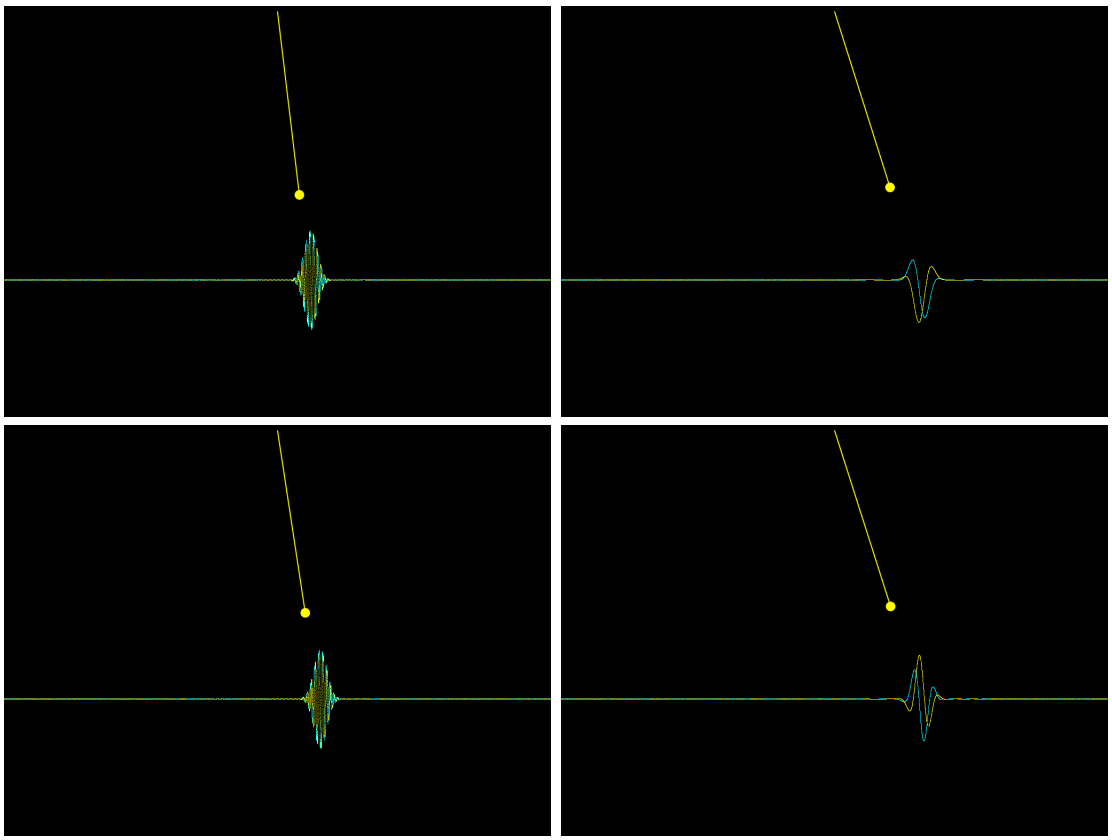

Figure 2.3: Screenshots from qpendulum

We can grasp even more properties of the quantum particle from the wave function. In the initial state, rapid oscillations correspond to a high value of p_0, and thus to a high velocity. This also holds for the wave function moving in qpendulum. When the particle is close to the centre (fig. 2.3, left column), the particle is moving fast, and there are rapid oscillations in the wave function. When it is close to the reversal point (right column), the particle is moving slowly, and the oscillations of the wave function are spatially slow.

In the left column of fig. 2.3 the oscillations are not easy to see. They are much easier to see in fig. 2.1 where the wave function is broader. This isn't just a question of visualisation, but this is Heisenberg's uncertainty principle at work. When the wave function is narrow in space (as in fig. 2.3), there cannot be many oscillations in it, which means that the momentum of the particle is not determined well. When the wave function is broad (as in fig. 2.1), there are enough oscillations to determine the momentum, but the broadness of the wave function implies an uncertainty of the position of the particle. Here Heisenberg's uncertainty principle becomes visible.

Heisenberg's uncertainty principle is also a feature of the Fourier transform. When we Fourier transform a narrow wave packet, the result is a broad wave packet, and vice versa.

As a further example, let's have another look at our initial state, eq. 2.3,

$$\psi(x,0) := e^{\frac{i}{\hbar}p_0 x - \left(\frac{x-x_0}{\Delta x}\right)^2}. \tag{2.16}$$

In momentum representation this state reads

$$\tilde{\psi}(p,0) = \frac{\sqrt{2}}{\hbar\,\Delta p}\, e^{-\frac{i}{\hbar}p x_0 - \left(\frac{p-p_0}{\Delta p}\right)^2}, \qquad \text{where} \qquad \Delta p := \frac{2\hbar}{\Delta x}. \tag{2.17}$$

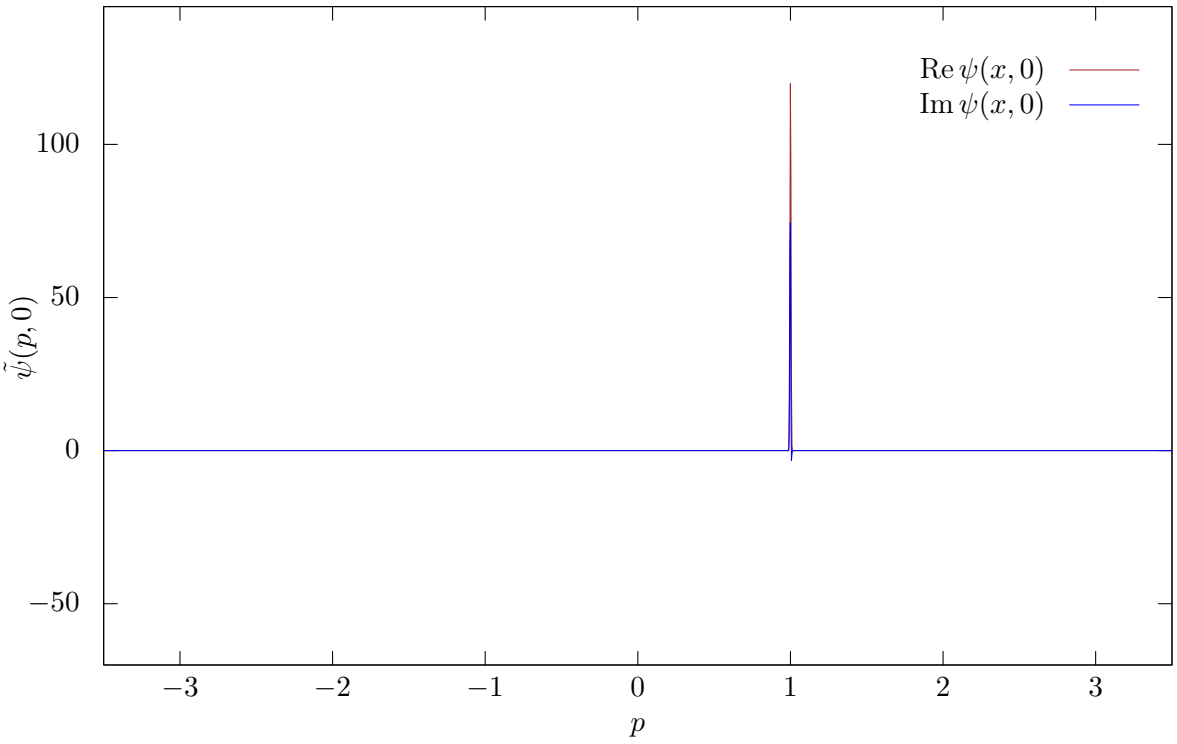

Figure 2.4: Gaussian wave packet with $x_0 = 1$, $p_0 = 1$, $\Delta x = 1$, $\hbar = 0.01$ in momentum representation

Note the different scalings of the y axis in this figure and in fig. 2.1.

Its graph is shown in fig. 2.4.

Both from the graph and from the formula (with a factor $\hbar$ from Δx to Δp) it is obvious that the width of the wave packet is much smaller in momentum representation than in position representation.

Since the norm of both wave functions must be the same, the amplitude is much higher in momentum representation (with $\hbar$ in the denominator).

▶ **Exercise 2.3:** Prove eq. 2.17.

Solution: To calculate the Fourier transform of

$$\psi(x,0) := e^{\frac{i}{\hbar}p_0 x - \left(\frac{x-x_0}{\Delta x}\right)^2} = e^{\frac{i}{\hbar}p_0 x} e^{-\left(\frac{x-x_0}{\Delta x}\right)^2} \tag{2.18}$$

we apply the well-known calculation rules for Fourier transforms.

- A prefactor e^{iax} results in a shift by $-a$ for k. Here, $a = \frac{p_0}{\hbar}$.
  Thus the prefactor $e^{\frac{i}{\hbar}p_0 x}$ results in a shift by $-\frac{p_0}{\hbar}$ for k, or a shift by $-p_0$ for p.
- Conversely the shift by $-x_0$ gets transformed to a prefactor $e^{-ikx_0} = e^{-\frac{i}{\hbar}px_0}$.
- $e^{-\alpha x^2}$ gets transformed to $\frac{1}{\sqrt{2\alpha}}\, e^{-\frac{k^2}{4\alpha}}$. Here, $\alpha = \frac{1}{\Delta x^2}$, and $k = \frac{p}{\hbar}$.
  Thus we can write down the exponent $-\frac{k^2}{4\alpha} = -\frac{1}{4}\Delta x^2\, \frac{p^2}{\hbar^2}$ as $-\frac{p^2}{\Delta p^2}$, where $\Delta p := \frac{2\hbar}{\Delta x}$.
  The prefactor becomes $\frac{1}{\sqrt{2\alpha}} = \frac{1}{\sqrt{2}}\Delta x = \frac{\sqrt{2}}{\hbar\,\Delta p}$.

Putting everything together we obtain

$$\tilde{\psi}(p,0) = \frac{\sqrt{2}}{\hbar\Delta p}\, e^{-\frac{i}{\hbar}px_0} e^{-\left(\frac{p-p_0}{\Delta p}\right)^2} = \frac{\sqrt{2}}{\hbar\Delta p}\, e^{-\frac{i}{\hbar}px_0 - \left(\frac{p-p_0}{\Delta p}\right)^2}. \quad \square \tag{2.19}$$

▶ **Exercise 2.4:** According to eq. 2.17, $\Delta x\,\Delta p = 2\hbar$. From Heisenberg's uncertainty relation one would expect $\Delta x\,\Delta p = \frac{1}{2}\hbar$ for Gaussian wave packets. Resolve this problem.

Solution: In eq. 2.17, Δx and Δp are the $\frac{1}{e}$ radiuses of the amplitudes of the wave functions. The quoted form of Heisenberg's uncertainty relation refers to something different, the standard deviations of the squared absolute values of Gaussian wave packets: $\sigma_x \cdot \sigma_p = \frac{1}{2}\hbar$.

By definition, the standard deviation of $e^{-\frac{x^2}{2\sigma^2}}$ is σ.

The squared absolute value of our wave function in position representation is $e^{-2\left(\frac{x-x_0}{\Delta x}\right)^2}$.
Thus our standard deviation is $2\sigma_x^2 = \frac{\Delta x^2}{2}$, or $\sigma_x = \frac{\Delta x}{2}$. Likewise $\sigma_p = \frac{\Delta p}{2}$.

So the product of our standard deviations is indeed $\sigma_x \cdot \sigma_p = \frac{\Delta x}{2} \cdot \frac{\Delta p}{2} = \frac{1}{4}\Delta x\,\Delta p = \frac{1}{2}\hbar$. $\square$

2.1.3 Understanding the Quantum Euler Method

Okay, what are we doing here?

- We want to solve a Schrödinger equation numerically.
- We have a time step operator

$$\psi(x, t+\Delta t) \approx e^{-\frac{i}{\hbar}\frac{p^2}{2m}\Delta t}\, e^{-\frac{i}{\hbar}V(x)\Delta t}\, \psi(x,t). \tag{2.20}$$

- Since p is a differential operator $-i\hbar\frac{\partial}{\partial x}$, it does not make sense to apply it in position representation. What does $e^{i\frac{\hbar}{2m}\frac{\partial^2}{\partial x^2}}$ even mean?
- Instead we represent the wave function *in a basis where the operator is diagonal* and apply it there. Then the operator boils down to a complex number (its eigenvalue) to which we can just apply the exponential. That's what $e^{i\frac{\hbar}{2m}\frac{\partial^2}{\partial x^2}}$ means.
- The same considerations hold for $V(x)$. It is a diagonal operator in position representation (point-wise multiplication; $V(x)$ is the eigenvalue of the operator for each x), so we apply it there.
- In momentum representation, $V(x)$ would be a differential operator which we cannot easily apply. When we imagine $V(x)$ as a matrix, it is diagonal in position representation (with the values of $V(x)$ as a real function on the diagonal, for the whole range of the index x), but a fully-occupied matrix in momentum representation.
- Likewise, p is a diagonal matrix in momentum representation, but a fully-occupied matrix in position representation.

By switching back and forth between position representation and momentum representation we only have to deal with diagonal matrices instead of fully-occupied ones. This saves *a lot* of memory and calculation time, $\mathcal{O}(n)$ instead of $\mathcal{O}(n^2)$, where n is the length of our arrays. This allows us to make the arrays much bigger than it would be possible if we had to deal with fully-occupied matrices.

We want to make our arrays as big as possible to make them as close as possible to theory, where their dimensions would be uncountably infinite. The limits of our simulations are set

by the Fourier transforms, which need $\mathcal{O}(n \log n)$ computing instructions and are thus a little slower than the point-wise operations we are using for applying our time step operators.

It is worth noting that our only approximation is that we apply $\frac{p^2}{2m}$ and $V(x)$ in sequence rather than simultaneously. In particular we don't approximate the exponentials. This ensures that our time step operator is unitary, i. e. it doesn't change the norm of the wave function.

2.1.4 Improving the Quantum Euler Method

So we have developed a quantum version of the explicit Euler method, and we can apply it to solve Schrödinger equations. How can we improve it?

When we apply $\frac{p^2}{2m}$ and $V(x)$ in sequence we can choose which one to apply first. However we'll get different results. This is because $\frac{p^2}{2m}$ and $V(x)$ do not commute, thus

$$e^{-\frac{i}{\hbar}\left(\frac{p^2}{2m}+V(x)\right)\Delta t} \neq e^{-\frac{i}{\hbar}\frac{p^2}{2m}\Delta t}\, e^{-\frac{i}{\hbar}V(x)\Delta t} \neq e^{-\frac{i}{\hbar}V(x)\Delta t}\, e^{-\frac{i}{\hbar}\frac{p^2}{2m}\Delta t}. \tag{2.21}$$

What we can do to minimise numerical errors is to take the arithmetic mean of both versions. In fact it is easy to prove (using the Baker-Campbell-Hausdorff theorem) that this really improves the result,

$$e^{-\frac{i}{\hbar}\left(\frac{p^2}{2m}+V(x)\right)\Delta t} = \frac{1}{2}\left(e^{-\frac{i}{\hbar}\frac{p^2}{2m}\Delta t}\, e^{-\frac{i}{\hbar}V(x)\Delta t} + e^{-\frac{i}{\hbar}V(x)\Delta t}\, e^{-\frac{i}{\hbar}\frac{p^2}{2m}\Delta t}\right) + \mathcal{O}(\Delta t^3). \tag{2.22}$$

This improved version of our 1st-order quantum Euler method is the quantum equivalent of the 2nd-order Heun method.

Apart from being more precise, this method gives us another advantage. While we are calculating the 2nd-order result, we get the result of the 1st-order method as a by-product. By comparing the 1st-order and the 2nd-order result we can estimate the error of our simulation and use this information to adapt the step size Δt.

This isn't just for convenience (because it saves calculation time), but it is necessary for solving certain differential equations at all, which actually require a different step size for different parts of the solution.

This method can be improved further to higher orders.

▶ **Exercise 2.5:** Prove eq. 2.22.

▶ **Exercise 2.6:** Improve the program qpendulum.cpp to use the quantum Heun method with adaptive step size instead of the plain quantum Euler method.

▶ **Exercise 2.7:** Set up the quantum version of the classical 4th-order Runge-Kutta method.

2.1.5 Units

In the computer it is easy to simulate a value of, say, $\hbar = 0.01$. However if we want our simulations to be more than just toys we must make them comparable to real-world experiments, where $2\pi\hbar = h = 6.626\,070\,15 \cdot 10^{-34}\,\mathrm{J\,s}$. (As of 20 May 2019 this value and the value of the elementary charge are fixed by the International System of Units, see [6].)

So what are our units?

Let δx, δt, and δm denote our units of length, time, and mass. Then in our simulations, $\hbar$ has the unit $\delta m\,\delta x^2\,\delta t^{-1}$. Later simulations will also involve the speed of light, c, which has the unit $\delta x\,\delta t^{-1}$, and a charge q, with unit δq. We can choose the mass and charge of our simulated particle to be connected to the mass and charge of a real-world particle, for instance an electron.

Now we can calculate the units of our simulation from the chosen numerical values of our constants. To avoid confusion, let $\hbar'$ be the numerical value of $\hbar$ in the simulation, as opposed to the actual $\hbar$, and do the same for c', m', and q'. Then our units mean

$$c = 299\,792\,458\,\tfrac{\mathrm{m}}{\mathrm{s}} = c'\,\tfrac{\delta x}{\delta t}, \tag{2.23}$$
$$\hbar = \tfrac{1}{2\pi} \cdot 6.626\,070\,15 \cdot 10^{-34}\,\mathrm{J\,s} = \hbar'\,\tfrac{\delta m\,\delta x^2}{\delta t}, \tag{2.24}$$
$$m = m_e = 9.109\,383\,56(11) \cdot 10^{-31}\,\mathrm{kg} = m'\,\delta m, \tag{2.25}$$
$$q = e = -1.602\,176\,634 \cdot 10^{-19}\,\mathrm{A\,s} = q'\,\delta q \tag{2.26}$$

$$\Rightarrow\ \delta m = \tfrac{1}{m'}\,m_e, \tag{2.27}$$
$$\delta q = \tfrac{1}{q'}\,e, \tag{2.28}$$
$$\delta x = \tfrac{c}{c'}\,\delta t, \tag{2.29}$$
$$\delta t = \tfrac{\hbar'}{\hbar}\,\delta m\,\delta x^2 = \tfrac{\hbar'}{\hbar}\,\delta m\,\left(\tfrac{c}{c'}\,\delta t\right)^2 \tag{2.30}$$

$$\Rightarrow\ \delta t = \tfrac{\hbar}{\hbar'}\,\tfrac{m'}{m_e}\,\tfrac{c'^2}{c^2} = \tfrac{m'\,c'^2}{\hbar'}\,\tfrac{\hbar}{m_e\,c^2}, \tag{2.31}$$
$$\delta x = \tfrac{\hbar}{\hbar'}\,\tfrac{m'}{m_e}\,\tfrac{c'}{c} = \tfrac{m'\,c'}{\hbar'}\,\tfrac{\hbar}{m_e\,c}. \tag{2.32}$$

As an example, consider an electron, which we simulate using $m' = 1$, $q' = 1$, $c' = 1$, and $\hbar' = 0.01$. Then our units get the values

$$\Rightarrow\ \delta m = m_e = 9.109\,383\,56(11) \cdot 10^{-31}\,\mathrm{kg}, \tag{2.33}$$
$$\delta q = e = -1.602\,176\,634 \cdot 10^{-19}\,\mathrm{A\,s}, \tag{2.34}$$
$$\delta t = \tfrac{1 \cdot 1^2}{0.01}\,\tfrac{\hbar}{m_e\,c^2} \approx 1.288\,089 \cdot 10^{-19}\,\mathrm{s}, \tag{2.35}$$
$$\delta x = \tfrac{1 \cdot 1}{0.01}\,\tfrac{\hbar}{m_e\,c} \approx 3.861\,593 \cdot 10^{-11}\,\mathrm{m}. \tag{2.36}$$

In this setup the length unit δx is close to the Bohr radius $a_0 = 5.291\,772\,109\,03(80) \cdot 10^{-11}\,\mathrm{m}$, and the time unit δt is the time a light ray needs to traverse it. This makes it suitable for investigating the dynamics of atoms. For investigating the dynamics of atomic nuclei a bigger value of $\hbar'$ and/or smaller values of m' and c' would make sense.

We now switch back from the notation $\hbar'$ for the numerical value in the simulation to just $\hbar$, and the same for c, m, and q.

2.2 Relativistic Quantum Mechanics

In this section we'll meet the Dirac equation, which is the Schrödinger equation of a relativistic particle and one of the ingredients of the Standard Model of quantum field theory. We'll study its free solutions analytically and apply the numerical methods developed in the previous section to simulate a relativistic quantum particle in arbitrary external electromagnetic fields.

2.2.1 The Free Dirac Equation

In the non-relativistic case, the Schrödinger equation of a free particle, i. e. of a particle with the energy – and thus the Hamiltonian –

$$E = E_{\text{kin}} = \tfrac{1}{2}mv^2 = \tfrac{p^2}{2m} = -\tfrac{\hbar^2}{2m}\tfrac{\partial^2}{\partial x^2} = H \tag{2.37}$$

reads

$$i\hbar\tfrac{\partial}{\partial t}\psi(x,t) = -\tfrac{\hbar^2}{2m}\tfrac{\partial^2}{\partial x^2}\psi(x,t). \tag{2.38}$$

It contains a first derivative with respect to t, but a second derivative with respect to x. This makes it incompatible with special relativity, where space and time can be mixed by Lorentz transformations. To make it compatible, derivatives with respect to time and space must be of the same order.

It is easy to transform an ordinary differential equation of second order to a system of two coupled ordinary differential equations of first order. While this doesn't immediately solve our problem, it gives us a hint how the solution could look like: We must extend the wave function from a complex-valued function to a vector-valued function, where the vector contains at least two complex numbers.

As Dirac found out, two complex numbers aren't enough, but the problem can be solved by extending the wave function to be *spinor*-valued, where a spinor is a vector with *four* complex components.

Then the Hamiltonian

$$H_\psi = -i\hbar c\sum_{j=1}^{3}\alpha_j\tfrac{\partial}{\partial x_j} + mc^2\alpha_4, \tag{2.39}$$

which acts on spinors, is Lorentz-invariant, i. e. compatible with special relativity.

The coefficients $\alpha_1, \ldots, \alpha_4$ aren't numbers, but matrices,

$$\alpha_1 = \begin{pmatrix} 0 & 0 & 0 & -i \\ 0 & 0 & -i & 0 \\ 0 & i & 0 & 0 \\ i & 0 & 0 & 0 \end{pmatrix}, \qquad \alpha_2 = \begin{pmatrix} 0 & 0 & 0 & -1 \\ 0 & 0 & 1 & 0 \\ 0 & 1 & 0 & 0 \\ -1 & 0 & 0 & 0 \end{pmatrix},$$

$$\alpha_3 = \begin{pmatrix} 0 & 0 & -i & 0 \\ 0 & 0 & 0 & i \\ i & 0 & 0 & 0 \\ 0 & -i & 0 & 0 \end{pmatrix}, \qquad \alpha_4 = \begin{pmatrix} 1 & 0 & 0 & 0 \\ 0 & 1 & 0 & 0 \\ 0 & 0 & -1 & 0 \\ 0 & 0 & 0 & -1 \end{pmatrix}. \tag{2.40}$$

This is just one of many equivalent representations of the Dirac matrices, all of which are commonly used. The notation used in this paper is after [7, § 28.4.3], where you can also find a mathematically exact and very inspiring approach to the Dirac equation by mathematical physics.

For later use we also note the matrices $\gamma_0, \ldots, \gamma_3$ with

$$\alpha_4 = \gamma_0, \qquad \text{and} \qquad \alpha_j = \gamma_0 \gamma_j \text{ for } j \in \{1, 2, 3\}, \tag{2.41}$$

spelled out

$$\gamma_0 = \begin{pmatrix} 1 & 0 & 0 & 0 \\ 0 & 1 & 0 & 0 \\ 0 & 0 & -1 & 0 \\ 0 & 0 & 0 & -1 \end{pmatrix}, \qquad \gamma_1 = \begin{pmatrix} 0 & 0 & 0 & -i \\ 0 & 0 & -i & 0 \\ 0 & -i & 0 & 0 \\ -i & 0 & 0 & 0 \end{pmatrix},$$
$$\gamma_2 = \begin{pmatrix} 0 & 0 & 0 & -1 \\ 0 & 0 & 1 & 0 \\ 0 & -1 & 0 & 0 \\ 1 & 0 & 0 & 0 \end{pmatrix}, \qquad \gamma_3 = \begin{pmatrix} 0 & 0 & -i & 0 \\ 0 & 0 & 0 & i \\ -i & 0 & 0 & 0 \\ 0 & i & 0 & 0 \end{pmatrix}. \tag{2.42}$$

Both sets of matrices are called *Dirac matrices*.

Substituting the relativistic Hamiltonian of kinetic energy, the *free Dirac Hamiltonian*, eq. 2.39, into the time-dependent Schrödinger equation, eq. 2.1,

$$i\hbar \tfrac{\partial}{\partial t} \psi(x,t) = H_\psi \psi(x,t), \tag{2.43}$$

yields the *free Dirac equation*,

$$i\hbar \tfrac{\partial}{\partial t} \psi(x,t) = -i\hbar c \sum_{j=1}^{3} \alpha_j \tfrac{\partial}{\partial x_j} \psi(x,t) + mc^2 \alpha_4 \, \psi(x,t), \tag{2.44}$$

which describes the quantum dynamics of a free relativistic particle.

2.2.2 Analytic Solutions of the Free Dirac Equation

As we have learned in subsection 2.1.1, we can solve the Schrödinger equation of a non-relativistic free particle exactly by transforming everything to momentum representation. Then the momentum operator, which contains a derivative with respect to x, reduces to point-wise multiplication by a number p, making the non-relativistic time step, eq. 2.10, very simple,

$$\tilde{\psi}(p, t + \Delta t) = e^{-\frac{i}{\hbar} \frac{p^2}{2m} \Delta t} \, \tilde{\psi}(p,t). \tag{2.45}$$

Doing the same for the free Dirac equation in momentum representation,

$$i\hbar \tfrac{\partial}{\partial t} \tilde{\psi}(p,t) = c \sum_{j=1}^{3} \alpha_j p_j \, \tilde{\psi}(p,t) + mc^2 \alpha_4 \, \tilde{\psi}(p,t), \tag{2.46}$$

results in

$$\tilde{\psi}(p, t + \Delta t) = \exp\left(-\tfrac{i}{\hbar} \Delta t \, c \sum_{j=1}^{3} \alpha_j \, p_j - \tfrac{i}{\hbar} \Delta t \, mc^2 \alpha_4 \right) \tilde{\psi}(p,t), \tag{2.47}$$

i. e. the exponential of $-\frac{i}{\hbar}\Delta t$ times the *momentum matrix*

$$\begin{aligned} P &= c \sum_{j=1}^{3} \alpha_j \, p_j + mc^2 \alpha_4 \\ &= \begin{pmatrix} mc^2 & 0 & -ic\,p_z & -ic\,p_x - c\,p_y \\ 0 & mc^2 & -ic\,p_x + c\,p_y & ic\,p_z \\ ic\,p_z & ic\,p_x + c\,p_y & -mc^2 & 0 \\ ic\,p_x - c\,p_y & -ic\,p_z & 0 & -mc^2 \end{pmatrix}. \end{aligned} \tag{2.48}$$

(We use the synonyms $p_x = p_1$, $p_y = p_2$, and $p_z = p_3$.)

The exponential of a diagonal matrix can be taken component-wise. To render this matrix diagonal we need to represent it in its eigenbasis. Thus the next step is to compute the four eigenvectors of this matrix, the *momentum eigenvectors* $\psi_{p,\sigma}$ for $\sigma \in \{0, 1, 2, 3\}$.

A straightforward calculation yields the eigenvalues E_σ,

$$E_0 = E_1 = E_+ := \sqrt{m^2c^4 + p^2c^2}, \qquad E_2 = E_3 = E_- := -\sqrt{m^2c^4 + p^2c^2} \tag{2.49}$$

with

$$p^2 := p_x^2 + p_y^2 + p_z^2, \tag{2.50}$$

and the eigenvectors $\psi_{p,\sigma}$,

$$\psi_{p,0} = \begin{pmatrix} 1 \\ 0 \\ B_{02} \\ B_{03} \end{pmatrix}, \quad \psi_{p,1} = \begin{pmatrix} 0 \\ 1 \\ B_{12} \\ B_{13} \end{pmatrix}, \quad \psi_{p,2} = \begin{pmatrix} B_{20} \\ B_{21} \\ 1 \\ 0 \end{pmatrix}, \quad \psi_{p,3} = \begin{pmatrix} B_{30} \\ B_{31} \\ 0 \\ 1 \end{pmatrix}, \tag{2.51}$$

with the coefficients

$$B_{02} = B_{20} = \frac{ic\,p_z}{E_+ + mc^2}, \qquad B_{03} = B_{21} = \frac{-c\,p_y + ic\,p_x}{E_+ + mc^2}, \tag{2.52}$$

$$B_{12} = B_{30} = \frac{c\,p_y + ic\,p_x}{E_+ + mc^2}, \qquad B_{13} = B_{31} = \frac{-ic\,p_z}{E_+ + mc^2}. \tag{2.53}$$

Now we can easily compute the time development of a quantum system according to the free Dirac equation in momentum representation. We decompose its wave function into momentum eigenstates,

$$\tilde{\psi}(p, t) = \sum_{\sigma=0}^{3} C_\sigma \psi_{p,\sigma}, \tag{2.54}$$

then the time development of each component is just a phase factor $e^{-\frac{i}{\hbar}E_\sigma \Delta t}$,

$$\tilde{\psi}(p, t + \Delta t) = e^{-\frac{i}{\hbar}H_\psi \Delta t}\,\tilde{\psi}(p, t) = \sum_{\sigma=0}^{3} e^{-\frac{i}{\hbar}E_\sigma \Delta t}\, C_\sigma \psi_{p,\sigma}. \tag{2.55}$$

There is one oddity in the Dirac equation which is worth discussing: Two of the four eigenvalues – kinetic energies – are negative. The corresponding eigenstates describe anti-particles, whereas the particles have positive kinetic energy.

A negative kinetic energy contradicts physical intuition. If the anti-particle loses energy when it accelerates one might think that it will get faster and faster just by itself. However the anti-particle won't do anything "just by itself". It needs a mechanism which causes it to change its state of motion, otherwise it won't accelerate or decelerate.

In our simulation as well as in the most advanced models of physics, quantum field theory and general relativity, there is no external mechanism which would, comparable to friction, cause a particle to minimise its energy. All mechanisms are inside the model.

In any case the negative energy doesn't cause problems in our simulation. We just have to keep in mind that an anti-particle moves in the opposite direction of its momentum vector when we prepare the initial state. Anyway we'll simplify things later by applying the Feynman-Stückelberg interpretation of anti-particles: By reversing their direction of time we render their kinetic energy positive.

▶ **Exercise 2.8:** Derive the above expressions for the momentum eigenvectors $\psi_{p,\sigma}$.

▶ **Exercise 2.9:** Prove that the momentum eigenvectors $\psi_{p,\sigma}$ are orthogonal for different σ.

▶ **Exercise 2.10:** Prove that the norm of the momentum eigenvectors is

$$|\psi_{p,\sigma}| = \sqrt{1 + \frac{p^2c^2}{mc^2 + \sqrt{m^2c^4 + p^2c^2}}} \tag{2.56}$$

for all $\sigma \in \{0, 1, 2, 3\}$.

2.2.3 The Dirac Equation with an External Field

There is a standard proceduce for the transition from a free system to a system with an external field A_μ, the so-called *minimal coupling*,

$$p_\mu \mapsto p_\mu - qA_\mu. \tag{2.57}$$

In our case, A_μ is the electromagnetic four-potential, the coupling constant q is the charge of our particle, and p_μ is the four-momentum,

$$p_0 = \tfrac{E}{c} = \tfrac{i\hbar}{c}\tfrac{\partial}{\partial t} = i\hbar\,\partial_0, \qquad p_j = i\hbar\tfrac{\partial}{\partial x_j} = i\hbar\,\partial_j \text{ for } j \in \{1, 2, 3\}. \tag{2.58}$$

This substitution has to be applied to the Lagrangian. Since we need to get familiar with this anyway, let's take the opportunity and derive the Dirac equation with an external field from its Lagrangian,

$$\mathcal{L}_\psi = \bar{\psi}\left(\sum_{\mu=0}^{3} i\hbar c\,\gamma_\mu\partial_\mu - mc^2\right)\psi. \tag{2.59}$$

To be precise, our Lagrangian is not a *Lagrangian function*, but a *Lagrangian density*, which applies to fields rather than to particles.

The minimal coupling $p_\mu \mapsto p_\mu - qA_\mu$ yields

$$\mathcal{L} = \bar{\psi}\left(\sum_{\mu=0}^{3} \gamma_\mu(i\hbar c\,\partial_\mu - qcA_\mu) - mc^2\right)\psi. \tag{2.60}$$

To derive the equations of motion we have to set up the Euler-Lagrange equations for the independent fields ψ and $\bar{\psi}$,

$$\frac{\partial\mathcal{L}}{\partial\bar{\psi}} - \sum_{\mu=0}^{3}\partial_\mu\left(\frac{\partial\mathcal{L}}{\partial(\partial_\mu\bar{\psi})}\right) = 0, \qquad \frac{\partial\mathcal{L}}{\partial\psi} - \sum_{\mu=0}^{3}\partial_\mu\left(\frac{\partial\mathcal{L}}{\partial(\partial_\mu\psi)}\right) = 0. \tag{2.61}$$

Let's start with the left one. We differentiate the Lagrangian with respect to $\bar{\psi}$ and to $\partial_\mu\bar{\psi}$ to get an equation of motion for ψ. Since $\mathcal{L}$ does not explictly depend on $\partial_\mu\bar{\psi}$, we have

$$\sum_{\mu=0}^{3}\partial_\mu\left(\frac{\partial\mathcal{L}}{\partial(\partial_\mu\bar{\psi})}\right) = 0, \tag{2.62}$$

and the equation of motion reads

$$\frac{\partial\mathcal{L}}{\partial\bar{\psi}} = \left(\sum_{\mu=0}^{3}\gamma_\mu(i\hbar c\,\partial_\mu - qcA_\mu) - mc^2\right)\psi = 0. \tag{2.63}$$

We extract the index zero from the sum and rearrange a little,

$$\gamma_0\, i\hbar c\, \partial_0 \psi + \sum_{j=1}^{3} \gamma_j (\, i\hbar c\, \partial_j - qcA_j)\psi - (mc^2 + \gamma_0 qcA_0)\psi = 0. \tag{2.64}$$

We isolate the time derivative ∂_0 on the left hand side and multiply the equation from the left by γ_0,

$$\gamma_0\gamma_0\, i\hbar c\, \partial_0 \psi = \sum_{j=1}^{3} \gamma_0\gamma_j(-i\hbar c\, \partial_j + qcA_j)\psi + (\gamma_0 mc^2 + \gamma_0\gamma_0 qcA_0)\psi. \tag{2.65}$$

With $\gamma_0\gamma_0 = 1$, $\gamma_0\gamma_j = \alpha_j$ for $j \in \{1,2,3\}$, $\gamma_0 = \alpha_4$, and $\partial_0 = \frac{1}{c}\frac{\partial}{\partial t}$ we arrive at the Dirac equation with an external field,

$$i\hbar \tfrac{\partial}{\partial t}\psi(x,t) = \sum_{j=1}^{3} \alpha_j \left(-i\hbar c\, \tfrac{\partial}{\partial x_j} + qcA_j\right) \psi(x,t) + (mc^2\alpha_4 + qcA_0)\psi(x,t). \tag{2.66}$$

For $q = 0$ this equation coincides with the free Dirac equation. So we have derived the free Dirac equation from its Lagrangian as a by-product.

When we repeat this procedure for the other Euler-Lagrange equation in eq. 2.61, we get the same equation for $\bar{\psi}$, but with reversed signs in front of $p_\mu = i\hbar\partial_\mu$ and qcA_μ. This is the so-called *adjoint Dirac equation*. When ψ is a solution of the Dirac equation, then $\bar{\psi} = \gamma_0\psi^*$ is a solution of the adjoint Dirac equation, and vice versa. So our "independent" fields ψ and $\bar{\psi}$ are in fact two representations of the same field.

▶ **Exercise 2.11:** Derive the adjoint Dirac equation with an external field, i. e. the Dirac equation with reversed signs in front of $p_\mu = i\hbar\partial_\mu$ and qcA_μ, starting from the other Euler-Lagrange equation in eq. 2.61.

Solution: With

$$\frac{\partial\mathcal{L}}{\partial\bar{\psi}} = \bar{\psi}\left(\sum_{\mu=0}^{3}\gamma_\mu qcA_\mu - mc^2\right), \qquad \frac{\partial\mathcal{L}}{\partial(\partial_\mu\bar{\psi})} = \bar{\psi}\, i\hbar c\,\gamma_\mu \tag{2.67}$$

the equation of motion reads

$$\begin{aligned}\frac{\partial\mathcal{L}}{\partial\bar{\psi}} - \sum_{\mu=0}^{3}\partial_\mu\left(\frac{\partial\mathcal{L}}{\partial(\partial_\mu\bar{\psi})}\right) &= \bar{\psi}\left(\sum_{\mu=0}^{3}\gamma_\mu qcA_\mu - mc^2\right) - \sum_{\mu=0}^{3}\partial_\mu\bar{\psi}\, i\hbar c\,\gamma_\mu \\ &= \left(\sum_{\mu=0}^{3}\gamma_\mu(-i\hbar c\,\partial_\mu + qcA_\mu) - mc^2\right)\bar{\psi} = 0,\end{aligned} \tag{2.68}$$

which is eq. 2.63 with $\bar{\psi}$ instead of ψ and with reversed signs in front of $p_\mu = i\hbar\partial_\mu$ and qcA_μ. □

▶ **Exercise 2.12:** Show that when ψ is a solution of the Dirac equation, then $\bar{\psi} = \gamma_0\psi^*$ is a solution of the adjoint Dirac equation, and vice versa.

2.2.4 Numeric Solution of the Dirac Equation with an External Field

It is possible to solve the Dirac equation with an external field analytically for special cases, including the hydrogen atom [7, § 28.5.4]. Here, however, we want to solve it numerically for the general case.

Our simple example from subsection 2.1.1 consisted of two operators, $\frac{p^2}{2m}$ which is diagonal in momentum representation, and $V(x)$ which is diagonal in position representation. The same decomposition is possible for the Dirac equation with an external field,

$$i\hbar\frac{\partial}{\partial t}\psi(x,t) = H\psi(x,t) \qquad \text{with} \qquad H = H_\psi + H_J, \tag{2.69}$$

where

$$H_\psi = -i\hbar c\sum_{j=1}^{3}\alpha_j\,\tfrac{\partial}{\partial x_j} + mc^2\alpha_4 \qquad \text{and} \qquad H_J = q\sum_{j=1}^{3}\alpha_j\,A_j + qcA_0. \tag{2.70}$$

In subsection 2.2.2 we have seen how to decompose a general wave function into eigenfunctions of the momentum matrix, eq. 2.48. This allows us to apply the time step operator $e^{-\frac{i}{\hbar}H_\psi\Delta t}$ to a wave function without approximation.

In addition we now have the interaction of the particle with the external field. It is diagonal in x (as opposed to a fully-occupied matrix which would involve an integral over x). Just like the momentum matrix is valid for a specific momentum p, we can speak of the interaction at a specific position x.

For fixed x, the interaction operator H_J is a matrix over spinor space, the *interaction matrix*

$$\begin{aligned} A &= q\sum_{j=1}^{3}\alpha_j\,A_j + qcA_0 \\ &= \begin{pmatrix} qcA_0 & 0 & -iqcA_z & -iqcA_x - qcA_y \\ 0 & qcA_0 & -iqcA_x + qcA_y & iqcA_z \\ iqcA_z & iqcA_x + qcA_y & qcA_0 & 0 \\ iqcA_x - qcA_y & -iqcA_z & 0 & qcA_0 \end{pmatrix}. \end{aligned} \tag{2.71}$$

(We use the synonyms $A_x = A_1$, $A_y = A_2$, and $A_z = A_3$.)

The structure of this matrix is similar enough to that of the momentum matrix that we can reuse the results from subsection 2.2.2 with the substitutions

$$c\,p_j \mapsto qcA_j \;\text{ for } j \in \{1,2,3\}, \qquad \pm mc^2 \mapsto qcA_0. \tag{2.72}$$

The eigenvalues are

$$E_0 = E_1 = E_+ := qcA_0 + qa, \qquad E_2 = E_3 = E_- := qcA_0 - qa \tag{2.73}$$

with

$$a := \sqrt{A_x^2 + A_y^2 + A_z^2}. \tag{2.74}$$

The interaction eigenvectors $\psi_{x,\sigma}$ have the same structure as the momentum eigenvectors $\psi_{p,\sigma}$,

$$\psi_{x,0} = \begin{pmatrix} 1 \\ 0 \\ B_{02} \\ B_{03} \end{pmatrix}, \quad \psi_{x,1} = \begin{pmatrix} 0 \\ 1 \\ B_{12} \\ B_{13} \end{pmatrix}, \quad \psi_{x,2} = \begin{pmatrix} B_{20} \\ B_{21} \\ 1 \\ 0 \end{pmatrix}, \quad \psi_{x,3} = \begin{pmatrix} B_{30} \\ B_{31} \\ 0 \\ 1 \end{pmatrix}, \tag{2.75}$$

with the coefficients

$$B_{02} = B_{20} = \frac{iA_z}{a}, \qquad B_{03} = B_{21} = \frac{-A_y + iA_x}{a}, \tag{2.76}$$

$$B_{12} = B_{30} = \frac{A_y + iA_x}{a}, \qquad B_{13} = B_{31} = \frac{-iA_z}{a}. \tag{2.77}$$

Now we can decompose the wave function in position representation into the eigenvectors of the interaction matrix and apply the time step operator $e^{-\frac{i}{\hbar}H_J\Delta t}$. It multiplies each eigenvector by a phase factor $e^{-\frac{i}{\hbar}E_\sigma\Delta t}$. After that we recombine the result to the wave function.

This allows us to apply the methods from subsection 2.1.1 and 2.1.4 for solving the Dirac equation with an external field.

There are some caveats when preparing the initial state, even without the external field.

In the non-relativistic case there was just one component. Now if we initialise just one component of the spinor, we prepare a superposition of three eigenstates. (The remaining one has a zero in this spinor component.) In particular we mix eigenstates with different signs of E_σ – particles and anti-particles – which will travel in opposite directions.

So if we really want to prepare an initial state with a well-defined momentum – which includes the question whether it is a particle or an anti-particle – we need to initialise a momentum eigenstate rather than a spinor component.

The external field doesn't exactly make things easier. It modifies the eigenstates of the total system in a way we can only simulate numerically, but we cannot compute analytically. (In the language of noncommutative geometry this is generalised curvature of the extended spacetime which bends the eigenstates.)

As a consequence, even preparing a momentum eigenstate results in a mixture of at least three different eigenstates, which involve particles as well as anti-particles and travel in opposite directions.

So there is no way to prepare a state which doesn't mix particles and anti-particles when there is an external field. However we can apply a trick. At the beginning we switch the external field off and prepare a "normal" momentum eigenstate. Then we slowly activate the external field, and the simulation takes the eigenstate with it.

Since this is just a simulation with no real fields involved, there is even an alternative. Instead of turning the external field off and on we can change the value of the coupling constant q. This alternate method will continue to work when the electromagnetic field is no longer external but a dynamic variable itself. It will allow us to shorten the distance between the prepared particles, thus extending the range of physical systems we can simulate.

To summarise, these are the steps to simulate a relativistic particle in an external field.

- Prepare an inital state as a momentum eigenstate (eq. 2.51), whose dependency on x is a Gaussian wave packet (eq. 2.3).
- Initially, set the external field to zero. Then switch it on slowly while the loop of the simulation is running.
- To simulate the action of the external field on the current state, decompose it into eigenstates of H_J (eq. 2.75), multiply the coefficient of each eigenvector $\psi_{x,\sigma}$ by its phase factor $e^{-\frac{i}{\hbar}E_\sigma\Delta t}$, and store the result back to the wave function.
- Fourier transform the wave function to momentum representation.
- To simulate the free propagation of the current state, decompose it into momentum eigenstates (eq. 2.51), multiply the coefficient of each eigenvector $\psi_{p,\sigma}$ by its phase factor $e^{-\frac{i}{\hbar}E_\sigma\Delta t}$, and store the result back to the wave function.

- Fourier transform the wave function back to position representation.
- Reiterate the time steps.

Figure 2.5 shows an implementation of this algorithm, a simulation of a two-dimensional relativistic quantum particle in a homogeneous external magnetic field in z direction, i. e. perpendicular to the screen or paper. The vector potential is $(-\frac{1}{2}\lambda y, \frac{1}{2}\lambda x, 0)$, where λ starts at 0 for $t = 0$, follows a $\sin^2$-shaped curve until it reaches -0.2 at $t = 2\pi$.

The images show

- the initial state at $t = 0$,
- the state at $t = 5$, where the particle has travelled to the right and the external magnetic field has almost reached its full strength,
- the state at $t = 20$, where the particle has started to orbit counterclockwise,
- and the state at $t = 130$, where the particle has completed its second orbit.

After that the particle continues to spread along its orbit, a rotating ellipsis.

The numeric parameters are $\hbar = 0.004$, $c = 1$, $m = 1$, $q = 1$, calculated in a grid of 4096×4096 points with a spatial separation of $\Delta x = 0.0035$. The numeric value of 0.2 of the external magnetic field corresponds to about $3.5 \cdot 10^6\,\mathrm{T}$, which is in the range of neutron stars. The images show a square area of about $13.8 \cdot 10^{-10}\,\mathrm{m}$ width and height. The particle orbits in a region of a few Ångström in diameter, which has the correct order of magnitude, compared to a classical calculation of the orbit.

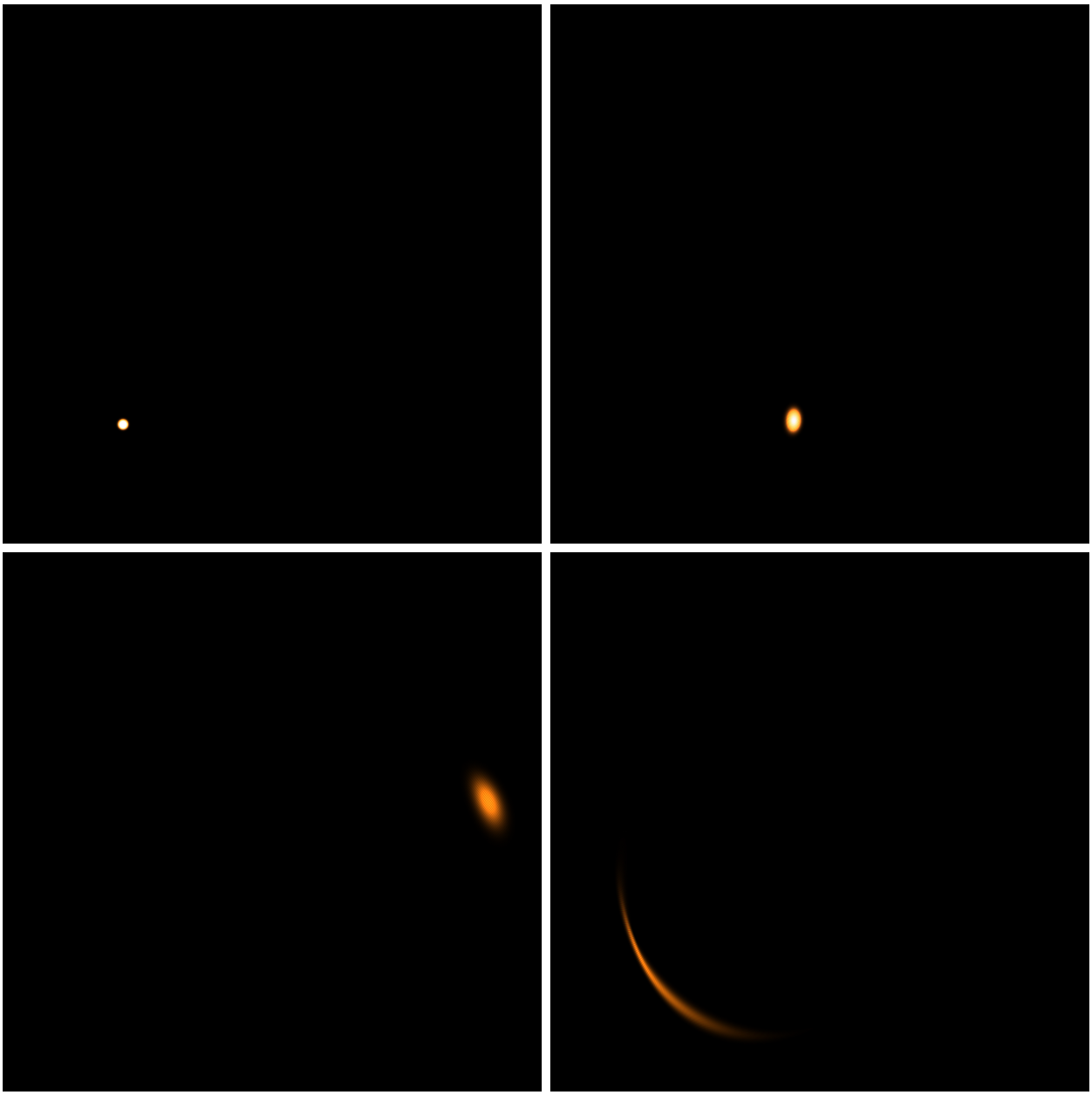

Figure 2.5: Simulation of a two-dimensional relativistic quantum particle in a homogeneous external magnetic field

2.3 Classical Electrodynamics

On the way to quantum electrodynamics, classical electrodynamics is two steps ahead of classical mechanics. It already uses wave functions to describe nature, and it is already compatible with special relativity.

The simplest consistent description of the electromagnetic field is already a relativistic one, the Maxwell equations. In fact special relativity emerged from the contradictions between Galilei's principle of relativity and the Maxwell equations, which predict that electromagnetic waves in the vacuum have always the same speed, seen from any reference frame. These contradictions led to Einstein's principle of relativity, where Lorentz transformations take the role of the Galilei transformations which govern classical mechanics, including non-relativistic quantum mechanics.

In this section we apply the methods from the previous sections to simulate a classical electromagnetic field, and we study its description in the Lagrangian and Hamiltonian formalisms. As we will see later, these are excellent preparations for simulating a field of photons.

2.3.1 The Maxwell Equations

In the previous section we simulated a relativistic quantum particle in an external electromagnetic field. We didn't assume anywhere that the field had any particular form or that it was static. It can be an arbitrary electromagnetic field $A_\mu(x,t)$, which we can store point-wise in an independent array.

At each position x and each time t, the components of A_μ are the electric Coulomb potential $A_0 = \frac{1}{c}\Phi$ and the magnetic vector potential $A = (A_x, A_y, A_z)$.

Most of the time, we will be using the four-potential A_μ instead of the electric field E and the magnetic flux density B for two reasons:

- A_μ directly enters the Dirac equation of a relativistic quantum particle.
- A_μ can be made Lorentz-invariant by using the Lorenz gauge.

In this sense the electromagnetic four-potential in Lorenz gauge is "the real thing", while the electric field and the magnetic flux density depend on the observer. For instance the Lorentz force of a classical charged particle moving in a magnetic field transforms to an electric force in a coordinate frame which moves together with the particle.

(Side note: The Lorentz transformation and the Lorentz force are named after Hendrik Antoon Lorentz, while the Lorenz gauge is named after Ludvig Lorenz.)

Now suppose that we have prepared an intial state for the electromagnetic field. Then its evolution in time is described by the Maxwell equations. In the vacuum, in absence of any charges or currents, and written in terms of the four-potential in Lorenz gauge they read

$$\Box A_\mu(x,t) = 0 \tag{2.78}$$

or, spelled out,

$$\tfrac{\partial^2}{\partial t^2} A_\mu(x,t) = c^2 \Delta A_\mu(x,t). \tag{2.79}$$

This equation for the four components of the four-potential ($\mu \in \{0,1,2,3\}$) has a similar structure as the Schrödinger equation. Both equations are hyperbolical partial differential equations, which relate a time derivative of a function to a spatial derivative of the same function.

But there is an important difference. Our non-relativistic Schrödinger equation (see subsection 2.1.1) was of first order in time and of second order in space. The Dirac equation (see section 2.2) is of first order both in time and in space. The vacuum Maxwell equation for the four-potential in Lorenz gauge (eq. 2.79) is of second order both in time and in space. A second-order derivative in time means that we cannot directly apply our methods to solve it numerically.

It is, of course, straightforward to convert it into a set of first-order differential equations by introducing the time derivative $\dot{A}_\mu(x,t)$ of $A_\mu(x,t)$ as a separate variable,

$$\frac{\partial}{\partial t} A_\mu(x,t) = \dot{A}_\mu(x,t), \tag{2.80}$$

$$\frac{\partial}{\partial t} \dot{A}_\mu(x,t) = c^2 \Delta A_\mu(x,t). \tag{2.81}$$

There is, however, an alternative formulation, which will prove beneficial later.

First we apply a Fourier transform to these equations. This turns the second-order spatial differential operator Δ into a multiplication by $(ik)^2 = -|k|^2$,

$$\frac{\partial}{\partial t} \tilde{A}_\mu(k,t) = \dot{\tilde{A}}_\mu(k,t), \tag{2.82}$$

$$\frac{\partial}{\partial t} \dot{\tilde{A}}_\mu(k,t) = -c^2 |k|^2 \tilde{A}_\mu(k,t), \tag{2.83}$$

where k is the vector of the spatial angular wavenumbers.

Later, $p = \hbar k$ will be the momentum of a photon. Thus we already use the name *momentum representation* for this k representation.

Now we define $\omega_k = |k|c$ and introduce the field

$$\alpha_\mu(k,t) := \tilde{A}_\mu(k,t) + \tfrac{i}{\omega_k} \dot{\tilde{A}}_\mu(k,t) \tag{2.84}$$

i. e. a complex field in momentum representation whose real part is the electromagnetic four-potential and whose imaginary part is, up to a factor of $\frac{1}{\omega_k}$, its time derivative.

Then

$$\begin{aligned}
\frac{\partial}{\partial t} \alpha_\mu(k,t) &= \frac{\partial}{\partial t} \tilde{A}_\mu(k,t) + \tfrac{i}{\omega_k} \frac{\partial}{\partial t} \dot{\tilde{A}}_\mu(k,t) \\
&= \dot{\tilde{A}}_\mu(k,t) - \tfrac{i}{\omega_k} c^2 |k|^2 \tilde{A}_\mu(k,t) \\
&= -i\omega_k \tfrac{i}{\omega_k} \dot{\tilde{A}}_\mu(k,t) - i\omega_k \tilde{A}_\mu(k,t) \\
&= -i\omega_k \, \alpha_\mu(k,t)
\end{aligned} \tag{2.85}$$

is a first-order differential equation for the complex wave function $\alpha_\mu(k,t)$, equivalent to the vacuum Maxwell equations in Lorenz gauge.

So we can, in momentum representation, transform our real-valued second-order differential equation into a complex-valued first-order differential equation. For the moment this just makes it easier to apply our numerical methods to it or to solve it analytically. (The solution is $\alpha_\mu(k, t+\Delta t) = e^{-i\omega_k \Delta t} \alpha_\mu(k,t)$.) Later this formulation of the Maxwell equations will become a key to the dynamics of photons.

▶ **Exercise 2.13:** Derive eq. 2.79 from the classical Maxwell equations and the Lorenz gauge $\nabla \cdot A + \frac{1}{c^2} \frac{\partial \Phi}{\partial t} = 0$.

▶ **Exercise 2.14:** Use the algorithm described in the previous sections to write a program which can simulate the time development of a classical electromagnetic wave in the vacuum.

▶ **Exercise 2.15:** Extend the software from the previous exercise to include charges and currents as sources of the electromagnetic field. You can either provide classical sources, or you can, by using the squared absolute value of a wave function as a density, simulate the classical electromagnetic field generated by a – non-relativistic or relativistic – quantum particle.

Hint: Simulate the interaction in position representation. Only the free development is easier to simulate in momentum representation.

2.3.2 Lagrangian Formulation of Classical Electrodynamics

In quantum field theory, including quantum electrodynamics, the Lagrangian forumlation has proven useful as a very compact way to describe physical systems – much more compact than differential equations.

In classical electrodynamics, where the vacuum Maxwell equations can be written $\Box A_\mu(x,t) = 0$, this is not yet the case. Nevertheless let's have a look at how the differential equations relate to the Lagrangian.

Like the Lagrangian of the Dirac equation, this Lagrangian is not a *Lagrangian function* for particles, but a *Lagrangian density* for fields.

The Lagrangian of classical electrodynamics reads

$$\mathcal{L}_A = -\tfrac{1}{4\mu_0} F_{\mu\nu} F^{\mu\nu}, \tag{2.86}$$

where $F_{\mu\nu}$ is the electromagnetic field tensor,

$$F_{\mu\nu} = \partial_\mu A_\nu - \partial_\nu A_\mu, \tag{2.87}$$

and μ_0 is the permeability of free space. (In theoretical physics, μ_0 is usually set to 1. We are keeping it here because it does not cause much trouble and we take the opportunity to investigate its role in the quantisation of the electromagnetic field. Also it can make it easier to compare our theoretical calculations with experimental data.)

As is customary in field theory, we are using, until the end of this chapter, upper and lower indices and the Einstein summation convention, known from special relativity. After that, this notation is likely to cause more confusion than clarity, so we will switch back to explicit summation symbols.

We are working with the Minkowski signature $(+,-,-,-)$. In particular,

- $A^\mu = (\frac{1}{c}\Phi, A_x, A_y, A_z)$ is the covariant four-potential (written $A_\mu(x,t)$ above),
- $A_\mu = (\frac{1}{c}\Phi, -A_x, -A_y, -A_z)$ is the contravariant four-potential,
- $\partial^\mu = (\frac{1}{c}\frac{\partial}{\partial t}, -\nabla)$ is the covariant four-gradient,
- $\partial_\mu = (\frac{1}{c}\frac{\partial}{\partial t}, \nabla)$ is the contravariant four-gradient,

and so on.

To see our Lagrangian at work, we will now derive the vacuum Maxwell equations, eq. 2.79, from the Lagrangian, eq. 2.86, and the Lorenz gauge

$$\partial_\mu A^\mu = \nabla \cdot A + \tfrac{1}{c^2}\dot{\Phi} = 0. \tag{2.88}$$

The Euler-Lagrange equation for the field A_κ reads

$$\frac{\partial \mathcal{L}_A}{\partial A_\kappa} = \partial_\lambda \left(\frac{\partial \mathcal{L}_A}{\partial(\partial_\lambda A_\kappa)} \right). \tag{2.89}$$

We first calculate the left-hand side. Since $\mathcal{L}_A$ as a function of A_κ and of $\partial_\lambda A_\kappa$ does in fact only depend on $\partial_\lambda A_\kappa$, the result is zero,

$$\begin{aligned}
\frac{\partial \mathcal{L}_A}{\partial A_\kappa} &= -\frac{1}{4\mu_0} \frac{\partial F_{\mu\nu} F^{\mu\nu}}{\partial A_\kappa} \\
&= -\frac{1}{4\mu_0} \frac{\partial (\partial_\mu A_\nu - \partial_\nu A_\mu)(\partial^\mu A^\nu - \partial^\nu A^\mu)}{\partial A_\kappa} \\
&= 0.
\end{aligned} \tag{2.90}$$

Next we calculate the right-hand side,

$$\begin{aligned}
\frac{\partial \mathcal{L}_A}{\partial(\partial_\lambda A_\kappa)} &= -\frac{1}{4\mu_0} \frac{\partial F_{\mu\nu} F^{\mu\nu}}{\partial(\partial_\lambda A_\kappa)} \\
&= -\frac{1}{4\mu_0} \frac{\partial}{\partial(\partial_\lambda A_\kappa)} (\partial_\mu A_\nu - \partial_\nu A_\mu)(\partial^\mu A^\nu - \partial^\nu A^\mu) \\
&= -\tfrac{1}{4\mu_0} \Big(\big(1 \cdot (\partial^\lambda A^\kappa - \partial^\kappa A^\lambda) - 1 \cdot (\partial^\kappa A^\lambda - \partial^\lambda A^\kappa)\big) \\
&\qquad + \big((\partial_\lambda A_\kappa - \partial_\kappa A_\lambda) \cdot 1 - (\partial_\kappa A_\lambda - \partial_\lambda A_\kappa) \cdot 1\big) \Big) \\
&= -\tfrac{1}{2\mu_0} (\partial^\lambda A^\kappa - \partial^\kappa A^\lambda + \partial_\lambda A^\kappa - \partial_\kappa A_\lambda) \\
&= \tfrac{1}{\mu_0} (\partial^\kappa A^\lambda - \partial^\lambda A^\kappa).
\end{aligned} \tag{2.91}$$

So our Euler-Lagrange equation reads

$$0 = \partial_\lambda (\partial^\kappa A^\lambda - \partial^\lambda A^\kappa) = \partial^\kappa \partial_\lambda A^\lambda - \Box A^\kappa. \tag{2.92}$$

Since $\partial_\lambda A^\lambda = 0$ due to the Lorenz gauge, we arrive at $\Box A^\kappa = 0$ (or $\Box A_\kappa(x,t) = 0$ in the notation used in the previous subsection), which is equivalent to the vacuum Maxwell equations, eq. 2.79.

To complete our considerations of the Lagrangian, and because we'll need it in the next subsection, we now express our Lagrangian in terms of the electric field $E = -\nabla\Phi - \dot{A}$ and of the magnetic flux density $B = \nabla \times A$. (If you don't want to go through these lenghty calculations, you can skip to the result $\mathcal{L}_A = \frac{1}{2\mu_0} \left(\frac{1}{c^2} E^2 - B^2\right)$, eq. 2.97, at the end of this subsection.)

We start by expressing $\mathcal{L}_A$ in terms of derivatives of A^μ,

$$\begin{aligned}
\mathcal{L}_A &= -\tfrac{1}{4\mu_0} F_{\mu\nu} F^{\mu\nu} \\
&= -\tfrac{1}{4\mu_0} (\partial_\mu A_\nu - \partial_\nu A_\mu)(\partial^\mu A^\nu - \partial^\nu A^\mu) \\
&= -\tfrac{1}{4\mu_0} (\partial_\mu A_\nu \, \partial^\mu A^\nu - \partial_\mu A_\nu \, \partial^\nu A^\mu - \partial_\nu A_\mu \, \partial^\mu A^\nu + \partial_\nu A_\mu \, \partial^\nu A^\mu) \\
&= -\tfrac{1}{2\mu_0} (\partial_\mu A_\nu \partial^\mu A^\nu - \partial_\mu A_\nu \, \partial^\nu A^\mu).
\end{aligned} \tag{2.93}$$

Here it makes sense to switch off Einstain summation convention and to look at the individual components. It is worth noting that raising or lowering an index of a component reverses its

sign for spatial indices, but it doesn't change the sign for temporal ones.

$$
\begin{aligned}
\partial_\mu A_\nu\, \partial^\mu A^\nu &= \partial_t A_t\, \partial^t A^t \\
&\quad + \partial_t A_x\, \partial^t A^x + \partial_t A_y\, \partial^t A^y + \partial_t A_z\, \partial^t A^z \\
&\quad + \partial_x A_t\, \partial^x A^t + \partial_y A_t\, \partial^y A^t + \partial_z A_t\, \partial^z A^t \\
&\quad + \partial_x A_x\, \partial^x A^x + \partial_y A_x\, \partial^y A^x + \partial_z A_x\, \partial^z A^x \\
&\quad + \partial_x A_y\, \partial^x A^y + \partial_y A_y\, \partial^y A^y + \partial_z A_y\, \partial^z A^y \\
&\quad + \partial_x A_z\, \partial^x A^z + \partial_y A_z\, \partial^y A^z + \partial_z A_z\, \partial^z A^y \\
&= \partial_t A_t\, \partial_t A_t \\
&\quad - \partial_t A_x\, \partial_t A_x - \partial_t A_y\, \partial_t A_y - \partial_t A_z\, \partial_t A_z \\
&\quad - \partial_x A_t\, \partial_x A_t - \partial_y A_t\, \partial_y A_t - \partial_z A_t\, \partial_z A_t \\
&\quad + \partial_x A_x\, \partial_x A_x + \partial_y A_x\, \partial_y A_x + \partial_z A_x\, \partial_z A_x \\
&\quad + \partial_x A_y\, \partial_x A_y + \partial_y A_y\, \partial_y A_y + \partial_z A_y\, \partial_z A_y \\
&\quad + \partial_x A_z\, \partial_x A_z + \partial_y A_z\, \partial_y A_z + \partial_z A_z\, \partial_z A_y \\
&= \tfrac{1}{c^4}\dot\Phi^2 - \tfrac{1}{c^2}\dot A^2 - \tfrac{1}{c^2}(\nabla\Phi)^2 \\
&\quad + (\partial_x A_x)^2 + (\partial_y A_x)^2 + (\partial_z A_x)^2 \\
&\quad + (\partial_x A_y)^2 + (\partial_y A_y)^2 + (\partial_z A_y)^2 \\
&\quad + (\partial_x A_z)^2 + (\partial_y A_z)^2 + (\partial_z A_z)^2,
\end{aligned}
\tag{2.94}
$$

$$
\begin{aligned}
\partial_\mu A_\nu\, \partial^\nu A^\mu &= \partial_t A_t\, \partial^t A^t \\
&\quad + \partial_t A_x\, \partial^x A^t + \partial_t A_y\, \partial^y A^t + \partial_t A_z\, \partial^z A^t \\
&\quad + \partial_x A_t\, \partial^t A^x + \partial_y A_t\, \partial^t A^y + \partial_z A_t\, \partial^t A^z \\
&\quad + \partial_x A_x\, \partial^x A^x + \partial_y A_x\, \partial^x A^y + \partial_z A_x\, \partial^x A^z \\
&\quad + \partial_x A_y\, \partial^y A^x + \partial_y A_y\, \partial^y A^y + \partial_z A_y\, \partial^y A^z \\
&\quad + \partial_x A_z\, \partial^z A^x + \partial_y A_z\, \partial^z A^y + \partial_z A_z\, \partial^y A^z \\
&= \partial_t A_t\, \partial_t A_t \\
&\quad - \partial_t A_x\, \partial_x A_t - \partial_t A_y\, \partial_y A_t - \partial_t A_z\, \partial_z A_t \\
&\quad - \partial_x A_t\, \partial_t A_x - \partial_y A_t\, \partial_t A_y - \partial_z A_t\, \partial_t A_z \\
&\quad + \partial_x A_x\, \partial_x A_x + \partial_y A_x\, \partial_x A_y + \partial_z A_x\, \partial_x A_z \\
&\quad + \partial_x A_y\, \partial_y A_x + \partial_y A_y\, \partial_y A_y + \partial_z A_y\, \partial_y A_z \\
&\quad + \partial_x A_z\, \partial_z A_x + \partial_y A_z\, \partial_z A_y + \partial_z A_z\, \partial_y A_z \\
&= \tfrac{1}{c^4}\dot\Phi^2 - \tfrac{2}{c^2}\dot A \cdot (\nabla\Phi) \\
&\quad + (\partial_x A_x)^2 + 2\,\partial_y A_x\, \partial_x A_y + 2\,\partial_z A_x\, \partial_x A_z \\
&\quad + (\partial_y A_y)^2 + 2\,\partial_z A_y\, \partial_y A_z + (\partial_z A_z)^2.
\end{aligned}
\tag{2.95}
$$

The difference of the two terms reads

$$
\begin{aligned}
-2\mu_0 \mathcal{L}_A &= \partial_\mu A_\nu\, \partial^\mu A^\nu - \partial_\mu A_\nu\, \partial^\nu A^\mu \\
&= \tfrac{1}{c^4}\dot\Phi^2 - \tfrac{1}{c^2}\dot A^2 - \tfrac{1}{c^2}(\nabla\Phi)^2 \\
&\quad + (\partial_x A_x)^2 + (\partial_y A_x)^2 + (\partial_z A_x)^2 \\
&\quad + (\partial_x A_y)^2 + (\partial_y A_y)^2 + (\partial_z A_y)^2 \\
&\quad + (\partial_x A_z)^2 + (\partial_y A_z)^2 + (\partial_z A_z)^2
\end{aligned}
$$

$$
\begin{aligned}
&- \tfrac{1}{c^4}\dot{\Phi}^2 + \tfrac{2}{c^2}\dot{A}\cdot(\nabla\Phi) \\
&- (\partial_x A_x)^2 - 2\,\partial_y A_x\,\partial_x A_y - 2\,\partial_z A_x\,\partial_x A_z \\
&- (\partial_y A_y)^2 - 2\,\partial_z A_y\,\partial_y A_z - (\partial_z A_z)^2 \\
= &-\tfrac{1}{c^2}\dot{A}^2 + \tfrac{2}{c^2}\dot{A}\cdot(\nabla\Phi) - \tfrac{1}{c^2}(\nabla\Phi)^2 \\
&+ (\partial_y A_x)^2 - 2\,\partial_y A_x\,\partial_x A_y + (\partial_x A_y)^2 \\
&+ (\partial_z A_x)^2 - 2\,\partial_z A_x\,\partial_x A_z + (\partial_x A_z)^2 \\
&+ (\partial_z A_y)^2 - 2\,\partial_z A_y\,\partial_y A_z + (\partial_y A_z)^2 \\
= &-\tfrac{1}{c^2}(\dot{A} - \nabla\Phi)^2 \\
&+ (\partial_y A_x - \partial_x A_y)^2 + (\partial_z A_x - \partial_x A_z)^2 + (\partial_z A_y - \partial_y A_z)^2 \\
= &-\tfrac{1}{c^2}E^2 + (\nabla\times A)^2 \\
= &\, B^2 - \tfrac{1}{c^2}E^2.
\end{aligned}
\tag{2.96}
$$

Thus our Lagrangian in terms of E and B reads

$$
\mathcal{L}_A = \tfrac{1}{2\mu_0}\left(\tfrac{1}{c^2}E^2 - B^2\right), \tag{2.97}
$$

or, with $\varepsilon_0 = \frac{1}{\mu_0 c^2}$,

$$
\mathcal{L}_A = \tfrac{1}{2}\left(\varepsilon_0 E^2 - \tfrac{1}{\mu_0}B^2\right). \tag{2.98}
$$

To get this result, we didn't need to use the Lorenz gauge $\partial_\mu A^\mu = 0$. It holds in any gauge.

2.3.3 Hamiltonian Formulation of Classical Electrodynamics

We are now ready for taking the last step in our preparation of classical electrodynamics for quantisation. We perform a Legendre transformation and derive the Hamiltonian of the electromagnetic field in the vacuum from its Lagrangian.

Again, to be precise, our Hamiltonian is a *Hamiltonian density* for fields. A *Hamiltonian function* for classical particles or a *Hamiltonian operator* for quantum wave functions do not make sense for a classical electromagnetic field. (Nevertheless we will derive both in the next chapter when quantising the electromagnetic field.)

The Legendre transformation reads

$$
\mathcal{H}_A = P^\nu\,\partial_0 A_\nu - \mathcal{L}_A, \tag{2.99}
$$

where

$$
P^\nu = \frac{\partial\mathcal{L}_A}{\partial(\partial_0 A_\nu)} \tag{2.100}
$$

is the conjugate momentum of A_ν.

Since we already know the Lagrangian $\mathcal{L}_A$ in terms of E and B, we proceed by expressing P^ν in terms of E and B as well.

$$
\begin{aligned}
P^\nu &= \frac{\partial\mathcal{L}_A}{\partial(\partial_0 A_\nu)} \\
&= \frac{\partial\left(-\frac{1}{4\mu_0}F_{0n}F^{0n}\right)}{\partial(\partial_0 A_\nu)} \\
&= \frac{\partial\left(-\frac{1}{4\mu_0}(\partial_0 A_\nu - \partial_\nu A_0)(\partial^0 A^\nu - \partial^\nu A^0)\right)}{\partial(\partial_0 A_\nu)}
\end{aligned}
$$

$$= -\tfrac{1}{4\mu_0} \frac{\partial(\partial_\mu A_\nu\, \partial^\mu A^\nu - \partial_\mu A_\nu\, \partial^\nu A^\mu - \partial_\nu A_\mu\, \partial^\mu A^\nu + \partial_\nu A_\mu\, \partial^\nu A^\mu)}{\partial(\partial_0 A_\nu)}$$
$$= -\tfrac{1}{4\mu_0} \frac{\partial(2\partial_0 A_\nu\, \partial_0 A_\nu - 2\partial_0 A_\nu\, \partial_\nu A_0 - 2\partial_\nu A_0\, \partial_0 A_\nu)}{\partial(\partial_0 A_\nu)}$$
$$= \tfrac{1}{\mu_0}\,(\partial_0 A_\nu - \partial_\nu A_0). \tag{2.101}$$

Up to this point we didn't make use of any gauge condition. Now we introduce, in addition to the Lorenz gauge $\nabla \cdot A + \frac{1}{c^2}\dot{\Phi}$, yet another gauge condition $\Phi = 0$. (Together with the Lorenz gauge this also implies $\nabla \cdot A = 0$. This additional gauge condition is not Lorentz-invariant.) Then $A_0 = 0$, and $E = -\nabla\Phi - \dot{A}$ simplifies to $E = -\dot{A}$. Thus we obtain

$$P^\nu = \tfrac{1}{\mu_0}\,(\partial_0 A_\nu - \partial_\nu A_0) = \tfrac{1}{\mu_0 c}\dot{A}_\nu = -\tfrac{1}{\mu_0 c}E \tag{2.102}$$

and

$$P^\nu\, \partial_0 A_\nu = \tfrac{1}{\mu_0 c}\dot{A}\, \tfrac{1}{c}\dot{A} = (-\tfrac{1}{\mu_0 c}E)(-\tfrac{1}{c}E) = \tfrac{1}{\mu_0 c^2}E^2. \tag{2.103}$$

Putting everything together, we obtain the Hamiltonian of the electromagnetic field in the vacuum, expressed in terms of E and B,

$$\begin{aligned}\mathcal{H}_A &= P^\nu\, \partial_0 A_\nu - \mathcal{L}_A \\ &= \tfrac{1}{2\mu_0 c^2}E^2 + \tfrac{1}{2}\big(B^2 - \tfrac{1}{\mu_0 c^2}E^2\big) \\ &= \tfrac{1}{2\mu_0}\big(\tfrac{1}{c^2}E^2 + B^2\big) \\ &= \tfrac{1}{2}\big(\varepsilon_0 E^2 + \tfrac{1}{\mu_0}B^2\big).\end{aligned} \tag{2.104}$$

For later use, we also express the Hamiltonian in terms of A and $\dot{A}$,

$$\mathcal{H}_A = \tfrac{1}{2\mu_0}\big(\tfrac{1}{c^2}\dot{A}^2 + (\nabla \times A)^2\big). \tag{2.105}$$

There is an interesting parallel between classical mechanics and classical electrodynamics. In classical mechanics, the Lagrangian and Hamiltonian functions read

$$L = T - V, \qquad H = T + V, \tag{2.106}$$

where T is the kinetic energy and V is the potential energy.

In classical electrodynamics the Lagrangian and Hamiltonian densities read

$$2\mu_0\mathcal{L}_A = \tfrac{1}{c^2}E^2 - B^2, \qquad 2\mu_0\mathcal{H}_A = \tfrac{1}{c^2}E^2 + B^2. \tag{2.107}$$

This suggests that $\frac{1}{c^2}E^2$ plays the role of a kinetic energy, and B^2 plays the role of a potential energy.

In fact in the next chapter, when we *quantise* the electromagnetic field, we will identify A and $\dot{A}$ as a pair of canonical coordinates. Then A will play the role of a coordinate, $\dot{A} = -E$ will be a momentum, $\frac{1}{2}|\dot{A}^2| = \frac{1}{2}E^2$ will be a kinetic energy, and $\frac{1}{2}k^2|A^2| = \frac{1}{2}B^2$ will implement the potential of a harmonic oscillator, which will give rise to the photon.

▶ **Exercise 2.16:** Derive the vacuum Maxwell equations as the Hamiltonian equations of motion (for fields) from their Hamiltonian density, eq. 2.104.

Chapter 3

Many Particles

This chapter addresses the peculiarities of many-particle quantum systems, which are very different from just multiple copies of single-particle quantum systems. After an introduction to *second quantisation*, where we encounter *creation* and *annihilation operators* and the *particle-number representation*, we will generalise our mathematical and numerical tools from one particle to many particles, thus re-developing quantum electrodynamics. Finally we'll have a brief look on the traditional, perturbative approach and its Feynman diagrams.

3.1 Mathematical Description of Many-Particle Quantum Systems

From the previous chapter we know how to describe a single quantum particle. In the non-relativistic case this was done via a complex-valued wave function and a hyperbolic partial differential equation, the Schrödinger equation. In the relativistic case the particle is described by a spinor-valued wave function and the Dirac equation, a particular Schrödinger equation which is Lorentz-invariant.

From classical mechanics we know that when we have a single particle, described by a vector, then we simply need two vectors to describe two particles. So we might conclude that we needed two complex-valued wave functions to describe two non-relativistic quantum particles, and two spinor-valued wave functions to describe two relativistic quantum particles.

Nature tells us that this is wrong in two ways. In many-particle quantum systems two new phenomena can be observed, *identical particles* and the *creation and annihilation of particles*.

3.1.1 Identical Particles

When we describe two quantum particles, for instance two electrons, by one wave function each, and we implement their Coulomb interaction by adding a potential $V(x_1, x_2) \sim \frac{1}{|x_1 - x_2|}$ to the Hamiltonian, we can calculate their scattering. Then the result is similar to the scattering of two classical particles, for instance two billard balls.

Scattering experiments with actual electrons reveal a very different result. For example, you can let two billard balls collide in such a way that the collision causes a turn by 90° for each of the balls. This is not possible when colliding electrons with the same spin. They avoid that angle. Why?

It turns out that we can describe the behaviour of electrons correctly when we assume that they are *identical*. They are not just alike, like coins of the same currency and value, but indeed identical, like equal amounts of money on your bank account. You can mark coins, so you can verify whether they were swapped or not. But you cannot mark two "different" Euros (or whatever currency you are using) on your bank account. If you swap them, *nothing* changes [8].

To describe identical particles mathematically, we must ensure that their joint wave function has some symmetry property with respect to permutations of the particles. When you swap two of them, physics must not change.

"Physics must not change" does not mean that the wave function itself must not change. There is a degree of freedom in the wave function which doesn't describe physics, its complex phase. It is acceptable when the joint wave function gets multiplied by an overall factor $\varphi \in \mathbb{C}$ with $|\varphi| = 1$ upon a permutation of the particles, since such a factor doesn't have any physical implications. (In mathematical physics, the state of a quantum system is defined as a *one-dimensional subspace* of the Hilbert space rather than a wave function of norm 1 [7, § 28.1.1]. The wave function we use in actual calculations is just a representative of the subspace.)

Actually we can already tell something about that φ. Imagine that we swap the same two particles two times. Then they will have their original places again, which is mathematically equivalent to doing nothing at all. After two transpositions, the wave functions must be identically the same as before, this time *including* the complex phase factor.

Since each transposition brings a factor of φ, this implies that $\varphi^2 = 1$, and thus $\varphi = \pm 1$.

It turns out that a theory which sets $\varphi = -1$ correctly describes the behaviour of electrons, positrons, muons, quarks and several other particles. For another family of particles, including *photons* which we'll encounter soon, we must set $\varphi = 1$ to make theory coincide with experiments.

A joint wave function which acquires a factor of -1 upon transposition of two particles is called *antisymmetric*. Then the particles are called *fermions* (after Enrico Fermi). A joint wave function which does not change upon transposition is called *symmetric*. Then the particles are called *bosons* (after Satyendranath Bose).

This explains why electrons with the same spin cannot scatter in an angle of 90°. The joint wave function of two scattering fermions, such as electrons, must be antisymmetric with respect to a transposition of the particles, i. e. change its sign. This implies that it must be zero in the bisecting plane between the electrons, where they had to fly when they were scattered by 90°.

▶ **Exercise 3.1:** Apply the methods developed in chapter 2 to simulate the "naïve" approach to scattering of two non-relativistic quantum particles by adding a Coulomb potential $V(x_1, x_2) \sim \frac{1}{|x_1 - x_2|}$ to the Hamiltonian, and verify that they behave indeed similarly to classical particles. (Only in the simulation, of course. In reality, they don't.)

3.1.2 Creation and Annihilation of Particles

Experiments have revealed yet another feature of quantum particles which we need to take into account when describing them mathematically. They can be created and annihilated, or turned into another sort of particle.

This implies that we cannot rely on the number of particles remaining constant. In particular, we cannot describe a system of N particles by using a Hilbert space of N independent wave

functions, interacting somehow. Instead, the N particles are just *one possible state* of the total system. Any other number of particles is a valid state as well. And the joint wave function of the quantum system takes each of those states as a valid basis state and spreads over all of them. That's what quantum wave functions do when offered a set of basis states.

This makes our Hilbert space much bigger than N independent wave functions.

To illustrate this, imagine two (distinguishable) quantum particles ψ and χ, which can take n states, each, for instance n positions in space. Then their wave functions have n components ψ_i, χ_i for $i \in \{1, \ldots, n\}$, each, which describe the amplitudes to find that particle at the ith position,

$$\psi = \begin{pmatrix} \psi_1 \\ \vdots \\ \psi_n \end{pmatrix}, \qquad \chi = \begin{pmatrix} \chi_1 \\ \vdots \\ \chi_n \end{pmatrix}. \tag{3.1}$$

Even this is not straightforward to imagine, for it includes cases where, say, ψ is at two positions at the same time.

Now one would, naïvely, expect the joint wave function Ψ to have $2n$ components,

$$\Psi = \begin{pmatrix} \psi_1 \\ \vdots \\ \psi_n \\ \chi_1 \\ \vdots \\ \chi_n \end{pmatrix} \qquad \text{(wrong)}. \tag{3.2}$$

Instead, each combination of ψ at some positions and χ at some other positions is a new basis state. The joint system can spread over all of them,

$$\Psi = \begin{pmatrix} \Psi_{1,1} \\ \vdots \\ \Psi_{n,1} \\ \vdots \\ \Psi_{1,n} \\ \vdots \\ \Psi_{n,n} \end{pmatrix} \qquad \text{(correct)}. \tag{3.3}$$

Each component $\Psi_{i,j}$ of Ψ has two indices i, j, where i labels the position of the ψ particle and j labels the position of the χ particle. Instead of $2n$ components, this vector has n^2 ones.

One example for a possible state is $\Psi_{1,7} = \frac{3}{5}$, $\Psi_{2,3} = \frac{4}{5}$, and $\Psi_{i,j} = 0$ for any other combination of i and j. This describes a mixed state where the amplitude to find ψ at position 1 and χ at position 7 in the same measurement is $\frac{3}{5}$, the amplitude to find ψ at position 2 and χ at position 3 in the same measurement is $\frac{4}{5}$, but the amplitude to measure anything else, including cases like ψ at position 1 and χ at position 3, is zero.

States like the example above are hard to write down as vectors. Here the bra-ket notation, known from nonrelativistic quantum theory, proves convenient. We write the vector as a linear combination of base vectors, which in turn are written as ket vectors with just the indices inside. Then the above example reads

$$\Psi = \tfrac{3}{5} \left|1, 7\right\rangle + \tfrac{4}{5} \left|2, 3\right\rangle. \tag{3.4}$$

This becomes even more important when the states of the particles, labelled $1, \ldots, n$ in this example, are no longer described by a discrete variable, but by a continuous one such as a position $x \in \mathbb{R}$ (or $x \in \mathbb{R}^3$ or even worse). Then the sum turns into an integral, for instance

$$\Psi = \int dx_\psi \int dx_\chi \left(\tfrac{3}{5} \delta(x_\psi - 1)\, \delta(x_\chi - 7) + \tfrac{4}{5} \delta(x_\psi - 2)\, \delta(x_\chi - 3) \right) |x_\psi, x_\chi\rangle \,. \tag{3.5}$$

Now imagine that our maximum number of particles is no longer 2, but infinite. Then we have arrived at our mathematical description of a many-particle quantum system. (Fortunately at least this infinity is a countable one, not a continuum.)

3.1.3 Creation and Annihilation of Identical Particles

So far our description of a many-particle quantum system only covers distinguishable particles. The next problem is to adapt it to describe identical particles.

The solution is to restrict our description to the subspace of the states which comply with the symmetry rules. How can we implement these rules?

A given two-particle state

$$\Psi = \begin{pmatrix} \Psi_{1,1} \\ \vdots \\ \Psi_{n,1} \\ \vdots \\ \Psi_{1,n} \\ \vdots \\ \Psi_{n,n} \end{pmatrix} = \sum_{i,j} \Psi_{i,j} \, |x_i, x_j\rangle \tag{3.6}$$

is symmetric when it doesn't change if we transpose the two particles,

$$\Psi_{i,j} = \Psi_{j,i} \quad \forall i, j, \tag{3.7}$$

and it is antisymmetric when it changes its sign upon transposition,

$$\Psi_{i,j} = -\Psi_{j,i} \quad \forall i, j. \tag{3.8}$$

This can be generalised to an arbitrary number N of particles. In the symmetric (bosonic) case this means that

$$\Psi_{i_1,\ldots,i_N} = \Psi_{P(i_1,\ldots,i_N)} \quad \forall i_1, \ldots, i_N \tag{3.9}$$

for all *permutations* P which mix the indices $i_1, \ldots, i_N$.

In the antisymmetric (fermionic) case we get a factor -1 for each transposition of two particles. Every permutation P of the particles can be decomposed into transpositions. It can be shown that for a given permutation P the number of its transpositions is either always an even number, or always an odd one. Thus we can speak of *even* and *odd permutations*.

For our antisymmetric many-particle states this means that they acquire a minus sign when the particles are mixed by an odd permutation, and they don't change when mixed by an even permutation,

$$\Psi_{i_1,\ldots,i_N} = \operatorname{sgn}(P)\, \Psi_{P(i_1,\ldots,i_N)} \quad \forall i_1, \ldots, i_N. \tag{3.10}$$

The symbol $\operatorname{sgn}(P)$ is called the *sign* (or *parity*) *of the permutation*. It is -1 for odd permutations and $+1$ for even ones, including the identity. (There are several common notations for the sign of a permutation.)

There is one important special situation. When we try to place two fermions *in the same state*, and we swap them, their joint wave function cannot change. On the other hand it must reverse its sign because of the antisymmetry. This is only possible when the joint wave function is identically zero. This means that it is not possible to have two fermions in precisely the same state. (In case you object that they *can* be in the same state when they are at different positions, remember that the position counts as a state, too.) This is called the *Pauli exclusion principle*.

3.1.4 Fock Space

The Schrödinger equations we have seen so far just propagate a single particle, but they don't mix the states of "different" (identical) particles. This ensures that when the initial state has the correct symmetry with respect to permutation of the particles, then the propagated state still has it.

This, however, is not enough to describe nature. Experiments have shown that quantum particles can be created, annihilated, or transformed into a different type of particle. How to set up a Schrödinger equation which describes these effects?

When we set up a Haniltonian which mixes particles we must ensure that it maps symmetric states to symmetric states and antisymmetric states to antisymmetric states. While this can be done in the basis we had set up in subsection 3.1.2, it is much easier to use a "toolbox" whose tools respect the symmetries automatically.

For this purpose the basis of combinations of "single particles" isn't well-suited. It contains too many states which aren't implemented by nature anyway, and we need to be careful to stay in the correct subspace all the time. Instead we switch to a basis which just contains the relevant states, the *Fock states*, which span a *Fock space*. This representation of many-particle quantum states is called the *occupation number representation*.

Each Fock state represents a state with a specific number of particles in a given state. What does that mean?

Let's revisit the example from subsection 3.1.2,

$$\Psi = \tfrac{3}{5} \left|1,7\right\rangle + \tfrac{4}{5} \left|2,3\right\rangle . \tag{3.11}$$

This state is neither symmetric nor antisymmetric, so it isn't suited to describe a system of two identical bosons or fermions. However we can *symmetrise* this state, i. e. project it on a symmetric or antisymmetric subspace.

Later, we'll mostly deal with the fermionic (antisymmetric) case, so let's focus on the bosonic (symmetric) case for now. Then the symmetrisation yields a new wave function,

$$\Psi_+ = \tfrac{1}{\sqrt{2}} \left(\tfrac{3}{5} \left|1,7\right\rangle + \tfrac{4}{5} \left|2,3\right\rangle + \tfrac{3}{5} \left|7,1\right\rangle + \tfrac{4}{5} \left|3,2\right\rangle \right) . \tag{3.12}$$

How to express this state in the Fock basis? It is a superposition of two symmetric two-particle states,

$$\Psi_+ = \underbrace{\tfrac{3}{5} \tfrac{1}{\sqrt{2}} \left(\left|1,7\right\rangle + \left|7,1\right\rangle \right)}_{=: \left|2_{1,7}\right\rangle} + \underbrace{\tfrac{4}{5} \tfrac{1}{\sqrt{2}} \left(\left|2,3\right\rangle + \left|3,2\right\rangle \right)}_{=: \left|2_{2,3}\right\rangle} . \tag{3.13}$$

$|2_{1,7}\rangle$ is a symmetric two-particle state with one boson – no matter which one – at position 1 and the other one at position 7. (As in subsection 3.1.2, "position" is just an example for a quantum state of the particle, an eigenstate of a quantum observable. It can also be a momentum, an angular momentum, or whatever. These observables are often called *quantum numbers*.)

The pure two-particle state $|2_{1,7}\rangle$ is *not* the same as a superpositon of two one-particle states,

$$|2_{1,7}\rangle = \tfrac{1}{\sqrt{2}}\left(|1,7\rangle + |7,1\rangle\right) \neq \tfrac{1}{\sqrt{2}}\left(|1\rangle + |7\rangle\right) = \tfrac{1}{\sqrt{2}}\left(|1_1\rangle + |1_7\rangle\right). \tag{3.14}$$

Also, each Fock state is a basis state which cannot be expressed via the other basis states,

$$|2_{1,7}\rangle + |2_{2,3}\rangle \neq |2_{1,3}\rangle + |2_{2,7}\rangle\,. \tag{3.15}$$

In many cases the state under consideration is clear from the context (for instance, a momentum eigenstate for a fixed momentum p), and the question is only how many particles occupy that state. In such cases the indices which denote the state are usually dropped, and the Fock states just read $|1\rangle$ for a one-particle state, $|2\rangle$ for a two-particle state, etc.

When there are just a few quantum numbers – for instance, if we restrict the number of "positions" in the example above to a maximum of 7 – then the position of the number inside the brackets is usually used to denote the quantum number, and the number itself denotes the number of particles in that state,

$$|2_{1,7}\rangle = |1,0,0,0,0,0,1\rangle\,, \tag{3.16}$$
$$|2_{2,3}\rangle = |0,1,1,0,0,0,0\rangle\,. \tag{3.17}$$

All this means that when you see something like $|2,3\rangle$ you should carefully check the context for what kind of object this notation currently stands for.

3.1.5 The Vacuum State

In fact the Fock basis is *not* a subset of the many-particle basis developed in subsection 3.1.2, but it contains one additional basis state, the *vacuum state*.

The vacuum state is always denoted $|0\rangle$. It is *not* the same as the zero vector. It is a valid wave function, a valid state of the many-particle system. It can take a complex phase as a prefactor, and it can be mixed with other states like any other basis vector. The vacuum state adds one dimension to the (infinitely-dimensional) Fock space.

Since the vacuum state doesn't contain any particles which could have quantum numbers, there is always just one vacuum state in Fock space.

Let's embrace this opportunity to understand the structure of Fock space by counting the number of N-boson states.

The number of one-particle states equals the number of orthogonal states a single particle can take (which can be an infinite number). When there are, for instance, 3 such states, then there are 3 orthogonal one-particle states, $|1,0,0\rangle$, $|0,1,0\rangle$, and $|0,0,1\rangle$. (Another notation would be $|1_1\rangle$, $|1_2\rangle$, and $|1_3\rangle$.)

The number of two-particle states is bigger. When there are, again, 3 orthogonal states a particle can take, then there are, in the bosonic case, 6 orthogonal two-particle states, $|2,0,0\rangle$, $|0,2,0\rangle$, $|0,0,2\rangle$, $|1,1,0\rangle$, $|0,1,1\rangle$, and $|1,0,1\rangle$ (or $|2_{1,1}\rangle$, $|2_{2,2}\rangle$, $|2_{3,3}\rangle$, $|2_{1,2}\rangle$, $|2_{2,3}\rangle$, and $|2_{1,3}\rangle$).

Staying in this example, there are 10 orthogonal three-boson states, $|3,0,0\rangle$, $|0,3,0\rangle$, $|0,0,3\rangle$, $|2,1,0\rangle$, $|2,0,1\rangle$, $|1,2,0\rangle$, $|0,2,1\rangle$, $|1,0,2\rangle$, $|0,1,2\rangle$, and $|1,1,1\rangle$.

To describe a state with up to three bosons which can take one of three states each, we need $1+3+6+10=20$ single-particle wave functions.

In general, the number of N-boson states where each boson can take n states, is given by the binomial coefficient

$$\left(\begin{array}{c} n+N-1 \\ N \end{array} \right). \tag{3.18}$$

▶ **Exercise 3.2:** Count the number of N-particle states where each particle can take n states in the fermionic (antisymmetric) case.

Hint: Fermions obey the Pauli exclusion principle.

Solution: Due to the Pauli exclusion principle it is not allowed to have two fermions in the same state. Thus we must distribute the N fermions over the n available states, and the solution is $\binom{n}{N}$ for $N \leq n$, and otherwise zero. In particular there are no fermionic N-particle states when N is bigger than the number n of states a single particle can take.

▶ **Exercise 3.3:** Count the number of N-particle states where each particle can take n states in the case of distinguishable particles.

Solution: For each new particle we must "insert" the vector of possible states into the already existing vector, which means to multiply the number of states by n. This yields n^N states for N distinguishable particles.

3.2 Many-Particle Operators

We are on the verge of extending quantum theory from one particle to many identical particles whose number is not constant, but it is a quantum property itself. As always when extending a well-known theory beyond its area of application, it is not *a priori* clear how the new theory will look like. We need to guess.

In the transition from Newton's classical physics to quantum theory this guess is named *quantisation*. We substitute two noncommutative operators – the differential operator $p = -i\hbar\frac{\partial}{\partial x}$ and the multiplication operator x – for the commutative variables p and x, which describe the state of a classical particle in the classical Hamiltonian function. From the result, the quantum Hamiltonian operator of the same system, we extract some data about the system. By comparing this theoretical prediction to experimental results we can check whether our guess was correct.

Now we are doing a similar guess again. We want to substitute many-particle operators for the single-particle ingredients of the quantum description of a single-particle system. We hope that the result describes the behaviour of a many-particle system correctly, i. e. in accordance with experiments. This second guess is called *second quantisation*.

To prepare this, we need to set up some many-particle operators which we can substitute into our equations. Since there are some fundamental differences between bosons and fermions, we'll do this separately for both types of particles.

3.2.1 Bosonic Number Operators

In the previous section we have set up the occupation number representation. Its basis states are the Fock states, which represent many-particle states with a well-defined number of particles. So it makes sense to construct an operator whose eigenstates are the Fock states with the particle numbers as the eigenvalues. This operator is called the *number operator*.

In the most simple case, where a bosonic system has just a single eigenstate, and the only question is how many bosons are in that state, we can write the number operator as a countably infinite matrix with respect to the Fock basis,

$$N = \begin{pmatrix} 0 & 0 & 0 & \dots & 0 & \dots \\ 0 & 1 & 0 & \dots & 0 & \dots \\ 0 & 0 & 2 & \dots & 0 & \dots \\ \vdots & \vdots & \vdots & \ddots & \vdots & \dots \\ 0 & 0 & 0 & \dots & m & \dots \\ \vdots & \vdots & \vdots & \vdots & \vdots & \ddots \end{pmatrix}. \tag{3.19}$$

Fortunately this simple case is all we need for doing quantum electrodynamics. (This is non-obvious and will be discussed in detail in section 3.3.) Nevertheless let's have a look at more general cases.

When the single-particle system has n eigenstates, then there are $\binom{n+N-1}{n}$ bosonic N-particle eigenstates. For example for $n = 2$ our basis has

1 eigenstate with 0 particles:	$\lvert 0\rangle$,
2 eigenstates with 1 particle:	$\lvert 1_{1,0}\rangle$, $\lvert 1_{0,1}\rangle$,
3 eigenstates with 2 particles:	$\lvert 2_{2,0}\rangle$, $\lvert 2_{1,1}\rangle$, $\lvert 2_{0,2}\rangle$,
4 eigenstates with 3 particles:	$\lvert 2_{3,0}\rangle$, $\lvert 2_{2,1}\rangle$, $\lvert 2_{1,2}\rangle$, $\lvert 2_{0,3}\rangle$,
and so on,	

and the matrix reads

$$N = \left(\begin{array}{c|ccc|ccc|c} 0 & 0 & 0 & 0 & 0 & 0 & 0 & \dots \\ \hline 0 & 1 & 0 & 0 & 0 & 0 & 0 & \dots \\ 0 & 0 & 1 & 0 & 0 & 0 & 0 & \dots \\ \hline 0 & 0 & 0 & 2 & 0 & 0 & 0 & \dots \\ 0 & 0 & 0 & 0 & 2 & 0 & 0 & \dots \\ 0 & 0 & 0 & 0 & 0 & 2 & 0 & \dots \\ \hline 0 & 0 & 0 & 0 & 0 & 0 & 3 & \dots \\ \vdots & \vdots & \vdots & \vdots & \vdots & \vdots & \vdots & \ddots \end{array}\right) . \tag{3.20}$$

In the most general case there can also be an infinite number of single-particle states.

The number operator is Hermitian; it is even real-valued and symmetric. Thus it is a good candidate for constructing operators for quantum observables, including the Hamiltonian.

3.2.2 Bosonic Ladder Operators

Now we can use the number operator to measure the number of particles in a given state, but we cannot change that number. For that purpose we set up a pair of two operators a_i^+, a_i, the so-called *creation and annihilation operators*, or *ladder operators*. They are defined by the property that they map one many-particle Fock state to the "next" one, i. e. a Fock state with one particle more or one particle less occupying a specific single-particle state.

In the simple case sketched above, where we examine bosons sharing just one single-particle state, the creation operator reads

$$a^+ |m\rangle = \sqrt{m+1}\ |m+1\rangle , \tag{3.21}$$

and the annihilation operator reads

$$a |m\rangle = \sqrt{m}\ |m-1\rangle . \tag{3.22}$$

In the slightly less simple case where each boson can be in one of n states, these operators operate on just one of the states, which is usually attached to the operator as an index,

$$a_4^+ |2_{1,7}\rangle = \sqrt{0+1}\ |3_{1,4,7}\rangle , \tag{3.23}$$

$$a_3 |2_{2,3}\rangle = \sqrt{2}\ |1_2\rangle . \tag{3.24}$$

($|2_{1,7}\rangle$ is a two-particle state, but it has no particle in the state number 4, thus the prefactor in eq. 3.23 reads $\sqrt{0+1}$, not $\sqrt{2+1}$. Analogous considerations hold for eq. 3.24.)

A creation operator (for the single-particle state number 3 in this example) acting on the vacuum state creates a particle,

$$a_3^+ |0\rangle = \sqrt{0+1}\ |1_3\rangle = |1_3\rangle , \tag{3.25}$$

and an annihilation operator acting on the vacuum state returns the zero vector,

$$a_3 |0\rangle = \sqrt{0}\ |0\rangle = 0. \tag{3.26}$$

Of course we cannot re-create the vacuum state from the zero vector. Whatever we multiply a zero with, it remains zero,

$$a_3^+ 0 = 0. \tag{3.27}$$

When we annihilate a many-particle state and immediately create it again, the state acquires the number of particles in it as a prefactor,

$$a_7^+ a_7 \left|2_{1,7}\right\rangle = a_7^+ \sqrt{1}\, \left|1_1\right\rangle = \sqrt{0+1}\,\sqrt{1}\, \left|2_{1,7}\right\rangle = 1 \cdot \left|2_{1,7}\right\rangle . \tag{3.28}$$

(Again, $\left|2_{1,7}\right\rangle$ is a two-particle state, but it has just one particle in the state number 7.)

This also holds for the vacuum state,

$$a_3^+ a_3 \left|0\right\rangle = 0 = 0 \cdot \left|0\right\rangle . \tag{3.29}$$

In other words, for a given state i, the combination $a_i^+ a_i$ of the ladder operators is a specialised number operator for that state,

$$a_i^+ a_i = N_i. \tag{3.30}$$

This is the reason behind the prefactors (featuring square roots) in front of the ladder operators.

For quantum electrodynamics we'll only need the simple case with just one single-particle state, shared by a potentially infinite number of bosons. In that case eq. 3.30 boils down to

$$a^+ a = N, \tag{3.31}$$

and we can write the ladder operators as – infinite – matrices

$$a^+ = \begin{pmatrix} 0 & 0 & 0 & \dots & 0 & \dots \\ \sqrt{1} & 0 & 0 & \dots & 0 & \dots \\ 0 & \sqrt{2} & 0 & \dots & 0 & \dots \\ 0 & 0 & \sqrt{3} & \dots & 0 & \dots \\ \vdots & \vdots & \vdots & \ddots & \vdots & \dots \\ 0 & 0 & 0 & \dots & \sqrt{m} & \dots \\ \vdots & \vdots & \vdots & \vdots & \vdots & \ddots \end{pmatrix}, \tag{3.32}$$

$$a = \begin{pmatrix} 0 & \sqrt{1} & 0 & 0 & \dots & 0 & \dots \\ 0 & 0 & \sqrt{2} & 0 & \dots & 0 & \dots \\ 0 & 0 & 0 & \sqrt{3} & \dots & 0 & \dots \\ \vdots & \vdots & \vdots & \vdots & \ddots & \vdots & \dots \\ 0 & 0 & 0 & 0 & \dots & \sqrt{m} & \dots \\ \vdots & \vdots & \vdots & \vdots & \vdots & \vdots & \ddots \end{pmatrix}. \tag{3.33}$$

These matrices are neither diagonal nor Hermitian, but a^+ is, as the notation suggests, the Hermitian conjugate of a, and vice versa. In the matrix of a^+ the first line is all zeroes; in the matrix of a the first column is all zeroes.

In the slightly less simple case of $n = 2$ single-particle eigenstates with the basis states

1 eigenstate with 0 particles:	$\left\|0\right\rangle$,
2 eigenstates with 1 particle:	$\left\|1_{1,0}\right\rangle$, $\left\|1_{0,1}\right\rangle$,
3 eigenstates with 2 particles:	$\left\|2_{2,0}\right\rangle$, $\left\|2_{1,1}\right\rangle$, $\left\|2_{0,2}\right\rangle$,
4 eigenstates with 3 particles:	$\left\|2_{3,0}\right\rangle$, $\left\|2_{2,1}\right\rangle$, $\left\|2_{1,2}\right\rangle$, $\left\|2_{0,3}\right\rangle$,
...	

the matrices read

$$a_1^+ = \left(\begin{array}{c|cc|ccc|c} 0 & 0 & 0 & 0 & 0 & 0 & \dots \\ \hline \sqrt{1} & 0 & 0 & 0 & 0 & 0 & \dots \\ 0 & 0 & 1 & 0 & 0 & 0 & \dots \\ \hline 0 & \sqrt{2} & 0 & 0 & 0 & 0 & \dots \\ 0 & 0 & \sqrt{1} & 0 & 0 & 0 & \dots \\ 0 & 0 & 0 & 0 & 0 & 1 & \dots \\ \hline \vdots & \vdots & \vdots & \vdots & \vdots & \vdots & \ddots \end{array}\right), \tag{3.34}$$

$$a_1 = \left(\begin{array}{c|cc|ccc|c} 0 & \sqrt{1} & 0 & 0 & 0 & 0 & \dots \\ \hline 0 & 0 & 0 & \sqrt{2} & 0 & 0 & \dots \\ 0 & 0 & 1 & 0 & \sqrt{1} & 0 & \dots \\ \hline 0 & 0 & 0 & 0 & 0 & 0 & \dots \\ 0 & 0 & 0 & 0 & 0 & 0 & \dots \\ 0 & 0 & 0 & 0 & 0 & 1 & \dots \\ \hline \vdots & \vdots & \vdots & \vdots & \vdots & \vdots & \ddots \end{array}\right). \tag{3.35}$$

$$a_2^+ = \left(\begin{array}{c|cc|ccc|c} 0 & 0 & 0 & 0 & 0 & 0 & \dots \\ \hline 0 & 1 & 0 & 0 & 0 & 0 & \dots \\ \sqrt{1} & 0 & 0 & 0 & 0 & 0 & \dots \\ \hline 0 & 0 & 0 & 1 & 0 & 0 & \dots \\ 0 & \sqrt{1} & 0 & 0 & 0 & 0 & \dots \\ 0 & 0 & \sqrt{2} & 0 & 0 & 0 & \dots \\ \hline \vdots & \vdots & \vdots & \vdots & \vdots & \vdots & \ddots \end{array}\right), \tag{3.36}$$

$$a_2 = \left(\begin{array}{c|cc|ccc|c} 0 & 0 & \sqrt{1} & 0 & 0 & 0 & \dots \\ \hline 0 & 1 & 0 & 0 & \sqrt{1} & 0 & \dots \\ 0 & 0 & 0 & 0 & 0 & \sqrt{2} & \dots \\ \hline 0 & 0 & 0 & 1 & 0 & 0 & \dots \\ 0 & 0 & 0 & 0 & 0 & 0 & \dots \\ 0 & 0 & 0 & 0 & 0 & 0 & \dots \\ \hline \vdots & \vdots & \vdots & \vdots & \vdots & \vdots & \ddots \end{array}\right). \tag{3.37}$$

In the general case there can be, again, an infinite number of single-particle states.

▶ **Exercise 3.4:** Extend the matrices above (eq. 3.34 to 3.37) to the three-particle basis states.

▶ **Exercise 3.5:** Construct the matrices of the bosonic ladder operators a_i^+ and a_i in the case of $n = 3$ single-particle states, covering at least the two-particle basis states.

3.2.3 Commutators of Bosonic Ladder-Operators

We have seen that when we first annihilate a particle and then recreate it, i. e. when we apply $a_i^+ a_i$, the result is the original state with a prefactor of the number of particles in it. Thus $a_i^+ a_i$ is a specialised number operator N_i for the state i.

When we first create a particle and then annihilate it again, i. e. when we apply $a_i\, a_i^+$, we get a similar result, but with another prefactor. When there are m bosons in the state i, then

$$a_i\, a_i^+ \left|m_i\right\rangle = a_i \sqrt{m+1}\, \left|(m+1)_i\right\rangle = (m+1)\left|m_i\right\rangle, \tag{3.38}$$

thus

$$a_i\, a_i^+ = N_i + 1 = a_i^+ a_i + 1, \tag{3.39}$$

or

$$a_i\, a_i^+ - a_i^+ a_i = [a_i, a_i^+] = 1. \tag{3.40}$$

This is a very important property of the ladder operators.

The square bracket $[a_i, a_i^+]$ is called the *commutator* of a_i and a_i^+. It can be used to re-order the ladder operators in a product.

This commutator holds for ladder operators for the same state i. For different states $i \neq j$ the ladder operators are independent. Then they commute, and their commutator is zero,

$$[a_i, a_j] = [a_i, a_j^+] = [a_i^+, a_j^+] = 0 \quad \text{for } i \neq j. \tag{3.41}$$

3.2.4 Constructing Bosonic Many-Particle States

The creation operators allow for yet another notation for many-particle states. To construct, for instance, a two-particle state with one boson in state 1 and "another" one in state 7, we can write

$$|2_{1,7}\rangle = a_1^+ a_7^+ \,|0\rangle\,. \tag{3.42}$$

(Since bosons are indistinguishable, we can speak of "another" boson just metaphorically.)

Since bosonic creation operators for different states commute, the order of the creation operators in front of the vacuum state does not matter,

$$|2_{1,7}\rangle = a_7^+ a_1^+ \,|0\rangle\,. \tag{3.43}$$

This notation of many-particle states is not much longer than the bra-ket notations, and it is less ambiguous. For this reason it is the preferred notation in literature.

When doing calculations with many-particle states, we can often combine ladder operators for the same state to specialised number operators for that state. If they are in the "wrong" order we can use the commutator to re-order them to make the combination possible.

As an example, let's write $(a_3 + a_2^+)(a_2 + a_3^+)\,|2_{2,3}\rangle$ as a linear combination of Fock states. It is clear that the result must contain $|0\rangle$ and $|4_{2,2,3,3}\rangle$, but what else?

$$\begin{aligned}
&(a_3 + a_2^+)(a_2 + a_3^+)\,|2_{2,3}\rangle \\
&= (a_3\, a_2 + a_3\, a_3^+ + a_2^+ a_2 + a_2^+ a_3^+)\, a_2^+ a_3^+ \,|0\rangle \\
&= a_3\, a_2\, a_2^+ a_3^+ \,|0\rangle + a_3\, a_3^+\, a_2^+ a_3^+ \,|0\rangle + a_2^+ a_2\, a_2^+ a_3^+ \,|0\rangle + a_2^+ a_3^+ a_2^+ a_3^+ \,|0\rangle \\
&= a_3\,(\underbrace{a_2\, a_2^+ - a_2^+ a_2}_{=1} + \underbrace{a_2^+ a_2}_{=N_2})\, a_3^+ \,|0\rangle + (\underbrace{a_3\, a_3^+ - a_3^+ a_3}_{=1} + \underbrace{a_3^+ a_3}_{=N_3})\, a_2^+ a_3^+ \,|0\rangle \\
&\quad + \underbrace{a_2^+ a_2}_{=N_2}\, a_2^+ a_3^+ \,|0\rangle + a_2^+ a_2^+ a_3^+ a_3^+ \,|0\rangle \\
&\qquad = N_2 = 1, \text{ because there is 1 boson in state 2 on the right} \\
&= a_3\,(1 + \underbrace{N_2}_{=0})\, a_3^+ \,|0\rangle \\
&\qquad\qquad = 0, \text{ because there is no boson in state 2 on the right} \\
&\quad + (1 + \underbrace{N_3}_{=1})\, a_2^+ a_3^+ \,|0\rangle \\
&\qquad\qquad = 1, \text{ because there is 1 boson in state 3 on the right} \\
&\quad + a_2^+ a_3^+ \,|0\rangle + a_2^+ a_2^+ a_3^+ a_3^+ \,|0\rangle
\end{aligned}$$

$$
\begin{aligned}
&= (\underbrace{a_3\, a_3^+ - a_3^+ a_3}_{=1} + \underbrace{a_3^+ a_3}_{=N_3=0,\text{ because there is no boson in state 3 on the right}}) \,|0\rangle \\
&\quad + 3a_2^+ a_3^+ \,|0\rangle + a_2^+ a_2^+ a_3^+ a_3^+ \,|0\rangle \\
&= |0\rangle + 3\, a_2^+ a_3^+ \,|0\rangle + a_2^+ a_2^+ a_3^+ a_3^+ \,|0\rangle \\
&= |0\rangle + 3\,|2_{2,3}\rangle + |4_{2,2,3,3}\rangle\,. \qquad (3.44)
\end{aligned}
$$

▶ **Exercise 3.6:** Write $(a_2 + a_3^+)(a_3 + a_2^+)\,|2_{2,3}\rangle$ as a linear combination of Fock states.

▶ **Exercise 3.7:** Write $(a_2^+ + a_3^+)(a_2 + a_3)\,|2_{2,3}\rangle$ as a linear combination of Fock states.

3.2.5 Fermionic Number Operators

We now construct the same types of operators for fermions, i. e. for particles whose wave function is antisymmetric upon transposition of two particles, rather than symmetric.

Again we construct the *number operator* by taking the Fock states as eigenstates and assigning the number of fermions in it as the eigenvalues. By applying N, each of its eigenstates gets multiplied by its eigenvalue, the number of fermions in the state.

There is, however, a crucial difference to bosons, the Pauli exclusion principle, which results from the antisymmetry of the wave function with respect to permutation of the particles. Since there can never be more than one fermion in the same state i, our matrices are much smaller.

For instance in the simple case, where the single-particle system has just 1 eigenstate, the matrix of the number operator N is not (countably) infinite-dimensional, but two-dimensional,

$$
N = \begin{pmatrix} 0 & 0 \\ 0 & 1 \end{pmatrix}. \qquad (3.45)
$$

The upper component of this matrix acts on the vacuum state and the lower one on the one-fermion state.

In the slightly less simple case, where the single-particle system has 2 eigenstates, the basis consists of the Fock states

$$
\begin{array}{ll}
\text{1 eigenstate with 0 particles:} & |0\rangle, \\
\text{2 eigenstates with 1 particle:} & |1_{1,0}\rangle,\ |1_{0,1}\rangle, \\
\text{1 eigenstate with 2 particles:} & |2_{1,1}\rangle.
\end{array}
$$

There are no many-particle eigenstates with more fermions than there are eigenstates in the single-particle system.

In this basis the matrix of N reads

$$
N = \left(\begin{array}{c|ccc} 0 & 0 & 0 & 0 \\ \hline 0 & 1 & 0 & 0 \\ 0 & 0 & 1 & 0 \\ \hline 0 & 0 & 0 & 2 \end{array}\right). \qquad (3.46)
$$

3.2.6 Fermionic Ladder Operators

We will now construct a pair c_i^+, c_i of ladder operators for fermions. (From section 3.4 on we will use bosonic and fermionic ladder operators together in the same equation, which is why

we call them c_i^+ and c_i here instead of re-using the notations a_i^+ and a_i. In section 4.4 we will also use the symbols b_i^+, b_i, d_i^+, and d_i for fermionic ladder operators.)

For the creation operator c_i^+ we must take into account that the Pauli exclusion principle doesn't allow to create another fermion in a state i which is already occupied by a fermion,

$$c_i^+ \left|1_i\right\rangle = 0. \tag{3.47}$$

Everything else is the same as in the bosonic case. The annihilation operator c_i maps a many-particle state with one fermion to the vacuum state,

$$c_i \left|1_i\right\rangle = \left|0\right\rangle. \tag{3.48}$$

The creation operator can "push up" the vacuum state to a one-particle state,

$$c_i^+ \left|0\right\rangle = \left|1_i\right\rangle, \tag{3.49}$$

and the annihilation operator can "push it down" to the zero vector,

$$c_i \left|0\right\rangle = 0. \tag{3.50}$$

As in the bosonic case, the product $c_i^+ c_i$ of fermionic ladder operators for the same state i is the specialised number operator for that state,

$$c_i^+ c_i \left|1_i\right\rangle = 1 \cdot \left|1_i\right\rangle = \left|1_i\right\rangle, \tag{3.51}$$

$$c_i^+ c_i \left|0\right\rangle = 0 \cdot \left|0\right\rangle = 0. \tag{3.52}$$

In the simple case, where the single-particle system has just 1 eigenstate, the matrices of the fermionic ladder operators read

$$c^+ = \begin{pmatrix} 0 & 0 \\ 1 & 0 \end{pmatrix}, \qquad c = \begin{pmatrix} 0 & 1 \\ 0 & 0 \end{pmatrix}, \tag{3.53}$$

and their product is the number operator

$$c^+ c = \begin{pmatrix} 0 & 0 \\ 0 & 1 \end{pmatrix} = N. \tag{3.54}$$

Again the upper components describe the operator's action on the vacuum state and the lower ones its action on the one-particle state.

In the case with 2 eigenstates in the single-particle system and with the Fock basis

$$\begin{array}{ll} \text{1 eigenstate with 0 particles:} & \left|0\right\rangle, \\ \text{2 eigenstates with 1 particle:} & \left|1_{1,0}\right\rangle, \left|1_{0,1}\right\rangle, \\ \text{1 eigenstate with 2 particles:} & \left|2_{1,1}\right\rangle, \end{array}$$

the matrices read

$$c_1^+ = \left(\begin{array}{c|cc|c} 0 & 0 & 0 & 0 \\ \hline 1 & 0 & 0 & 0 \\ 0 & 0 & 1 & 0 \\ \hline 0 & 0 & 1 & 0 \end{array}\right), \qquad c_1 = \left(\begin{array}{c|cc|c} 0 & 1 & 0 & 0 \\ \hline 0 & 0 & 0 & 0 \\ 0 & 0 & 1 & 1 \\ \hline 0 & 0 & 0 & 0 \end{array}\right), \tag{3.55}$$

$$c_2^+ = \left(\begin{array}{c|cc|c} 0 & 0 & 0 & 0 \\ \hline 0 & 1 & 0 & 0 \\ 1 & 0 & 0 & 0 \\ \hline 0 & 1 & 0 & 0 \end{array}\right), \qquad c_2 = \left(\begin{array}{c|cc|c} 0 & 0 & 1 & 0 \\ \hline 0 & 1 & 0 & 1 \\ 0 & 0 & 0 & 0 \\ \hline 0 & 0 & 0 & 0 \end{array}\right). \tag{3.56}$$

When working with ladder operators, they are usually denoted by their symbols rather than by their matrices. Nevertheless, two-dimensional fermionic matrices will play a major role in section 4.4, when we'll investigate the relation between fermions and anti-fermions.

3.2.7 Anti-Commutators of Fermionic Ladder-Operators

We have seen that the product $c_i^+ c_i$ of fermionic ladder operators for the same state i results in a specialised number operator N_i, which counts the number of fermions in that state. Let's review the mechanism behind this.

First, c_i tries to annihilate a fermion in the given state. If the state is occupied, i. e. we apply the number operator to the one-fermion state $|1_i\rangle$, we get the vacuum state. After that we apply the creation operator c_i^+, which maps the vacuum state back to the one-fermion state,

$$c_i^+ c_i \, |1_i\rangle = c_i^+ \, |0\rangle = |1_i\rangle \, . \tag{3.57}$$

If the state is not occupied, i. e. we apply the number operator to the vacuum state $|0\rangle$, we get the zero vector. When we apply the creation operator c_i^+ to it, it remains zero,

$$c_i^+ c_i \, |0\rangle = c_i^+ \, 0 = 0. \tag{3.58}$$

Now what kind of operator do we get when we reverse the order of the fermionic ladder operators in the product? What is $c_i \, c_i^+$ applied to a fermionic state?

First, c_i^+ tries to create a fermion in the given state. If the state is not occupied, i. e. we apply our "reversed number operator" to the vacuum state $|0\rangle$, we get the one-fermion state $|1_i\rangle$. After that we apply the annihilation operator c_i, which maps the one-fermion state back to the vacuum state,

$$c_i \, c_i^+ \, |0\rangle = c_i \, |1_i\rangle = |0\rangle \, . \tag{3.59}$$

If the state is occupied, i. e. we apply our operator to the one-fermion state $|1_i\rangle$, we get the zero vector. When we apply the annihilation operator c_i to it, it remains zero,

$$c_i \, c_i^+ \, |1_i\rangle = c_i \, 0 = 0. \tag{3.60}$$

So our "reversed number operator" $c_i \, c_i^+$ does essentially the same as the "normal" number operator, but with the roles of the one-fermion state and of the vacuum state reversed.

This "reversed number operator" will become important when investigating the relation between fermions and anti-fermions in section 4.4, thus we give it a name, *anti-number operator*.

When we apply the sum of both operators, $c_i \, c_i^+ + c_i^+ c_i$, to a fermionic state, then the "normal" number operator keeps the one-fermion state and maps the vacuum state to zero, while the anti-number operator does the opposite. So their sum maps every fermionic state to itself,

$$(c_i \, c_i^+ + c_i^+ c_i) \, |1_i\rangle = 0 + |1_i\rangle = |1_i\rangle \, , \tag{3.61}$$

$$(c_i \, c_i^+ + c_i^+ c_i) \, |0\rangle = |0\rangle + 0 = |0\rangle \, . \tag{3.62}$$

In other words, we get the identity map,

$$c_i \, c_i^+ + c_i^+ c_i = [c_i, c_i^+]_+ = 1. \tag{3.63}$$

As in the bosonic case, this is a very important property of the ladder operators.

$[c_i, c_i^+]_+ = c_i \, c_i^+ + c_i^+ c_i$ is called the *anticommutator* of c_i and c_i^+. It can also be written $\{c_i, c_i^+\}$. To avoid confusion, the "normal" commutator, which is important in the bosonic case, can be written with a minus sign as an index, $[a_i, a_i^+]_- = a_i \, a_i^+ - a_i^+ a_i$.

For fermionic ladder operators for different states $i \neq j$ the anticommutator is zero,

$$[c_i, c_j]_+ = [c_i, c_j^+]_+ = [c_i^+, c_j^+]_+ = 0 \quad \text{for } i \neq j, \tag{3.64}$$

which means that these operators *anticommute*,

$$c_i \, c_j = -c_j \, c_i, \quad c_i \, c_j^+ = -c_j^+ c_i, \quad c_i^+ c_j^+ = -c_j^+ c_i^+ \quad \text{for } i \neq j. \tag{3.65}$$

3.2.8 Constructing Fermionic Many-Particle States

Like in the bosonic case, we can construct fermionic many-particle states by applying creation operators to the vacuum state.

To construct, for instance, a two-particle state with one fermion in state 1 and "another" one in state 7, we can write

$$|2_{1,7}\rangle = c_1^+ c_7^+ |0\rangle . \tag{3.66}$$

The creation operators for different states anticommute, thus the order of the creation operators in front of the vacuum state does matter,

$$|2_{1,7}\rangle = c_1^+ c_7^+ |0\rangle = -c_7^+ c_1^+ |0\rangle = -|2_{7,1}\rangle . \tag{3.67}$$

Again, when doing calculations with many-particle states, we can often combine ladder operators for the same state to specialised number operators. If they are in the "wrong" order we can use the anticommutator to re-order them to make the combination possible.

Another important property of fermionic ladder operators is that, due to the Pauli exclusion principle, the product of each of them with itself is zero.

To get familiar with this, let's calculate an example. What is $(c_3 + c_2^+)(c_2 + c_3^+)\,|2_{2,3}\rangle$ expressed as a linear combination of Fock states?

$$\begin{aligned}
&(c_3 + c_2^+)(c_2 + c_3^+)\,|2_{2,3}\rangle \\
&= (c_3\,c_2 + c_3\,c_3^+ + c_2^+ c_2 + c_2^+ c_3^+)\,c_2^+ c_3^+\,|0\rangle \\
&= c_3\,c_2\,c_2^+ c_3^+\,|0\rangle + c_3\,c_3^+\,c_2^+ c_3^+\,|0\rangle + c_2^+ c_2\,c_2^+ c_3^+\,|0\rangle + c_2^+ c_3^+ c_2^+ c_3^+\,|0\rangle \\
&= c_3\,c_2\,c_2^+ c_3^+\,|0\rangle - c_3\,c_2^+ \underbrace{c_3^+ c_3}_{=0}\,|0\rangle + c_2^+ c_2\,c_2^+ c_3^+\,|0\rangle - \underbrace{c_2^+ c_2^+}_{=0}\,\underbrace{c_3^+ c_3}_{=0}\,|0\rangle \\
&= c_3\,(\underbrace{c_2\,c_2^+ + c_2^+ c_2}_{=1} - \underbrace{c_2^+ c_2}_{=N_2})\,c_3^+\,|0\rangle \\
&\quad + \underbrace{c_2^+ c_2}_{=N_2=1,\text{ because there is 1 fermion in state 2 on the right}}\,c_2^+ c_3^+\,|0\rangle \\
&= c_3(1 - \underbrace{N_2}_{=0,\text{ because there is no fermion in state 2 on the right}})\,c_3^+\,|0\rangle + c_2^+ c_3^+\,|0\rangle \\
&= (\underbrace{c_3\,c_3^+ + c_3^+ c_3}_{=1} - \underbrace{c_3^+ c_3}_{=N_3=0,\text{ because it acts on the vacuum state}})\,|0\rangle + c_2^+ c_3^+\,|0\rangle \\
&= |0\rangle + |2_{2,3}\rangle .
\end{aligned} \tag{3.68}$$

Instead of expanding $c_3\,c_3^+$ to $c_3\,c_3^+ + c_3^+ c_3 - c_3^+ c_3 = 1 - c_3^+ c_3$, we can also directly see that $c_3\,c_3^+\,|0\rangle = |0\rangle$ because $c_3\,c_3^+$ is an anti-number operator, which maps the vacuum state to itself and the one-particle state (state number 3 in this case) to zero.

3.3 Second Quantisation

Now we are ready for *second quantisation*, i. e. for substituting many-particle operators, so-called *field operators*, into equations made to describe single particles in the hope that the resulting equations will describe many-particle systems correctly.

This substitution will be done in the Hamiltonian function, derived from the Lagrangian density.

The operators are to be substituted for the wave functions. In literature, they also take the role of the wave function as the dynamical variable, or parts of it. When this is done completely, i. e. we have a static wave function and time-dependent operators, it is called the *Heisenberg picture*. When parts of the dynamics remain in the wave function, i. e. both the wave function and the operators are time-dependent, it is called the *Dirac picture* or *interaction picture*. This is where the famous Feynman diagrams get defined.

For compatibility with the traditional approach, we will first construct the time-dependent versions of the field operators. In chapter 4 the dynamics will reside completely in the wave function, just like in chapter 2. This is called the *Schrödinger picture*.

3.3.1 Photons

In this subsection we implement the *quantisation of the electomagnetic field*.

We don't immediately substitute a many-particle operator into a single-particle equation. Instead we follow essentially the customary path of quantisation of the electromagnetic field as found in textbooks (e. g. in [9, § 2]), with the modification that we are directly using the four-potential A_μ and its time derivative $\dot{A}_\mu$ as our canonical coordinates instead of position-independent versions of them.

The procedure is as follows.

- We investigate the classical electromagnetic field in *momentum representation*, i. e. we decompose the classical wave function $A_\mu(x,t)$ into plane waves, labelled by the angular wavenumber vector k.
- In the classical electromagnetic field we identify a pair of canonical coordinates. It consists, for each k, of the four-potential A_μ and its time derivative $\dot{A}_\mu$.
- We investigate, for each k and each μ, the system we got in the previous step. It turns out to have the structure of a harmonic oscillator.
- We substitute a differential operator for the "momentum" coordinate and a multiplication operator for the "position" coordinate, thus turning, for each k and μ, the classical harmonic oscillator into a quantum system. This is *first quantisation* of the electromagnetic field.
- We identify the eigenstates of each of these quantum systems with a Fock space over a quantum system with just one single-particle state.
- We reinterpret the result as a *second quantisation*, i. e. a substitution of a many-particle operator into a classical equation.

The last step will be postponed to the next subsection.

As noted in section 2.3 (eq. 2.79), the vacuum Maxwell equations are a second-order differential

equation for the four-potential $A_\mu(x,t)$, a field with four real-valued components,

$$\frac{\partial^2}{\partial t^2} A_\mu(x,t) = c^2 \Delta A_\mu(x,t). \tag{3.69}$$

We can convert this partial differential equation to an ordinary one by applying a Fourier transform. Then each derivative with respect to x turns into a factor of ik. Thus the Laplace operator Δ turns into a factor of $-|k|^2$, and we obtain the *momentum representation* of the vacuum Maxwell equations,

$$\frac{\partial^2}{\partial t^2} \tilde{A}_\mu(k,t) = -c^2 |k|^2 \tilde{A}_\mu(k,t). \tag{3.70}$$

This is an ordinary differential equation for $\tilde{A}_\mu(t)$ with parameter k. It has the same structure as the equation of motion of a classical one-dimensional harmonic oscillator with the coordinate $\tilde{A}_\mu(t)$ and the angular frequency $\omega_k = c|k|$.

With a hypothetical mass m we introduce a momentum

$$\tilde{P}_\mu = m\dot{\tilde{A}}_\mu \tag{3.71}$$

and take a shortcut to the classical Hamiltonian function

$$H_{k,\mu} = \tfrac{1}{2} m \dot{\tilde{A}}_\mu^2 + \tfrac{1}{2} m \omega_k^2 \tilde{A}_\mu^2 = \tfrac{\tilde{P}_\mu^2}{2m} + \tfrac{1}{2} m \omega_k^2 \tilde{A}_\mu^2. \tag{3.72}$$

Our hypothetical mass m is *not* the photon mass. In this equation it is dimensionless and its choice doesn't affect our results, so it can safely be set to 1. For now it is just here to make it easier to recognise the parallels of this system to a harmonic oscillator.

Now we apply the rules of first quantisation to this harmonic oscillator. The coordinate $\tilde{A}_\mu$ turns into a multiplication operator. We substitute the differential operator $-i\hbar \frac{\partial}{\partial \tilde{A}_\mu}$ for the momentum $\tilde{P}_\mu$ and obtain the quantum Hamiltonian operator

$$H_{k,\mu} = -\tfrac{\hbar^2}{2m} \tfrac{\partial^2}{\partial \tilde{A}_\mu^2} + \tfrac{1}{2} m \omega_k^2 \tilde{A}_\mu^2 \tag{3.73}$$

and the Schrödinger equation

$$i\hbar \tfrac{\partial}{\partial t} \Psi(\tilde{A}_\mu, t) = -\tfrac{\hbar^2}{2m} \tfrac{\partial^2}{\partial \tilde{A}_\mu^2} \Psi(\tilde{A}_\mu, t) + \tfrac{1}{2} m \omega_k^2 \tilde{A}_\mu^2 \Psi(\tilde{A}_\mu, t). \tag{3.74}$$

The quantum harmonic oscillator is a well-known system. Its eigenstates read

$$\Psi_n(\tilde{A}_\mu, t) = \tfrac{1}{\sqrt{2^n n!}} \left(\tfrac{m\omega_k}{\pi\hbar}\right)^{\frac{1}{4}} e^{-\frac{m\omega_k \tilde{A}_\mu^2}{2\hbar}} H_n\left(\sqrt{\tfrac{m\omega_k}{\hbar}} \tilde{A}_\mu\right) e^{-\frac{i}{\hbar} E_n t} \tag{3.75}$$

where $n \in \mathbb{N}_0$, and H_n denotes the *Hermite polynomials*,

$$H_n(x) = (-1)^n e^{\frac{1}{2}x^2} \tfrac{d^n}{dx^n} e^{-\frac{1}{2}x^2}. \tag{3.76}$$

The feature we are interested in are the energy levels allowed by quantum mechanics for this system, its energy eigenvalues

$$E_n = \hbar\omega_k \left(n + \tfrac{1}{2}\right). \tag{3.77}$$

They are independent of our hypothetical mass m. In contrast to our "coordinate" $\tilde{A}_\mu$, which is actually an electromagnetic four-potential, the E_n are indeed energies (since $\hbar\omega_k$ is an energy). These are the energy levels allowed for an electromagnetic field at the angular wavenumber vector k (which is still present inside $\omega_k = c|k|$ and acts as a parameter for our quantum system).

All this looks somewhat divorced from reality, but it has been introduced to explain experimental results, the *photoelectric effect*. Experiments have shown that the energy transfer by an electromagnetic wave happens in portions of $\Delta E = \hbar\omega_k = \hbar c|k|$. Similar to an atom, whose electrons can absorb and emit portions of energy which correspond to the differences between its energy eigenvalues, the energy of an electromagnetic field can only change in portions which depend on the wavelength (via the angular wavenumber vector k). This is our *first quantisation* of the electromagnetic field.

Before we proceed to second quantisation, let's have a look at the physical implications of our findings so far.

- The electromagnetic field with a specific angular wavenumber vector k can absorb and emit energies in portions of $\Delta E = \hbar\omega_k = \hbar c|k|$. This is in accordance with experimental results (photoelectric effect).
- The state with sharp k is not a quantum eigenstate, but it belongs to a classical field. The quantisation doesn't happen between x and p (or between x and k), but between the electromagnetic four-potential $\tilde{A}_\mu(k,t)$ and its time derivative.
- This implies that we have a quantum uncertainty relation between the electromagnetic four-potential $\tilde{A}_\mu(k,t)$ and its derivative with respect to time, which can be translated to a quantum uncertainty relation between the magnetic and the electric field. This uncertainty has been measured experimentally [10].
- In addition we have a *classical* uncertainty relation between the position x and the angular wavenumber vector k. To get a sharp value of k the spatial extent of the electromagnetic field would have to be infinite. In reality it will always be finite. To compose a finite field we need many frequencies and thus many angular wavenumber vectors k.
- As soon as we localise an electromagnetic field it can no longer have a sharp value of k and thus of $\hbar\omega_k$. In this sense we have a classical uncertainty relation between the position x of an electromagnetic wave and its energy portion $\hbar\omega_k$.

Now, where are the photons?

We now interpret the energy portion $\hbar\omega_k$ as the kinetic energy carried by a particle, the *photon*. (As we will see later, a photon also carries a momentum, so it makes indeed sense to treat it as a particle.)

Photons aren't actual particles, but energy levels. When we treat them as particles they are identical, so we want to use many-particle quantum operators to describe them, in particular a number operator. In fact we already have an operator which is quite similar to a bosonic number operator, the Hamiltonian of our "harmonic oscillator", eq. 3.73. In the basis of its eigenstates, eq. 3.75, its (infinite) matrix reads

$$H_{k,\mu} = \begin{pmatrix} \left(0+\frac{1}{2}\right)\hbar\omega_k & 0 & 0 & \dots \\ 0 & \left(1+\frac{1}{2}\right)\hbar\omega_k & 0 & \dots \\ 0 & 0 & \left(2+\frac{1}{2}\right)\hbar\omega_k & \dots \\ \vdots & \vdots & \vdots & \ddots \end{pmatrix}. \tag{3.78}$$

In this Hilbert space (which depends on k) we now define a pair of bosonic ladder operators $a^+_{k,\mu}, a_{k,\mu}$, which take us from one eigenstate $\Psi_n(\tilde{A}_\mu)$ to the next one,

$$a^+_{k,\mu}\Psi_n = \sqrt{n+1}\,\Psi_{n+1}, \tag{3.79}$$

$$a_{k,\mu}\Psi_n = \sqrt{n}\,\Psi_{n-1}. \tag{3.80}$$

Then we can write our Hamiltonian as

$$H_{k,\mu} = \hbar\omega_k\left(a^+_{k,\mu}a_{k,\mu} + \tfrac{1}{2}\right) = \hbar\omega_k\left(N_{k,\mu} + \tfrac{1}{2}\right), \tag{3.81}$$

where $N_{k,\mu} = a^+_{k,\mu}a_{k,\mu}$ is a bosonic number operator for the quantised electromagnetic field at the angular wavenumber vector k and in the component μ of the four-potential.

This interpretation of the differences between the energy levels of the electromagnetic field allowed by first quantisation as the energies of identical particles is our *second quantisation* of the electromagnetic field.

At this point, two observations should be noted.

- The indices k and μ do *not* label single-particle states. Instead we have, for each angular wavenumber vector k and each component μ, one Fock space over just one single-particle state.
- In the case of the electromagnetic field, second quantisation does not actually introduce any new physics. It just reinterprets the results of first quantisation.

▶ **Exercise 3.8:** Express $a^+_{k,\mu}$ and $a_{k,\mu}$ via $\tilde{A}_\mu$ and $\tilde{P}_\mu$.

3.3.2 Field Operators

So we got a many-particle operator, the number operator N_k, for photons with the angular wavenumber vector k. However the bosonic structure resulted from harmonic oscillators, which already were in the system. So where exactly did we substitute a many-particle operator?

In first quantisation, we substitute operators on a Hilbert space for the real-valued variables x and p in the classical Hamiltonian. This is what we did in the previous subsection for the momentum representation of A_μ and $\dot{A}_\mu$, see eq. 3.73. This suggests that we have to insert a many-particle operator into the classical Hamiltonian of the Maxwell equations in momentum representation. Since we already know the result, this allows us to deduce the form of the many-particle operator to be substituted. This can help us to develop a systematic way to do the same for other physical systems.

For this purpose we need the classical Hamiltonian of the Maxwell equations, expressed in terms of $A_\mu(x,t)$ and $\dot{A}_\mu(x,t)$, in momentum representation.

We already know the classical Hamiltonian of the Maxwell equations, expressed in terms of $A_\mu(x,t)$ and $\dot{A}_\mu(x,t)$ in position representation, eq. 2.105,

$$\mathcal{H}_A = \tfrac{1}{2\mu_0}\left(\tfrac{1}{c^2}\dot{A}_\mu(x,t)^2 + \big(\nabla \times A_\mu(x,t)\big)^2\right). \tag{3.82}$$

To proceed, we express $A_\mu(x,t)$ in momentum representation, i. e. as a superposition of real-valued plane waves,

$$A_\mu(x,t) = \tfrac{1}{\sqrt{2}}\int d^3k\, A_{k,\mu}\, e^{i(kx-\omega_k t)} + A^*_{k,\mu}\, e^{-i(kx-\omega_k t)}, \tag{3.83}$$

where $\omega_k = c|k|$. The coefficients $A_{k,\mu}$ can be obtained from $A_\mu(x,t)$ via a Fourier transform. The specific choice $\frac{1}{\sqrt{2}}$ for the prefactor does not really affect the results. It is chosen to make it easier to recognise the physical meaning of $A_{k,\mu}$ later.

Now we can express the ingredients of $\mathcal{H}_A$ in momentum representation.

$$\begin{aligned}
\dot{A}_\mu(x,t) &= \tfrac{\partial}{\partial t} A_\mu(x,t) \\
&= \tfrac{\partial}{\partial t}\tfrac{1}{\sqrt{2}}\int d^3k\, A_{k,\mu}\, e^{i(kx-\omega_k t)} + A^*_{k,\mu}\, e^{-i(kx-\omega_k t)} \\
&= \tfrac{1}{\sqrt{2}}\int d^3k\, (-i\omega_k) A_{k,\mu}\, e^{i(kx-\omega_k t)} + (ik) A^*_{k,\mu}\, e^{-i(kx-\omega_k t)},
\end{aligned} \tag{3.84}$$

$$
\begin{aligned}
\dot{A}_\mu(x,t)^2 &= \tfrac{1}{2}\left(\int d^3k\,(-i\omega_k)A_{k,\mu}\,e^{i(kx-\omega_k t)} + (ik)A^*_{k,\mu}\,e^{-i(kx-\omega_k t)}\right)\\
&\qquad\left(\int d^3k'\,(-i\omega_{k'})A_{k',\mu}\,e^{i(k'x-\omega_{k'} t)} + (ik)A^*_{k',\mu}\,e^{-i(k'x-\omega_{k'} t)}\right)\\
&= \tfrac{1}{2}\int d^3k\int d^3k'\,(-\omega_k\omega_{k'})\,A_{k,\mu}A_{k',\mu}\,e^{i(k+k')x}\,e^{-i(\omega_k+\omega_{k'})t}\\
&\qquad + (\omega_k\omega_{k'})\,A_{k,\mu}A^*_{k',\mu}\,e^{i(k-k')x}\,e^{-i(\omega_k-\omega_{k'})t}\\
&\qquad + (\omega_k\omega_{k'})\,A^*_{k,\mu}A_{k',\mu}\,e^{i(-k+k')x}\,e^{-i(-\omega_k+\omega_{k'})t}\\
&\qquad + (-\omega_k\omega_{k'})\,A^*_{k,\mu}A^*_{k',\mu}\,e^{i(-k-k')x}\,e^{-i(-\omega_k-\omega_{k'})t},
\end{aligned}
\tag{3.85}
$$

$$
\begin{aligned}
\nabla\times A_\mu(x,t) &= \nabla\times\tfrac{1}{\sqrt{2}}\int d^3k\,A_{k,\mu}\,e^{i(kx-\omega_k t)} + A^*_{k,\mu}\,e^{-i(kx-\omega_k t)}\\
&= \tfrac{1}{\sqrt{2}}\int d^3k\,\nabla\times A_{k,\mu}\,e^{i(kx-\omega_k t)} + \nabla\times A^*_{k,\mu}\,e^{-i(kx-\omega_k t)}\\
&= \tfrac{1}{\sqrt{2}}\int d^3k\,(ik)\times A_{k,\mu}\,e^{i(kx-\omega_k t)} + (-ik)\times A^*_{k,\mu}\,e^{-i(kx-\omega_k t)},
\end{aligned}
\tag{3.86}
$$

$$
\begin{aligned}
\big(\nabla\times A_\mu(x,t)\big)^2 &= \tfrac{1}{2}\left(\int d^3k\,(ik)\times A_{k,\mu}\,e^{i(kx-\omega_k t)} + (-ik)\times A^*_{k,\mu}\,e^{-i(kx-\omega_k t)}\right)\\
&\qquad\left(\int d^3k'\,(ik')\times A_{k',\mu}\,e^{i(k'x-\omega_{k'} t)} + (-ik')\times A^*_{k',\mu}\,e^{-i(k'x-\omega_{k'} t)}\right)\\
&= \tfrac{1}{2}\int d^3k\int d^3k'\,\big((ik)\times A_{k,\mu}\big)\big((ik')\times A_{k',\mu}\big)e^{i(k+k')x}\,e^{-i(\omega_k+\omega_{k'})t}\\
&\qquad + \big((ik)\times A_{k,\mu}\big)\big(-(ik')\times A^*_{k',\mu}\big)e^{i(k-k')x}\,e^{-i(\omega_k-\omega_{k'})t}\\
&\qquad + \big((-ik)\times A^*_{k,\mu}\big)\big((ik')\times A_{k',\mu}\big)e^{i(-k+k')x}\,e^{-i(-\omega_k+\omega_{k'})t}\\
&\qquad + \big((-ik)\times A^*_{k,\mu}\big)\big((-ik')\times A^*_{k',\mu}\big)e^{i(-k-k')x}\,e^{-i(-\omega_k-\omega_{k'})t}.
\end{aligned}
\tag{3.87}
$$

We put the ingredients together to form the Hamiltonian density,

$$
\begin{aligned}
\mathcal{H}_A &= \tfrac{1}{2\mu_0}\Big(\tfrac{1}{c^2}\dot{A}_\mu(x,t)^2 + \big(\nabla\times A_\mu(x,t)\big)^2\Big)\\
&= \tfrac{1}{4\mu_0}\int d^3k\int d^3k'\,\tfrac{1}{c^2}(-\omega_k\omega_{k'})\,A_{k,\mu}A_{k',\mu}\,e^{i(k+k')x}\,e^{-i(\omega_k+\omega_{k'})t}\\
&\qquad + \tfrac{1}{c^2}(\omega_k\omega_{k'})\,A_{k,\mu}A^*_{k',\mu}\,e^{i(k-k')x}\,e^{-i(\omega_k-\omega_{k'})t}\\
&\qquad + \tfrac{1}{c^2}(\omega_k\omega_{k'})\,A^*_{k,\mu}A_{k',\mu}\,e^{i(-k+k')x}\,e^{-i(-\omega_k+\omega_{k'})t}\\
&\qquad + \tfrac{1}{c^2}(-\omega_k\omega_{k'})\,A^*_{k,\mu}A^*_{k',\mu}\,e^{i(-k-k')x}\,e^{-i(-\omega_k-\omega_{k'})t}\\
&\qquad + \big((ik)\times A_{k,\mu}\big)\big((ik')\times A_{k',\mu}\big)e^{i(k+k')x}\,e^{-i(\omega_k+\omega_{k'})t}\\
&\qquad + \big((ik)\times A_{k,\mu}\big)\big((-ik')\times A^*_{k',\mu}\big)e^{i(k-k')x}\,e^{-i(\omega_k-\omega_{k'})t}\\
&\qquad + \big((-ik)\times A^*_{k,\mu}\big)\big((ik')\times A_{k',\mu}\big)e^{i(-k+k')x}\,e^{-i(-\omega_k+\omega_{k'})t}\\
&\qquad + \big((-ik)\times A^*_{k,\mu}\big)\big((-ik')\times A^*_{k',\mu}\big)e^{i(-k-k')x}\,e^{-i(-\omega_k-\omega_{k'})t}.
\end{aligned}
\tag{3.88}
$$

We switch from the Hamiltonian density to the Hamiltonian function by integrating over x. The integral turns the exponentials $e^{i(k+k')x}$ into Dirac distributions $\delta(\pm k\pm k')$. After that we carry out the integral over k', which enforces $k'=\pm k$.

$$
H_A = \int d^3x\,\mathcal{H}_A
$$

$$
\begin{aligned}
&= \tfrac{1}{4\mu_0}\int d^3x \int d^3k \int d^3k' \, \tfrac{1}{c^2}(-\omega_k\omega_{k'})\, A_{k,\mu}A_{k',\mu}\, e^{i(k+k')x}\, e^{-i(\omega_k+\omega_{k'})t} \\
&\qquad + \tfrac{1}{c^2}(\omega_k\omega_{k'})\, A_{k,\mu}A^*_{k',\mu}\, e^{i(k-k')x}\, e^{-i(\omega_k-\omega_{k'})t} \\
&\qquad + \tfrac{1}{c^2}(\omega_k\omega_{k'})\, A^*_{k,\mu}A_{k',\mu}\, e^{i(-k+k')x}\, e^{-i(-\omega_k+\omega_{k'})t} \\
&\qquad + \tfrac{1}{c^2}(-\omega_k\omega_{k'})\, A^*_{k,\mu}A^*_{k',\mu}\, e^{i(-k-k')x}\, e^{-i(-\omega_k-\omega_{k'})t} \\
&\qquad + \big((ik)\times A_{k,\mu}\big)\big((ik')\times A_{k',\mu}\big) e^{i(k+k')x}\, e^{-i(\omega_k+\omega_{k'})t} \\
&\qquad + \big((ik)\times A_{k,\mu}\big)\big((-ik')\times A^*_{k',\mu}\big) e^{i(k-k')x}\, e^{-i(\omega_k-\omega_{k'})t} \\
&\qquad + \big((-ik)\times A^*_{k,\mu}\big)\big((ik')\times A_{k',\mu}\big) e^{i(-k+k')x}\, e^{-i(-\omega_k+\omega_{k'})t} \\
&\qquad + \big((-ik)\times A^*_{k,\mu}\big)\big((-ik')\times A^*_{k',\mu}\big) e^{i(-k-k')x}\, e^{-i(-\omega_k-\omega_{k'})t} \\
&= \tfrac{1}{4\mu_0}\int d^3k \int d^3k' \, \tfrac{1}{c^2}(-\omega_k\omega_{k'})\, A_{k,\mu}A_{k',\mu}\, \delta(k+k')\, e^{-i(\omega_k+\omega_{k'})t} \\
&\qquad + \tfrac{1}{c^2}(\omega_k\omega_{k'})\, A_{k,\mu}A^*_{k',\mu}\, \delta(k-k')\, e^{-i(\omega_k-\omega_{k'})t} \\
&\qquad + \tfrac{1}{c^2}(\omega_k\omega_{k'})\, A^*_{k,\mu}A_{k',\mu}\, \delta(-k+k')\, e^{-i(-\omega_k+\omega_{k'})t} \\
&\qquad + \tfrac{1}{c^2}(-\omega_k\omega_{k'})\, A^*_{k,\mu}A^*_{k',\mu}\, \delta(-k-k')\, e^{-i(-\omega_k-\omega_{k'})t} \\
&\qquad + \big((ik)\times A_{k,\mu}\big)\big((ik')\times A_{k',\mu}\big)\, \delta(k+k')\, e^{-i(\omega_k+\omega_{k'})t} \\
&\qquad + \big((ik)\times A_{k,\mu}\big)\big((-ik')\times A^*_{k',\mu}\big)\, \delta(k-k')\, e^{-i(\omega_k-\omega_{k'})t} \\
&\qquad + \big((-ik)\times A^*_{k,\mu}\big)\big((ik')\times A_{k',\mu}\big)\, \delta(-k+k')\, e^{-i(-\omega_k+\omega_{k'})t} \\
&\qquad + \big((-ik)\times A^*_{k,\mu}\big)\big((-ik')\times A^*_{k'}\big)\, \delta(-k-k')\, e^{-i(-\omega_k-\omega_{k'})t} \\
&= \tfrac{1}{4\mu_0}\int d^3k \, \tfrac{1}{c^2}(-\omega_k\omega_{-k})\, A_{k,\mu}A_{-k,\mu}\, e^{-i(\omega_k+\omega_{-k})t} \\
&\qquad + \tfrac{1}{c^2}(\omega_k\omega_k)\, A_{k,\mu}A^*_k\, e^{-i(\omega_k-\omega_k)t} \\
&\qquad + \tfrac{1}{c^2}(\omega_k\omega_k)\, A^*_{k,\mu}A_k\, e^{-i(-\omega_k+\omega_k)t} \\
&\qquad + \tfrac{1}{c^2}(-\omega_k\omega_{-k})\, A^*_{k,\mu}A^*_{-k,\mu}\, e^{-i(-\omega_k-\omega_{-k})t} \\
&\qquad + \big((ik)\times A_{k,\mu}\big)\big((-ik)\times A_{-k,\mu}\big)\, e^{-i(\omega_k+\omega_{-k})t} \\
&\qquad + \big((ik)\times A_{k,\mu}\big)\big((-ik)\times A^*_{k,\mu}\big)\, e^{-i(\omega_k-\omega_k)t} \\
&\qquad + \big((-ik)\times A^*_{k,\mu}\big)\big((ik)\times A_{k,\mu}\big)\, e^{-i(-\omega_k+\omega_k)t} \\
&\qquad + \big((-ik)\times A^*_{k,\mu}\big)\big((ik)\times A^*_{-k,\mu}\big)\, e^{-i(-\omega_k-\omega_{-k})t} \\
&= \tfrac{1}{4\mu_0}\int d^3k \, \tfrac{1}{c^2}(-\omega_k^2)\, A_{k,\mu}A^*_{k,\mu}\, e^{-2i\omega_k t} \\
&\qquad + \tfrac{2}{c^2}\omega_k^2\, A^*_{k,\mu}A_{k,\mu} \\
&\qquad + \tfrac{1}{c^2}(-\omega_k^2)\, A^*_{k,\mu}A_{k,\mu}\, e^{2i\omega_k t} \\
&\qquad + \big((ik)\times A_{k,\mu}\big)\big((-ik)\times A^*_{k,\mu}\big) e^{-2i\omega_k t} \\
&\qquad + 2\big((ik)\times A_{k,\mu}\big)\big((-ik)\times A^*_{k,\mu}\big) \\
&\qquad + \big((-ik)\times A^*_{k,\mu}\big)\big((ik)\times A_{k,\mu}\big) e^{2i\omega_k t}. \qquad (3.89)
\end{aligned}
$$

Using the Lagrange identity

$$|a\times b|^2 = |a|^2|b|^2 - (a\cdot b)^2 \qquad (3.90)$$

we transform

$$\big((ik)\times A_{k,\mu}\big)\big((-ik)\times A^*_{k,\mu}\big) = \big|(ik)\times A_{k,\mu}\big|^2 = k^2 A_{k,\mu}A^*_{k,\mu} - (ik\cdot A_{k,\mu})^2. \qquad (3.91)$$

Since $k \cdot A_{k,\mu} = 0$ due to our gauge condition $\nabla \cdot A_\mu(x,t) = 0$, we can continue with

$$\begin{aligned} H_A &= \tfrac{1}{4\mu_0} \int d^3k \, \tfrac{1}{c^2}(-\omega_k^2)\, A_{k,\mu} A^*_{k,\mu}\, e^{-2i\omega_k t} + \tfrac{2}{c^2}\omega_k^2\, A^*_{k,\mu} A_{k,\mu} + \tfrac{1}{c^2}(-\omega_k^2)\, A^*_{k,\mu} A_{k,\mu}\, e^{2i\omega_k t} \\ &\qquad + k^2 A_{k,\mu} A^*_{k,\mu}\, e^{-2i\omega_k t} + 2k^2 A_{k,\mu} A^*_{k,\mu} + k^2 A_{k,\mu} A^*_{k,\mu}\, e^{2i\omega_k t} \\ &= \tfrac{1}{4\mu_0} \int d^3k \, \tfrac{2}{c^2} \dot{A}^*_{k,\mu} \dot{A}_{k,\mu} + 2k^2 A_{k,\mu} A^*_{k,\mu} \end{aligned} \tag{3.92}$$

and arrive at the Hamiltonian function of the electromagnetic field in the vacuum in momentum representation,

$$H_A = \int d^3x \, \mathcal{H}_A = \tfrac{1}{\mu_0 c^2} \int d^3k \, \tfrac{1}{2} \dot{A}_{k,\mu} \dot{A}^*_{k,\mu} + \tfrac{1}{2} k^2 c^2 A_{k,\mu} A^*_{k,\mu}. \tag{3.93}$$

At this point we should wonder what a Hamiltonian *function* for a field is good for. Don't we need a Hamiltonian *density* to describe the dynamics of a field?

To understand what we just did, let's remember the conjugate momentum P_μ of the canonical coordinate A_μ, eq. 2.102,

$$P_\mu = \tfrac{1}{\mu_0 c} \dot{A}_\mu, \tag{3.94}$$

as obtained from the Lagrangian. (In subsection 2.3.3 it was written P^μ and used with Einstein summation convention.)

When we express H_A through $P_{k,\mu} = \tfrac{1}{\mu_0 c} \dot{A}_{k,\mu}$,

$$\begin{aligned} H_A &= \int d^3k \, \tfrac{\mu_0}{2\mu_0^2 c^2} \dot{A}_{k,\mu} \dot{A}^*_{k,\mu} + \tfrac{1}{2\mu_0 c^2} k^2 c^2 A_{k,\mu} A^*_{k,\mu} \\ &= c \int d^3k \, \tfrac{1}{2}(\mu_0 c) |P_{k,\mu}|^2 + \tfrac{1}{2} \tfrac{1}{\mu_0 c} \omega_k^2 |A_{k,\mu}|^2 \\ &= c \int d^3k \, \tfrac{|P_{k,\mu}|^2}{2m} + \tfrac{1}{2} m \omega_k^2 |A_{k,\mu}|^2 \qquad \text{with } m = \tfrac{1}{\mu_0 c}, \end{aligned} \tag{3.95}$$

we obtain, for each k, the classical Hamiltonian function of a harmonic oscillator.

We have found, still on the classical level, a description of the electromagnetic field as an infinite ensemble of particles, oscillating harmonically. At the same stroke we have justified our shortcut to the classical Hamiltonian of the electromagnetic field, eq. 3.72, and identified our hypothetical mass m as the reciprocal of $\mu_0 c$, thus identifying $\tfrac{1}{\mu_0 c} = c\,\varepsilon_0$ as an "inertia of the electromagnetic field".

(Side note: This beautiful detail would remain hidden if we worked with $\mu_0 = c = 1$.)

So even the classical electromagnetic field in momentum representation behaves like an infinite ensemble of decoupled harmonic oscillators, one for each angular wavenumber vector $k \in \mathbb{R}^3$ and for each $\mu \in \{0,1,2,3\}$. Now we can proceed and quantise it.

From the previous subsection we know that the result is

$$H_A = \int d^3k \sum_{\mu=0}^{3} H_{k,\mu} = \int d^3k \sum_{\mu=0}^{3} \hbar\omega_k \left(a^+_{k,\mu} a_{k,\mu} + \tfrac{1}{2} \right). \tag{3.96}$$

However this time we can compare it to the classical Hamiltonian function im momentum representation we just calculated from the Lagrangian density,

$$H_A = \int d^3x \, \mathcal{H}_A = \tfrac{1}{\mu_0 c^2} \int d^3k \, \tfrac{1}{2} \dot{A}_{k,\mu} \dot{A}^*_{k,\mu} + \tfrac{1}{2} k^2 c^2 A_{k,\mu} A^*_{k,\mu}. \tag{3.97}$$

What do we have to substitute for what in eq. 3.97 in order to obtain eq. 3.96?

We have the fundamental problem that $A^*_{k,\mu}$ and $A_{k,\mu}$ commute, while $a^+_{k,\mu}$ and $a_{k,\mu}$ don't. To address this problem, we apply the commutator relation between $a^+_{k,\mu}$ and $a_{k,\mu}$,

$$[a_{k,\mu}, a^+_{k,\mu}]_- = a_{k,\mu}\, a^+_{k,\mu} - a^+_{k,\mu} a_{k,\mu} = 1, \tag{3.98}$$

and make eq. 3.96 more symmetric,

$$a^+_{k,\mu} a_{k,\mu} + \tfrac{1}{2} = a^+_{k,\mu} a_{k,\mu} + \tfrac{1}{2}(a_{k,\mu}\, a^+_{k,\mu} - a^+_{k,\mu} a_{k,\mu}) = \tfrac{1}{2}(a^+_{k,\mu} a_{k,\mu} + a_{k,\mu}\, a^+_{k,\mu}), \tag{3.99}$$

$$H_A = \int d^3k \sum_{\mu=0}^{3} \hbar\omega_k \left(a^+_{k,\mu} a_{k,\mu} + \tfrac{1}{2}\right) = \int d^3k \sum_{\mu=0}^{3} \tfrac{1}{2}\hbar\omega_k (a^+_{k,\mu} a_{k,\mu} + a_{k,\mu}\, a^+_{k,\mu}). \tag{3.100}$$

When we compare this to eq. 3.97,

$$\begin{aligned} H_A &= \tfrac{1}{\mu_0 c^2} \int d^3k\, \tfrac{1}{2} \dot{A}_{k,\mu} \dot{A}^*_{k,\mu} + \tfrac{1}{2} k^2 c^2 A_{k,\mu} A^*_{k,\mu} \\ &= \int d^3k\, \tfrac{1}{2} \tfrac{1}{\mu_0 c^2} \left(\omega_k^2 A^*_{k,\mu} A_{k,\mu} + k^2 c^2 A_{k,\mu} A^*_{k,\mu}\right) \\ &= \int d^3k\, \tfrac{1}{2} \tfrac{\omega_k}{\mu_0 c^2}\, \omega_k \left(A^*_{k,\mu} A_{k,\mu} + A_{k,\mu} A^*_{k,\mu}\right), \end{aligned} \tag{3.101}$$

we find that we can get the many-particle Hamiltonian operator from the classical Hamiltonian function by substituting

$$\tfrac{\omega_k}{\mu_0 c^2} A^*_{k,\mu} A_{k,\mu} = \sum_{\mu=0}^{3} \hbar\, a^+_{k,\mu} a_{k,\mu}, \qquad \tfrac{\omega_k}{\mu_0 c^2} A_{k,\mu} A^*_{k,\mu} = \sum_{\mu=0}^{3} \hbar\, a_{k,\mu}\, a^+_{k,\mu}, \tag{3.102}$$

or

$$A_{k,\mu} = \sqrt{\tfrac{\hbar\mu_0 c^2}{\omega_k}}\, a_{k,\mu}, \qquad A^*_{k,\mu} = \sqrt{\tfrac{\hbar\mu_0 c^2}{\omega_k}}\, a^+_{k,\mu}. \tag{3.103}$$

(The sum over μ arises from the scalar product between the four-vectors $A_{k,\mu}$ and $A^*_{k,\mu}$.)

Initially (eq. 3.83), $A_{k,\mu}$ and $A^*_{k,\mu}$ themselves were substituted for $A_\mu(x,t)$,

$$A_\mu(x,t) = \tfrac{1}{\sqrt{2}} \int d^3k\, A_{k,\mu}\, e^{i(kx-\omega_k t)} + A^*_{k,\mu}\, e^{-i(kx-\omega_k t)}. \tag{3.104}$$

So we can interpret the quantisation of the electromagnetic field as a substitution of the many-particle operator

$$\hat{A}_\mu(x,t) = \int d^3k \sqrt{\tfrac{\hbar\mu_0 c^2}{2\omega_k}} \left(a_{k,\mu}\, e^{i(kx-\omega_k t)} + a^+_{k,\mu}\, e^{-i(kx-\omega_k t)}\right) \tag{3.105}$$

for the electromagnetic field $A_\mu(x,t)$ in its classical Hamiltonian function, which we derived from its Lagrangian density.

This operator is called the *field operator* of the electromagnetic field.

As already noted, this "second quantisation" of the electromagnetic field is just a reinterpretation of its first quantisation, where we performed a transition from an infinite system of decoupled classical harmonic oscillators to an infinite system of decoupled quantum harmonic oscillators.

The use of this reinterpretation is a hint how to do the transition from a single-particle wave function to a many-particle wave function in a system which does not have this structure by

itself. The recipe for second quantisation is to construct a field operator out of ladder operators and momentum eigenstates of the system, and then to substitute it for the wave function in the classical Hamiltonian function we obtained from the Lagrangian density.

This will be our method for the second quantisation of the Dirac equation, which is not just a reinterpretation, but acutally conveys new physics.

▶ **Exercise 3.9:** Show how to obtain the coefficients $A_{k,\mu}$ in eq. 3.83 from a given $A_\mu(x,t)$.

Hint: Use a Fourier transform.

3.3.3 Second Quantisation of the Free Dirac Equation

We want to substitute field operators into the Hamiltonian function of the free Dirac equation. For this we need field operators and the Hamiltonian function of the free Dirac equation.

We start by calculating the Hamiltonian density of the free Dirac equation. From subsection 2.2.3, eq. 2.59, we know its Lagrangian density,

$$\mathcal{L}_\psi = \bar{\psi}\left(\sum_{\mu=0}^{3} i\hbar c\,\gamma_\mu\partial_\mu - mc^2\right)\psi. \tag{3.106}$$

The variables of $\mathcal{L}_\psi$ are the independent fields $\bar{\psi}(x,t)$ and $\psi(x,t)$ and their time derivatives $\partial_0\bar{\psi}(x,t)$ and $\partial_0\psi(x,t)$.

A Legendre transformation takes us from the Lagrangian to the Hamiltonian,

$$\begin{aligned}\mathcal{H}_\psi &= \frac{\partial\mathcal{L}_\psi}{\partial(\partial_0\bar{\psi})}\,\partial_0\bar{\psi} + \frac{\partial\mathcal{L}_\psi}{\partial(\partial_0\psi)}\,\partial_0\psi - \mathcal{L}_\psi \\ &= 0 + \bar{\psi}\,i\hbar c\,\gamma_0\,\partial_0\psi - \bar{\psi}\left(\sum_{\mu=0}^{3} i\hbar c\,\gamma_\mu\partial_\mu - mc^2\right)\psi \\ &= \bar{\psi}\left(\sum_{j=1}^{3} -i\hbar c\,\gamma_j\partial_j + mc^2\right)\psi. \end{aligned}\tag{3.107}$$

With $\bar{\psi} = \gamma_0\psi^*$ we get

$$\mathcal{H}_\psi = \psi^*\left(-i\hbar c\sum_{j=1}^{3}\alpha_j\partial_j + mc^2\alpha_4\right)\psi, \tag{3.108}$$

i. e. we reproduce the free Dirac Hamiltonian operator, eq. 2.39, with ψ^* and ψ attached to the left and to the right. This Hamiltonian density is the expectation value of the Hamiltonian operator of free fermions in the state ψ.

Next we construct field operators to be substituted for ψ and ψ^*.

In the case of the electromagnetic field we decomposed one real-valued field $A_\mu(x,t)$ into plane waves, which resulted in pairs $A_{k,\mu}$ and $A^*_{k,\mu}$ of the coefficients in momentum representation.

In the case of the Dirac equation the wave functions don't need to be real-valued, but instead we already have the independent variables ψ and ψ^*. Thus it makes sense to start by writing down ψ^* and ψ in momentum representation,

$$\psi(x,t) = \int d^3p \sum_{\sigma=0}^{3} \langle\psi_{p,\sigma}|\psi(x,t)\rangle\; e^{-\frac{i}{\hbar}(px - E_{p,\sigma}t)}, \tag{3.109}$$

$$\psi^*(x,t) = \int d^3p \sum_{\sigma=0}^{3} \langle \psi(x,t) | \psi_{p,\sigma} \rangle \; e^{\frac{i}{\hbar}(px - E_{p,\sigma}t)}. \tag{3.110}$$

with the energy eigenvalues $E_{p,\sigma} = \sqrt{m^2c^4 + p^2c^2}$ for $\sigma \in \{0,1\}$ and $E_{p,\sigma} = -\sqrt{m^2c^4 + p^2c^2}$ for $\sigma \in \{2,3\}$.

$\psi_{p,\sigma}$ denotes normalised versions of our momentum eigenvectors, eq. 2.51. The scalar product of $\psi(x,t)$ with $\psi_{p,\sigma}$ extracts the coefficient for the momentum representation of $\psi(x,t)$. When we do the same for $\psi^*(x,t)$ we must reverse the order of the factors in the scalar product.

We construct our field operators by attaching fermionic ladder operators $c^+_{p,\sigma}$ and $c_{p,\sigma}$ to the eigenstates $\psi_{p,\sigma}$ and $\psi^*_{p,\sigma}$,

$$\hat{\psi}(x,t) = \int d^3p \sum_{\sigma=0}^{3} \psi_{p,\sigma} c_{p,\sigma} \, e^{-\frac{i}{\hbar}(px - E_{p,\sigma}t)}, \tag{3.111}$$

$$\hat{\psi}^*(x,t) = \int d^3p \sum_{\sigma=0}^{3} c^+_{p,\sigma} \psi^*_{p,\sigma} \, e^{\frac{i}{\hbar}(px - E_{p,\sigma}t)}. \tag{3.112}$$

We are approaching the point where this work significantly deviates from the established path to quantum electrodynamics, as found in literature. Thus two remarks seem to be appropriate.

- In literature, the field operators are usually constructed from $\bar{\psi}$ and ψ rather than ψ^* and ψ. Both descriptions are equivalent. With $\bar{\psi}$ the Dirac matrix γ_0 in $\bar{\psi} = \gamma_0 \psi^*$ is attached to the wave function; with ψ^* it is seen as part of the Hamiltonian density.
- These are the time-dependent versions of the field operators as found in literature. They are needed for doing time-ordered perturbation theory, which will be presented in subsection 3.4.2. Later we will work with time-independent field operators, which don't have $-E_{p,\sigma}t$ in the exponentials. Of course we can get them, when needed, by setting $t = 0$.

Before we go on and insert these field operators into the Hamiltonian function, let's try to understand how they work. What exactly do they map to what, and what does that mean physically?

First, let's have a look at the structure of the Fock space these operators act on.

Like in the case of the photons, we do not construct a Fock space over the uncountably infinite set of single-particle momentum eigenstates, but we construct one Fock space for each p. However unlike in the case of the photons, we have four single-particle states labelled by σ, which populate the same Fock space – as opposed to the four independent components of $A_{k,\mu}$. (To be precise, they are not physically independent, but their independent parts span separate Fock spaces.)

Now the field operators act on fermionic many-particle wave functions. These wave functions have the structure

$$\psi(x,t) = \int d^3p_0 \sum_{\sigma_0=0}^{3} \psi_{\sigma_0}(p_0,t) \, c^+_{p_0,\sigma_0} \, |0\rangle \, . \tag{3.113}$$

Here, $c^+_{p_0,\sigma_0} \, |0\rangle$ is a basis state, a one-fermion Fock state in momentum representation. We construct a general state by combining many of these basis states, attaching coefficients $\psi_{\sigma_0}(p_0,t)$. This coefficient function $\psi_{\sigma_0}(p_0,t)$ gives us four complex numbers, one for each σ_0, at each momentum p_0 at each time t.

In other words, $\psi_{\sigma_0}(p_0,t)$ is the spinor-valued wave function of a single fermion.

When $c_{p,\sigma}$ acts on the wave function eq. 3.113, it extracts the coefficient of the one-fermion Fock basis state $c^+_{p,\sigma}\,|0\rangle$,

$$c_{p,\sigma}\int d^3p_0\sum_{\sigma_0=0}^{3}\psi_{\sigma_0}(p_0,t)\,c^+_{p_0,\sigma_0}\,|0\rangle=\psi_\sigma(p,t). \tag{3.114}$$

This works because $c_{p,\sigma}c^+_{p_0,\sigma_0}\,|0\rangle$ is only nonzero when $p=p_0$ and $\sigma=\sigma_0$.

In fact eq. 3.113 is not the most general many-fermion wave function for it lacks contributions of the vacuum state. Those contributions have the structure

$$\Omega(x,t)=\int d^3p_0\;\Omega(p_0,t)\,|0\rangle \tag{3.115}$$

with a complex-valued coefficient wave function $\Omega(p_0,t)$.

When $c_{p,\sigma}$ acts on this vacuum wave function, the result is always zero, because $c_{p,\sigma}\,|0\rangle=0$. So the fermionic vacuum wave function doesn't play any role at this point. Nevertheless let's note that there is not simply the same vacuum $|0\rangle$ everywhere, with just a complex number as its coefficient, but the coefficient of the vacuum state is a wave function, too.

Let's continue to understand how the field operator $\hat\psi(x,t)$ acts on a many-fermion wave function. After $c_{p,\sigma}$ has extracted one component of the spinor-valued coefficient function $\psi_{\sigma_0}(p_0,t)$, we multiply it by the momentum eigenstate amplitude vector $\psi_{p,\sigma}$. This turns the component, a complex number, into a spinor vector.

Finally, the field operator multiplies the spinor by the phase factor $e^{-\frac{i}{\hbar}(px-E_{p,\sigma}t)}$ of the plane wave.

The other field operator $\hat\psi^*_{p,\sigma}$ works the other way round. It accepts a spinor, then extracts a single component by multiplying it with the momentum eigenstate amplitude vector $\psi^*_{p,\sigma}$. After that it uses the creation operator $c^+_{p,\sigma}$ to insert that complex number as a component into the coefficient function $\psi_{\sigma_0}(p_0,t)$ of the result, again multiplying it by a phase factor $e^{\frac{i}{\hbar}(px-E_{p,\sigma}t)}$ of a plane wave.

In summary, $\hat\psi(x,t)$ maps a many-fermion wave function to a spinor, and $\hat\psi^*(x,t)$ maps a spinor to a many-fermion wave function.

Now we are ready for constructing the many-particle Hamiltonian operator H_ψ for free fermions by substituting the field operators into the Hamiltonian function. For this purpose we substitute them into the Hamiltonian density and integrate over x,

$$\begin{aligned}
H_\psi &= \int d^3x\;\hat\psi^*(x,t)\left(-i\hbar c\sum_{j=1}^{3}\alpha_j\partial_j+mc^2\alpha_4\right)\hat\psi(x,t),\\
&= \int d^3x\int d^3p\sum_{\sigma=0}^{3}\int d^3p'\sum_{\sigma'=0}^{3}\\
&\quad c^+_{p',\sigma'}\psi^*_{p',\sigma'}\,e^{\frac{i}{\hbar}(p'x-E_{p',\sigma'}t)}\left(\sum_{j=1}^{3}-i\hbar c\,\alpha_j\partial_j+mc^2\alpha_4\right)\psi_{p,\sigma}c_{p,\sigma}\,e^{-\frac{i}{\hbar}(px-E_{p,\sigma}t)}\\
&= \int d^3x\int d^3p\sum_{\sigma=0}^{3}\int d^3p'\sum_{\sigma'=0}^{3}\\
&\quad c^+_{p',\sigma'}\psi^*_{p',\sigma'}\left(\sum_{j=1}^{3}-i\hbar c\,\alpha_j\partial_j+mc^2\alpha_4\right)\psi_{p,\sigma}c_{p,\sigma}\,e^{-\frac{i}{\hbar}(p-p')x}\,e^{\frac{i}{\hbar}(E_{p,\sigma}-E_{p',\sigma'})t}.
\end{aligned} \tag{3.116}$$

The integral over x turns the exponential of $p - p'$ into a δ distribution, which allows us to carry out the integral over p'.

$$\begin{aligned} H_\psi = &\int d^3p \sum_{\sigma=0}^{3} \int d^3p' \sum_{\sigma'=0}^{3} \\ &c^+_{p',\sigma'} \psi^*_{p',\sigma'} \left(\sum_{j=1}^{3} -i\hbar c\, \alpha_j \partial_j + mc^2 \alpha_4 \right) \psi_{p,\sigma}\, c_{p,\sigma}\, \delta(p-p') e^{\frac{i}{\hbar}(E_{p,\sigma} - E_{p',\sigma'})t} \\ = &\int d^3p \sum_{\sigma=0}^{3} \sum_{\sigma'=0}^{3} c^+_{p,\sigma'} \psi^*_{p,\sigma'} \left(\sum_{j=1}^{3} -i\hbar c\, \alpha_j \partial_j + mc^2 \alpha_4 \right) \psi_{p,\sigma} c_{p,\sigma}\, e^{\frac{i}{\hbar}(E_{p,\sigma} - E_{p,\sigma'})t}. \end{aligned} \tag{3.117}$$

$\psi_{p,\sigma}$ is an eigenvector of the momentum matrix

$$P = \sum_{j=1}^{3} -i\hbar c\, \alpha_j \partial_j + mc^2 \alpha_4. \tag{3.118}$$

Thus the momentum matrix does not affect the orthogonality of $\psi_{p,\sigma}$ and $\psi^*_{p,\sigma'}$ for $\sigma \neq \sigma'$. This allows us to carry out the sum over σ', which removes the explicit time dependency and gives us the many-particle Hamiltonian operator for free fermions,

$$H_\psi = \int d^3p \sum_{\sigma=0}^{3} c^+_{p,\sigma} \psi^*_{p,\sigma} \left(\sum_{j=1}^{3} -i\hbar c\, \alpha_j \partial_j + mc^2 \alpha_4 \right) \psi_{p,\sigma} c_{p,\sigma}. \tag{3.119}$$

Again, before we carry on, let's try to understand how this operator works. What exactly does this Hamiltonian operator map to what, and what does that mean physically?

Of course, being a Hamiltonian operator for many fermions, it maps a many-fermion state to another many-fermion state.

- The $c_{p,\sigma}$ on the right extracts the coefficient wave function $\psi_\sigma(p,t)$ from the many-fermion state $\psi(x,t)$ (see eq. 3.113) it acts on.
- Multiplication of that component, a complex number, by the momentum eigenstate amplitude vector $\psi_{p,\sigma}$ turns it into a spinor.
- The momentum matrix propagates that spinor, just as it does in the free Dirac equation, turning it into another spinor.
- After that, multiplication by $\psi^*_{p,\sigma}$ extracts one component, a complex number.
- Finally, $c^+_{p,\sigma}$ inserts that complex number as a component into the coefficient wave function of the resulting many-fermion wave function.

In other words, our many-particle Hamiltonian H_ψ acts on the coefficient wave function $\psi(x,t)$ just like the single-particle Hamiltonian of the Dirac equation acts on a single-particle wave function. The behaviour of free fermions in the many-particle case is precisely the same as in the one-particle case.

The only new thing is the vacuum state, which gets mapped to zero. With a zero on the right-hand side of the Schrödinger equation, this state does not change at all, so it doesn't contribute anything physically interesting.

The interesting things happen in the interaction between fermions and photons.

3.4 Interaction Between Fermions and Photons

Now, after we have quantised the electromagnetic field, and after we have applied second quantisation to the free Dirac equation, we can proceed to quantum electrodynamics, the science of the interaction between fermions and photons, the indistinguishable particles which resulted from both quantisations.

The recipe is the second quantisation of the interaction Hamiltonian, which we obtain from the Lagrangian. The steps are:

- Derive the interaction Hamiltonian from the Lagrangian of quantum electrodynamics.
- Insert the field operators into the Hamiltonian.

The result will be the Hamiltonian operator of quantum electrodynamics, which describes the interaction between fermions and photons.

After that, the next steps could be to set up the Schrödinger equation, to prepare a wave function of fermions and photons, and to study its time development. This will the subject of the next chapter, and it will be the main result of this work.

In this section we will instead have a brief look on time-ordered perturbation theory, the traditional approach to quantum electrodynamics and to quantum field theory in general.

3.4.1 The Hamiltonian of Quantum Electrodynamics

To obtain the Hamiltonian of quantum electrodynamics, we set up its Lagrangian and apply a Legendre transform.

So far we have met the Lagrangian densities of the free Dirac equation,

$$\mathcal{L}_\psi = \bar{\psi}\left(\sum_{\mu=0}^{3} i\hbar c\,\gamma_\mu\partial_\mu - mc^2\right)\psi \tag{3.120}$$

and of classical electrodynamics

$$\mathcal{L}_A = -\tfrac{1}{4\mu_0}F_{\mu\nu}F^{\mu\nu}. \tag{3.121}$$

To have both in one Lagrangian, we can simply add them. To account for the interaction between both fields, we apply the minimal coupling $p_\mu \mapsto p_\mu - qA_\mu$. The result is the Lagrangian of quantum electrodynamics,

$$\begin{aligned}\mathcal{L} &= \bar{\psi}\left(\sum_{\mu=0}^{3}\gamma_\mu(i\hbar c\,\partial_\mu - qcA_\mu) - mc^2\right)\psi - \tfrac{1}{4\mu_0}F_{\mu\nu}F^{\mu\nu}. \\ &= \mathcal{L}_\psi + \mathcal{L}_A + \mathcal{L}_J \end{aligned}\tag{3.122}$$

with the new term

$$\mathcal{L}_J = \bar{\psi}\left(qc\sum_{\mu=0}^{3}\gamma_\mu A_\mu\right)\psi. \tag{3.123}$$

We already have derived the many-particle Hamiltonian densities $\mathcal{H}_\psi$ and $\mathcal{H}_A$ from $\mathcal{L}_\psi$ and $\mathcal{L}_A$. Let's complete the job and do the same for $\mathcal{L}_J$.

Since $\mathcal{L}_J$ does does not explicitly depend on any derivatives of its variables, its Legendre transform, the interaction Hamiltonian density of quantum electrodynamics, reads

$$\mathcal{H}_J = -\mathcal{L}_J = \bar{\psi}\left(-qc\sum_{\mu=0}^{3}\gamma_\mu A_\mu\right)\psi = \psi^*\left(-qc\sum_{\mu=0}^{3}\gamma_0\gamma_\mu A_\mu\right)\psi. \tag{3.124}$$

We substitute the field operators for ψ^*, ψ, and A_μ, and obtain

$$\begin{aligned}
\mathcal{H}_J &= \hat{\psi}^*(x,t)\left(-qc\sum_{\mu=0}^{3}\gamma_0\gamma_\mu\hat{A}_\mu\right)\hat{\psi}(x,t) \\
&= \left(\int d^3p'\sum_{\sigma'=0}^{3} c^+_{p',\sigma'}\psi^*_{p',\sigma'}\, e^{\frac{i}{\hbar}(p'x-E_{p',\sigma'}t)}\right) \\
&\quad \left(-qc\sum_{\mu=0}^{3}\gamma_0\gamma_\mu\int d^3k\,\sqrt{\tfrac{\hbar\mu_0c^2}{2\omega_k}}\left(a_{k,\mu}\, e^{i(kx-\omega_kt)} + a^+_{k,\mu}\, e^{-i(kx-\omega_kt)}\right)\right) \\
&\quad \left(\int d^3p\sum_{\sigma=0}^{3}\psi_{p,\sigma}c_{p,\sigma}\, e^{-\frac{i}{\hbar}(px-E_{p,\sigma}t)}\right) \\
&= -qc\int d^3p'\sum_{\sigma'=0}^{3}\int d^3p\sum_{\sigma=0}^{3}\int d^3k\sum_{\mu=0}^{3} c^+_{p',\sigma'}\psi^*_{p',\sigma'}\, e^{\frac{i}{\hbar}(p'x-E_{p',\sigma'}t)} \\
&\qquad\qquad \gamma_0\gamma_\mu\sqrt{\tfrac{\hbar\mu_0c^2}{2\omega_k}}\left(a_{k,\mu}\, e^{i(kx-\omega_kt)} + a^+_{k,\mu}\, e^{-i(kx-\omega_kt)}\right) \\
&\qquad\qquad \psi_{p,\sigma}c_{p,\sigma}\, e^{-\frac{i}{\hbar}(px-E_{p,\sigma}t)}.
\end{aligned} \tag{3.125}$$

Now we could integrate over x, set up the full Hamiltonian operator of quantum electrodynamics, $H = H_\psi + H_A + H_J$, and use it in a Schrödinger equation. We are postponing this to chapter 4.

At this point, the traditional approach to quantum electrodynamics is a different one, time-ordered perturbation theory. Since there is plenty of literature about this method (see, for instance, [9, chapter VIII]), the following subsection 3.4.2 will only give a brief introduction.

3.4.2 Time-Ordered Perturbation Theory

Solving the Schrödinger equation for $H = H_\psi + H_A + H_J$ is nontrivial, even with the aid of computers. The following perturbative approach renders the problem manageable, even analytically. It was developed at the end of the 1940s by Dyson, Feynman, Stückelberg, *et al.*

The results of these calculations are consistent with experimental results up to a very high accuracy, both in explaining new experimental findings as well as in correctly predicting new phenomena. It got extended from quantum electrodynamics, which describes electrons, positrons, and electromagnetic interaction, to the Standard Model of particle physics, describing quarks and leptons, electroweak and strong (gluon) interaction, and the Higgs mechanism. It is the most successful theory ever developed in physics.

Time-ordered perturbation theory treats the interaction H_J as a small perturbation of the free time development $H_0 = H_\psi + H_A$ and as a time-dependent operator $H_J(t)$, which acts on a time-dependent wave function $\Psi(t)$. This picture, where both the operators and the wave functions can be time-dependent, is the *interaction picture* (or *Dirac picture*) of quantum theory.

Fortunately, we already have the time-dependent operators at hand. When we calculated the operators H_ψ, H_A, and H_J (with H_J only as a Hamiltonian density $\mathcal{H}_J$ so far), we substituted time-dependent field operators for the one-particle wave functions in the single-particle Hamiltonians, thus already constructing time-dependent operators. (In fact this explicit time dependency went away when we calculated H_ψ and H_A, so these operators are the same in the Schrödinger and the interaction picture. H_J, however, remains time-dependent.)

Equivalently, we could have constructed our field operators as time-independent operators. Then we would get the time-dependent $H_J(t)$ from the time-independent $H_J(0)$ via

$$H_J(t) = e^{\frac{i}{\hbar}H_0 t}\, H_J(0)\, e^{-\frac{i}{\hbar}H_0 t}. \tag{3.126}$$

We are now interested in calculating scattering amplitudes, which can be compared to experimental results. For this purpose we let an initial many-particle state evolve and calculate the amplitude to obtain a specific final state.

As an example, let the initial state consist of two fermions (such as electrons) in specific momentum eigenstates p_i, σ_1 and p_2, σ_2. Then the initial many-particle wave function reads

$$\Psi(t_0) = c^+_{p_2,\sigma_2} c^+_{p_1,\sigma_1} |0\rangle\,. \tag{3.127}$$

We let this two-fermion state evolve for some time $t_1 - t_0$ and let the fermions interact. After that we probe the many-particle wave function for specific states, for instance states which again consist of two fermions in momentum eigenstates, p_3, σ_3 and p_4, σ_4. We get the amplitude

$$S = \langle 0|\, c_{p_3,\sigma_3} c_{p_4,\sigma_4} \Psi(t_1) \tag{3.128}$$

for a scattering event with ingoing momentum eigenstates p_1, σ_1 and p_2, σ_2 and with outgoing momentum eigenstates p_3, σ_3 and p_4, σ_4. This is called *Møller scattering*.

The problem is how to calculate $\Psi(t_1)$ from $\Psi(t_0)$.

In the Schrödinger picture (see next chapter), the solution is to solve the Schrödinger equation

$$i\hbar \tfrac{\partial}{\partial t}\Psi(t) = (H_0 + H_J)\Psi(t). \tag{3.129}$$

In the interaction picture, the free evolution has already been taken account of in the explicit time dependency of $H_J(t)$. Thus eq. 3.129 simplifies to

$$i\hbar \tfrac{\partial}{\partial t}\Psi(t) = H_J(t)\Psi(t) \tag{3.130}$$

(with a different $\Psi(t)$, yet containing the same information).

With a time-independent H_J, the solution would be

$$\Psi(t_1) = e^{-\frac{i}{\hbar}(t_1 - t_0)H_J}\Psi(t_0). \tag{3.131}$$

This does not work with a time-dependent H_J, except when the time interval $t_1 - t_0$ is infinitesimal. If $H_J(t)$ was an ordinary function, we could repair this by using an integral instead of a plain multiplication,

$$\Psi(t_1) = \exp\left(-\tfrac{i}{\hbar}\int_{t_0}^{t_1} H_J(t)\, dt\right)\Psi(t_0). \tag{3.132}$$

However this makes use of the property $e^{x+y} = e^x\, e^y$, which only holds when x and y commute. $H_J(t)$, however, contains ladder operators, which don't commute.

Time-ordered perturbation theory solves this problem by expanding the exponential to its power series up to the order we are interested in. Then we apply, in each term of the expansion, the commutator rules for the ladder operators inside $H_J(t)$ to arrange them in the correct time order. This is called a *time-ordered product* and written using a symbolic "operator" $\mathcal{T}$,

$$\Psi(t_1) = \mathcal{T}\left(\exp\left(-\tfrac{i}{\hbar}\int_{t_0}^{t_1} H_J(t)\, dt\right)\right)\Psi(t_0)$$

$$= \left(\sum_{j=0}^{\infty} \frac{\left(-\frac{i}{\hbar}\right)^j}{j!} \mathcal{T} \left(\int_{t_0}^{t_1} H_J(t)\, dt \right)^j \right) \Psi(t_0). \tag{3.133}$$

Now we can use this to calculate the scattering amplitude

$$\begin{aligned} S &= \langle 0 |\, c_{p_3,\sigma_3} c_{p_4,\sigma_4} \Psi(t_1) \\ &= \langle 0 |\, c_{p_3,\sigma_3} c_{p_4,\sigma_4} \left(\sum_{j=0}^{\infty} \frac{\left(-\frac{i}{\hbar}\right)^j}{j!} \mathcal{T} \left(\int_{t_0}^{t_1} H_J(t)\, dt \right)^j \right) c^+_{p_2,\sigma_2} c^+_{p_1,\sigma_1} |0\rangle \,. \end{aligned} \tag{3.134}$$

The remaining problem is to calculate the time-ordered j-fold product of an integral with itself. For this purpose we insert the interaction Hamiltonian operator

$$H_J(t) = \int d^3x\ \mathcal{H}_J, \tag{3.135}$$

with $\mathcal{H}_J$ as in eq. 3.125, into the expression for the scattering amplitude, eq. 3.134. We obtain

$$\begin{aligned} S = \langle 0 |\, c_{p_3,\sigma_3} c_{p_4,\sigma_4} \Bigg(\sum_{j=0}^{\infty} \frac{\left(-\frac{i}{\hbar}\right)^j}{j!} \mathcal{T} \Bigg(\int_{t_0}^{t_1} dt \int d^3x \\ (-qc) \int d^3p' \sum_{\sigma'=0}^{3} \int d^3p \sum_{\sigma=0}^{3} \int d^3k \sum_{\mu=0}^{3} c^+_{p',\sigma'} \psi^*_{p',\sigma'}\, e^{\frac{i}{\hbar}(p'x - E_{p',\sigma'}t)}\, \gamma_0 \gamma_\mu \\ \sqrt{\tfrac{\hbar\mu_0 c^2}{2\omega_k}} \Big(a_{k,\mu}\, e^{i(kx-\omega_k t)} + a^+_{k,\mu}\, e^{-i(kx-\omega_k t)} \Big) \psi_{p,\sigma} c_{p,\sigma}\, e^{-\frac{i}{\hbar}(px - E_{p,\sigma}t)} \Bigg)^j \Bigg) c^+_{p_2,\sigma_2} c^+_{p_1,\sigma_1} |0\rangle \,. \end{aligned} \tag{3.136}$$

For each j in the sum, this expression contains the product of $2j+4$ fermionic ladder operators, two for the ingoing state $c^+_{p_2,\sigma_2} c^+_{p_1,\sigma_1} |0\rangle$, two for the outgoing state $\langle 0 |\, c_{p_3,\sigma_3} c_{p_4,\sigma_4}$, and two "inner" ones, $c^+_{p',\sigma'}$ and $c_{p,\sigma}$, for each copy of $\mathcal{H}_J$ inside the jth power of the integral.

When two integrals of $\mathcal{H}_J$ get multiplied, only those combinations of ladder operators contribute a nonzero result, where a $c_{p,\sigma}$ meets a $c^+_{p,\sigma}$ for the same p, σ. This is because the whole expression acts on the vacuum state, both on the left and on the right, and the combination $c_{p,\sigma} c^+_{p,\sigma}$ is the anti-number operator, which maps the vacuum state to itself and everything else to zero. This procedure of combining ladder operators is called *contraction*.

All nonzero contributions can be imagined as "paths" from the ingoing state to the outgoing one. Spelling out the sum over j in S,

$$S = \sum_{j=0}^{\infty} \frac{\left(-\frac{i}{\hbar}\right)^j}{j!} S_j, \tag{3.137}$$

the contributions of order j are of the type

$$S_0 = \langle 0 |\, c_{p_3,\sigma_3} c_{p_4,\sigma_4} \cdots c^+_{p_2,\sigma_2} c^+_{p_1,\sigma_1} |0\rangle \,, \tag{3.138}$$

$$\begin{aligned} S_1 = {} & \langle 0 |\, c_{p_3,\sigma_3} c_{p_4,\sigma_4} \cdots c^+_{p'=p_4,\sigma'=\sigma_4} \gamma\, c_{p=p_2,\sigma=\sigma_2} \cdots c^+_{p_2,\sigma_2} c^+_{p_1,\sigma_1} |0\rangle \\ & + \langle 0 |\, c_{p_3,\sigma_3} c_{p_4,\sigma_4} \cdots c^+_{p'=p_3,\sigma'=\sigma_3} \gamma\, c_{p=p_1,\sigma=\sigma_1} \cdots c^+_{p_2,\sigma_2} c^+_{p_1,\sigma_1} |0\rangle \\ & + \langle 0 |\, c_{p_3,\sigma_3} c_{p_4,\sigma_4} \cdots c^+_{p'=p_3,\sigma'=\sigma_3} \gamma\, c_{p=p_2,\sigma=\sigma_2} \cdots c^+_{p_2,\sigma_2} c^+_{p_1,\sigma_1} |0\rangle \\ & + \langle 0 |\, c_{p_3,\sigma_3} c_{p_4,\sigma_4} \cdots c^+_{p'=p_4,\sigma'=\sigma_4} \gamma\, c_{p=p_1,\sigma=\sigma_1} \cdots c^+_{p_2,\sigma_2} c^+_{p_1,\sigma_1} |0\rangle \,. \end{aligned} \tag{3.139}$$

At this point we can already see that S_0 is zero except when the ingoing and the outgoing states coincide. Also it can be shown that S_1 is always zero (see exercise 3.11).

For $j = 2$ there are two integrals over p and p', each. We rename the new ones to p'' and p'''. To save space, we drop the indices σ, considering them included in p.

$$\begin{aligned} S_2 = &\langle 0| c_{p_3} c_{p_4} \cdots c^+_{p'=p_4} \gamma\, c_{p=p_2} \cdots c^+_{p'''=p_3} \gamma\, c_{p''=p_1} \cdots c^+_{p_2} c^+_{p_1} |0\rangle \\ &+ \langle 0| c_{p_3} c_{p_4} \cdots c^+_{p'=p_3} \gamma\, c_{p=p_1} \cdots c^+_{p'''=p_4} \gamma\, c_{p''=p_2} \cdots c^+_{p_2} c^+_{p_1} |0\rangle \\ &+ \langle 0| c_{p_3} c_{p_4} \cdots c^+_{p'=p_3} \gamma\, c_{p=p_2} \cdots c^+_{p'''=p_4} \gamma\, c_{p''=p_1} \cdots c^+_{p_2} c^+_{p_1} |0\rangle \\ &+ \langle 0| c_{p_3} c_{p_4} \cdots c^+_{p'=p_4} \gamma\, c_{p=p_1} \cdots c^+_{p'''=p_3} \gamma\, c_{p''=p_2} \cdots c^+_{p_2} c^+_{p_1} |0\rangle \,. \end{aligned} \tag{3.140}$$

(This example intentionally uses the same order as the example in [9, § 73], where the scattering amplitude is actually calculated.)

Figure 3.1 illustrates the "paths" from the ingoing to the outgoing states corresponding to the four rows of eq. 3.140. In the figure the paths go from left to right; in the equation the ingoing state is on the right, and the paths go to the left.

Contracting the operators is only possible when they are neighbours in the product. Since all p and σ in this expression are different, the fermionic ladder operators from different field operators are independent, so they anticommute. Since each field operator contains two ladder operators, the field operators commute, and we can sort them as we need them. However when we swap the ladder operators in the ingoing or outgoing states, we get a factor of -1.

This means that we can, while contracting ladder operators, change the order of the inner field operators "on the fly", but when we change the order of the ladder operators of the ingoing or outgoing states, we must keep track of the sign.

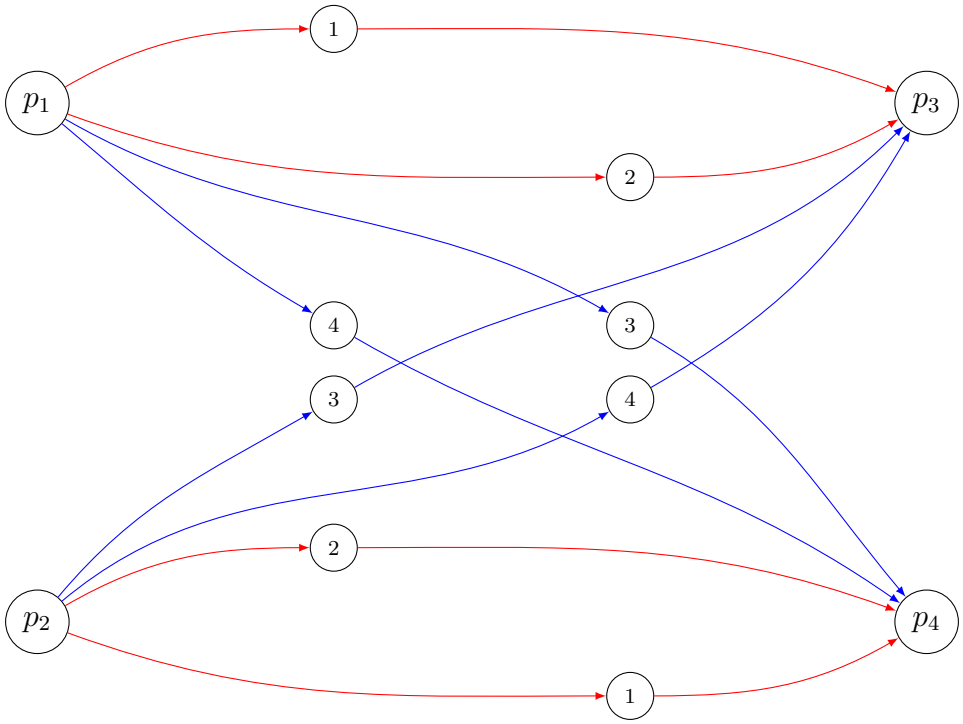

Figure 3.1: "Paths" from the ingoing to the outgoing state for S_2

The numbers correspond to the rows in eq. 3.140 and 3.141. The horizontal alignment is reversed with respect to the equations. Red lines correspond to the left Feynman diagram in fig. 3.2, blue lines to the right one.

It turns out that we must flip the ladder operators of the ingoing states on the right in the lower two lines,

$$\begin{aligned} S_2 = &\langle 0| \, c_{p_3} c_{p_4} \cdots c^+_{p'=p_4} \gamma \, c_{p=p_2} \cdots c^+_{p'''=p_3} \gamma \, c_{p''=p_1} \cdots c^+_{p_2} c^+_{p_1} \, |0\rangle \\ &+ \langle 0| \, c_{p_3} c_{p_4} \cdots c^+_{p'=p_3} \gamma \, c_{p=p_1} \cdots c^+_{p'''=p_4} \gamma \, c_{p''=p_2} \cdots c^+_{p_2} c^+_{p_1} \, |0\rangle \\ &- \langle 0| \, c_{p_3} c_{p_4} \cdots c^+_{p'=p_3} \gamma \, c_{p=p_2} \cdots c^+_{p'''=p_4} \gamma \, c_{p''=p_1} \cdots c^+_{p_1} c^+_{p_2} \, |0\rangle \\ &- \langle 0| \, c_{p_3} c_{p_4} \cdots c^+_{p'=p_4} \gamma \, c_{p=p_1} \cdots c^+_{p'''=p_3} \gamma \, c_{p''=p_2} \cdots c^+_{p_1} c^+_{p_2} \, |0\rangle \, . \end{aligned} \tag{3.141}$$

After this we can contract all ladder operators. In the two upper lines we first contract p_4 and p_2 and then p_3 and p_1. In the two lower lines, after having swapped the ladder operators in the ingoing state, we first contract p_4 and p_1 and then p_3 and p_2.

The two positive and the two negative contributions only differ among each other by the names of their inner indices, thus we can combine them,

$$\begin{aligned} S_2 = &\, 2 \, \langle 0| \, c_{p_3} c_{p_4} \cdots c^+_{p'=p_4} \gamma \, c_{p=p_2} \cdots c^+_{p'''=p_3} \gamma \, c_{p''=p_1} \cdots c^+_{p_2} c^+_{p_1} \, |0\rangle \\ &- 2 \, \langle 0| \, c_{p_3} c_{p_4} \cdots c^+_{p'=p_3} \gamma \, c_{p=p_2} \cdots c^+_{p'''=p_4} \gamma \, c_{p''=p_1} \cdots c^+_{p_1} c^+_{p_2} \, |0\rangle \, . \end{aligned} \tag{3.142}$$

(Of course one has to verify that the factors abbreviated "$\cdots$" match, too.)

This leaves us with two types of contributions to S_2.

From order $j = 3$ on it gets much more complicated since there are multiple ways to contract the inner ladder operators. Then the time-ordering becomes relevant, too: When two inner ladder operators get contracted, the one with the earlier time must be on the right of the one with the later time.

In order not to lose overview, symbols have been developed to keep track of the different types of contributions, *Feynman diagrams*.

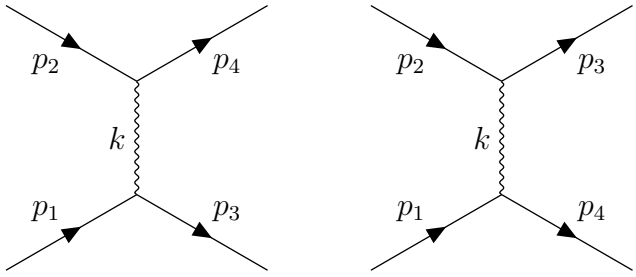

Figure 3.2: Second-order Feynman diagrams for Møller scattering

Figure 3.2 shows the Feynman diagrams for the positive (left) and the negative (right) contribution to S_2. The arrow lines visualise which fermionic ladder operators get contracted with which partners. The wavy lines visualise contributions by the photons, which we haven't discussed above; they are simply part of the "$\cdots$".

There are elaborate rules for working with Feynman diagrams, which make it possible to keep the overview over all contributions to the scattering amplitude even for higher orders.

Furthermore, Feynman diagrams provide an interpretation of the interaction between particles and waves, which accommodates human intuition. For instance the Feynman diagrams in fig. 3.2 can be interpreted as a fermion emitting a photon, which is then absorbed by another fermion. This intuitive approach can be helpful in the interpretation of the results.

Now how to calculate the scattering amplitude?

After having calculated all contributions to S up to the desired order, we can substitute them for $\mathcal{H}_J$ in eq. 3.136. After that we let $t_0 \to -\infty$ and $t_1 \to \infty$, and we carry out the integrals over t and x, thus integrating over spacetime. Then the exponentials coming from $\mathcal{H}_J$ turn into four-dimensional δ distributions, which enable us to carry out more integrals. In many cases, including our example of second-order Møller scattering, the result can even be calculated analytically.

This brief introduction omits several important aspects of time-ordered perturbation theory, most prominently the handling of anti-fermions. This specific problem will be addressed, using other, but related means, in the next chapter, section 4.4. For other aspects of time-ordered perturbation theory, please refer to literature. (See, for instance, [9, chapters VIII–XIV].)

As written above, this method is extremely successful. Does it have any downsides?

When it comes to higher orders, some of the integrals produced by time-ordered perturbation theory diverge. To solve this problem, a method named *renormalisation* has been developed, which makes it possible to extract useful information even from the diverging integrals.

The main drawback of time-ordered perturbation theory is that it cannot, as of 2021, be successfully applied to gravity. So far all attempts have led to nonrenormalisable divergences.

The next chapter will describe a new method for doing calculations with many-particle quantum fields, which is compatible with gravity.

▶ **Exercise 3.10:** Prove eq. 3.130.

Hint: Use variation of parameters.

Solution: Following the method of variation of parameters we decompose $\Psi(t)$ into solutions of the homogeneous differential equation. In the fermionic case these are momentum eigenstates, thus we denote them $\psi_p(t)$ or $|p\rangle$.

Then we substitute the ansatz with time-dependent coefficients $C_p(t)$,

$$\Psi(t) = \int d^3p \; C_p(t)\psi_p(t), \tag{3.143}$$

into the full Schrödinger equation, eq. 3.129, obtaining

$$\begin{aligned}
(H_0 + H_J)\Psi(t) &= \int d^3p \; (H_0 + H_J)\, C_p(t)\, \psi_p(t) \\
&= \int d^3p \int d^3p' \; E_{p,\sigma}\, C_p(t)\, |p\rangle + C_p(t)\, |p'\rangle \langle p'| \, H_J \, |p\rangle \\
&= \int d^3p \int d^3p' \; E_{p,\sigma}\, C_p(t)\psi_p(t) + C_p(t)\psi_{p'}(t) \langle p'| \, H_J \, |p\rangle \,, \qquad (3.144) \\
i\hbar\tfrac{\partial}{\partial t}\Psi(t) &= i\hbar\tfrac{\partial}{\partial t} \int d^3p \; C_p(t)\, \psi_p(t) \\
&= i\hbar \int d^3p \; \tfrac{\partial}{\partial t}\big(C_p(t)\, \psi_p(t)\big) \\
&= i\hbar \int d^3p \; \tfrac{\partial}{\partial t} C_p(t)\, \psi_p(t) - \tfrac{i}{\hbar} E_{p,\sigma}\, C_p(t)\, \psi_p(t) \\
&= \int d^3p \; i\hbar\tfrac{\partial}{\partial t} C_p(t)\, \psi_p(t) + E_{p,\sigma}\, C_p(t)\, \psi_p(t). \qquad (3.145)
\end{aligned}$$

Equating the coefficients yields

$$i\hbar\tfrac{\partial}{\partial t}C_p(t) + E_{p,\sigma}\, C_p(t) \;= E_{p,\sigma}\, C_p(t) + \int d^3p'\; C_{p'}(t)\, \langle p|\, H_J\, |p'\rangle \tag{3.146}$$

and thus

$$i\hbar\tfrac{\partial}{\partial t}C_p(t) = \int d^3p'\; C_{p'}(t)\, \langle p|\, H_J\, |p'\rangle\,, \tag{3.147}$$

or, identifying $C_p(t)$ as the coefficients of our new $\Psi(t)$,

$$i\hbar\tfrac{\partial}{\partial t}\, \langle p|\Psi\rangle = \int d^3p'\, \langle p|\, H_J\, |p'\rangle\, \langle p'|\Psi\rangle\,, \tag{3.148}$$

or

$$i\hbar\tfrac{\partial}{\partial t}\Psi(t) = H_J(t)\Psi(t). \quad \square \tag{3.149}$$

Remark: When we decompose $\Psi(t)$ into time-independent versions ψ_p of $\psi_p(t)$, i. e. solutions of the time-independent Schrödinger equation $H_0\Psi(t) = E\,\Psi(t)$ rather than the homogeneous time-dependent Schrödinger equation $i\hbar\frac{\partial}{\partial t}\Psi(t) = H_0\Psi(t)$, the result is

$$i\hbar\tfrac{\partial}{\partial t}\,\Psi(t) = e^{\frac{i}{\hbar}H_0 t} H'_J(t)\, e^{-\frac{i}{\hbar}H_0 t}\,\Psi(t) \tag{3.150}$$

instead of eq. 3.130, where $H'_J(t)$ denotes the representation of $H_J(t)$ in the basis of the time-independent ψ_p.

▶ **Exercise 3.11:** Explain why S_1 is zero.

Hint: Consider the photons.

Solution: The factors "$\cdots$" in the expression for S_1 contain photonic ladder operators, either $a_{k,\mu}$ or $a^+_{k,\mu}$. The contribution of $a_{k,\mu}$ can only be nonzero when there is an $a^+_{k,\mu}$ on the right, and the contribution of $a^+_{k,\mu}$ can only be nonzero when there is an $a_{k,\mu}$ on the left. Since we have only fermionic states on both sides, $a_{k,\mu}$ and $a^+_{k,\mu}$ can only provide factors of zero. $\square$

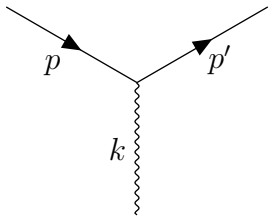

Figure 3.3: Feynman diagram: vertex

Remark: In the language of Feynman diagrams each $c^+_{p,\sigma}a_{k,\mu}c_{p',\sigma'}$ or $c^+_{p,\sigma}a^+_{k,\mu}c_{p',\sigma'}$ is depicted by a *vertex* with three lines as shown in fig. 3.3. The rules for dealing with Feynman diagrams demand that every line, which isn't an ingoing or outgoing state or an external field, must be connected to a vertex. In the case of S_1 this is not possible.

This rule is related to conservation of four-momentum. When we represent the four-momenta symbolically by their spatial components, we can write conservation of four-momentum in the total process as $p_1 + p_2 = p_3 + p_4$. In addition we have, for each application of $\mathcal{H}_J$, a local conservation of four-momentum, which becomes visible when we carry out the integral over spacetime. Then the exponentials turn into four-dimensional δ distributions, which enforce $p' \pm \hbar k - p = 0$ for each application of $\mathcal{H}_J$. In S_1 we apply $\mathcal{H}_J$ just once, so conservation of four-momentum implies $k = 0$, which does not make sense.

Chapter 4

Quantum Electrodynamics in the Schrödinger Picture

In this chapter we develop and implement a new method for calculating the dynamics of many-particle quantum systems. It works in the Schrödinger picture by setting up the many-particle Schrödinger equation and solving it numerically.

This method is very different from time-ordered perturbation theory in that it doesn't expand the exponential in the time development operator into its power series. Instead it works in the eigenbasis of the exponent, thus allowing for a non-perturbative treatment of the exponential. That way the problem boils down to the numeric solution of a nonlinear hyperbolic partial differential equation – just like a numerical approach to general relativity. Thus the extension of this method to include gravity should be straightforward by design. On the other hand it is a nontrivial result of this work that this method can be applied to many-particle quantum field theory at all, in particular to pair annihilation and creation.

Our model system is quantum electrodynamics. Generalisation of this method to other quantum systems, up to the full Standard Model, is expected to be intricate, but possible.

Unlike time-ordered perturbation theory, whose Feynman diagrams look like schematic drawings of colliding particles but describe in fact abstract contractions of ladder operators, this method directly simulates colliding particles in position representation. Its output are many-particle wave functions over spacetime.

4.1 The Hamiltonian of Quantum Electrodynamics in the Schrödinger Picture

In section 3.3 we have calculated the Hamitonian operators of free photons and free fermions,

$$H_A = \int d^3k \sum_{\mu=0}^{3} \tfrac{1}{2}\hbar\omega_k (a^+_{k,\mu} a_{k,\mu} + a_{k,\mu}\, a^+_{k,\mu}) \tag{4.1}$$

and

$$H_\psi = \int d^3p \sum_{\sigma=0}^{3} c^+_{p,\sigma} \psi^*_{p,\sigma} \left(\sum_{j=1}^{3} -i\hbar c\, \alpha_j \partial_j + mc^2 \alpha_4 \right) \psi_{p,\sigma} c_{p,\sigma}. \tag{4.2}$$

Although we substituted time-dependent field operators into the Hamiltonian densities, both Hamiltonian operators turned out time-independent, so we can directly use them in the Schrödinger picture.

To complete the Hamiltonian of quantum electrodynamics, $H = H_\psi + H_A + H_J$, we still need the interaction Hamiltonian H_J.

In subsection 3.4.1 we have calculated the Hamiltonian density $\mathcal{H}_J$ of the interaction between photons and fermions. Again we substituted time-dependent field operators into the Hamiltonian densities. In the calculation of H_ψ and H_A the explicit time dependency vanished in the transition from the Hamiltonian density to the Hamiltonian operator. This time the explicit time dependency is still present in the Hamiltonian density, which makes it suitable for use in the interaction picture as it has been done in subsection 3.4.2. To make it usable in the Schrödinger picture, we substitute $t = 0$, thus transferring the time dependency from the field operators to the wave function.

Our time-independent many-particle interaction Hamiltonian density reads

$$\begin{aligned}
\mathcal{H}_J &= \hat{\psi}^* \left(-qc \sum_{\mu=0}^{3} \gamma_0 \gamma_\mu \hat{A}_\mu \right) \hat{\psi} \\
&= \left(\int d^3p' \sum_{\sigma'=0}^{3} c^+_{p',\sigma'} \psi^*_{p',\sigma'} \, e^{\frac{i}{\hbar} p' x} \right) \\
&\quad \left(-qc \sum_{\mu=0}^{3} \gamma_0 \gamma_\mu \int d^3k \, \sqrt{\tfrac{\hbar \mu_0 c^2}{2\omega_k}} \left(a_{k,\mu} \, e^{ikx} + a^+_{k,\mu} \, e^{-ikx} \right) \right) \\
&\quad \left(\int d^3p \sum_{\sigma=0}^{3} \psi_{p,\sigma} c_{p,\sigma} \, e^{-\frac{i}{\hbar} px} \right) \\
&= -qc \int d^3p' \sum_{\sigma'=0}^{3} \int d^3p \sum_{\sigma=0}^{3} \int d^3k \sum_{\mu=0}^{3} c^+_{p',\sigma'} \psi^*_{p',\sigma'} \, e^{\frac{i}{\hbar} p' x} \\
&\qquad \gamma_0 \gamma_\mu \sqrt{\tfrac{\hbar \mu_0 c^2}{2\omega_k}} \left(a_{k,\mu} \, e^{ikx} + a^+_{k,\mu} \, e^{-ikx} \right) \\
&\qquad \psi_{p,\sigma} c_{p,\sigma} \, e^{-\frac{i}{\hbar} px} \\
&= -qc \int d^3p' \sum_{\sigma'=0}^{3} \int d^3p \sum_{\sigma=0}^{3} \int d^3k \sum_{\mu=0}^{3} \\
&\qquad c^+_{p',\sigma'} \psi^*_{p',\sigma'} \, \gamma_0 \gamma_\mu \sqrt{\tfrac{\hbar \mu_0 c^2}{2\omega_k}} \, a_{k,\mu} \psi_{p,\sigma} c_{p,\sigma} \, e^{\frac{i}{\hbar}(p' + \hbar k - p)x} \\
&\qquad + c^+_{p',\sigma'} \psi^*_{p',\sigma'} \, \gamma_0 \gamma_\mu \sqrt{\tfrac{\hbar \mu_0 c^2}{2\omega_k}} \, a^+_{k,\mu} \psi_{p,\sigma} c_{p,\sigma} \, e^{\frac{i}{\hbar}(p' - \hbar k - p)x}.
\end{aligned} \tag{4.3}$$

We turn the Hamiltonian density with the field operators into a Hamiltonian operator by integrating over x. Again, this integral turns the exponentials into δ distributions which allow us to carry out one further integral. We choose the one over k.

$$\begin{aligned}
H_J &= \int d^3x \, \mathcal{H}_J \\
&= -qc \int d^3p' \sum_{\sigma'=0}^{3} \int d^3p \sum_{\sigma=0}^{3} \int d^3k \sum_{\mu=0}^{3} \\
&\qquad c^+_{p',\sigma'} \psi^*_{p',\sigma'} \, \gamma_0 \gamma_\mu \sqrt{\tfrac{\hbar \mu_0 c^2}{2\omega_k}} \, a_{k,\mu} \psi_{p,\sigma} c_{p,\sigma} \, \delta(p' + \hbar k - p) \\
&\qquad + c^+_{p',\sigma'} \psi^*_{p',\sigma'} \, \gamma_0 \gamma_\mu \sqrt{\tfrac{\hbar \mu_0 c^2}{2\omega_k}} \, a^+_{k,\mu} \psi_{p,\sigma} c_{p,\sigma} \, \delta(p' - \hbar k - p)
\end{aligned}$$

$$= -qc \int d^3p' \sum_{\sigma'=0}^{3} \int d^3p \sum_{\sigma=0}^{3} \sum_{\mu=0}^{3} \\ c^+_{p',\sigma'} \psi^*_{p',\sigma'} \gamma_0 \gamma_\mu \, a_\mu(p-p') \, \psi_{p,\sigma} c_{p,\sigma} \\ + c^+_{p',\sigma'} \psi^*_{p',\sigma'} \gamma_0 \gamma_\mu \, a^+_\mu(p'-p) \, \psi_{p,\sigma} c_{p,\sigma} \tag{4.4}$$

with

$$a_\mu(\hbar k) = \sqrt{\tfrac{\hbar \mu_0 c^2}{2\omega_k}} \, a_{k,\mu} \qquad \text{and} \qquad a^+_\mu(\hbar k) = \sqrt{\tfrac{\hbar \mu_0 c^2}{2\omega_k}} \, a^+_{k,\mu}. \tag{4.5}$$

The right halves of the two lowermost lines in eq. 4.4, together with the integral over p,

$$\int d^3p \; a_\mu(p-p') \, \psi_{p,\sigma} c_{p,\sigma} \qquad \text{and} \qquad \int d^3p \; a^+_\mu(p'-p) \, \psi_{p,\sigma} c_{p,\sigma}, \tag{4.6}$$

are convolutions, i. e. integrals of the type

$$f(p') * g(p') = \int d^3p \, f(p) \, g(p'-p). \tag{4.7}$$

This means that we can apply the convolution theorem

$$\mathcal{F}\big(f(p') * g(p')\big)(x) = (2\pi)^{\frac{3}{2}} \, \mathcal{F}\big(f(p')\big)(x) \, \mathcal{F}\big(g(p')\big)(x) \tag{4.8}$$

to transform the convolutions in momentum representation into point-wise products in position representation,

$$\int d^3p \; a_\mu(p-p') \, \psi_{p,\sigma} c_{p,\sigma} = (2\pi)^{\frac{3}{2}} \, \mathcal{F}^{-1}\Big(\mathcal{F}\big(a_\mu(-p')\big)(x) \, \mathcal{F}\big(\psi_{p',\sigma} c_{p',\sigma}\big)(x)\Big)(p'), \tag{4.9}$$

$$\int d^3p \; a^+_\mu(p'-p) \, \psi_{p,\sigma} c_{p,\sigma} = (2\pi)^{\frac{3}{2}} \, \mathcal{F}^{-1}\Big(\mathcal{F}\big(a^+_\mu(p')\big)(x) \, \mathcal{F}\big(\psi_{p',\sigma} c_{p',\sigma}\big)(x)\Big)(p'). \tag{4.10}$$

Normally, we use a Fourier transform to switch from position to momentum representation and a reverse Fourier transform to switch back. To render eq. 4.9 and 4.10 more compatible with physical intuition, we swap $\mathcal{F}$ and $\mathcal{F}^{-1}$. Then the arguments get minus signs,

$$\int d^3p \; a_\mu(p-p') \, \psi_{p,\sigma} c_{p,\sigma} = (2\pi)^{\frac{3}{2}} \, \mathcal{F}\Big(\mathcal{F}^{-1}\big(a_\mu(p')\big)(x) \, \mathcal{F}^{-1}\big(\psi_{-p',\sigma} c_{-p',\sigma}\big)(x)\Big)(p'), \tag{4.11}$$

$$\int d^3p \; a^+_\mu(p'-p) \, \psi_{p,\sigma} c_{p,\sigma} = (2\pi)^{\frac{3}{2}} \, \mathcal{F}\Big(\mathcal{F}^{-1}\big(a^+_\mu(-p')\big)(x) \, \mathcal{F}^{-1}\big(\psi_{-p',\sigma} c_{-p',\sigma}\big)(x)\Big)(p'). \tag{4.12}$$

With the abbreviations

$$a_{x,\mu} := \mathcal{F}^{-1}\big(a_\mu(p')\big)(x), \tag{4.13}$$

$$a^+_{x,\mu} := \mathcal{F}^{-1}\big(a^+_\mu(-p')\big)(x) = \mathcal{F}^{-1}\big(a_\mu(p')\big)^*(x), \tag{4.14}$$

$$\psi_{x,\sigma} c_{x,\sigma} := \mathcal{F}^{-1}\big(\psi_{-p',\sigma} c_{-p,\sigma}\big)(x) = \mathcal{F}^{-1}\big(\psi^*_{p',\sigma} c_{p,\sigma}\big)^*(x) \tag{4.15}$$

we can write down the time-independent Hamiltonian operator of the interaction between fermions and photons,

$$H_J = -(2\pi)^{\frac{2}{3}} \, qc \int d^3p \sum_{\sigma'=0}^{3} \sum_{\sigma=0}^{3} \sum_{\mu=0}^{3} c^+_{p,\sigma'} \psi^*_{p,\sigma'} \gamma_0 \gamma_\mu \, \mathcal{F}(a_{x,\mu} \psi_{x,\sigma} c_{x,\sigma})(p) \\ + c^+_{p,\sigma'} \psi^*_{p,\sigma'} \gamma_0 \gamma_\mu \, \mathcal{F}\big(a^+_{x,\mu} \psi_{x,\sigma} c_{x,\sigma}\big)(p)$$

$$= -(2\pi)^{\frac{2}{3}}\, qc \int d^3p \sum_{\sigma'=0}^{3} \sum_{\sigma=0}^{3} c^+_{p,\sigma'} \psi^*_{p,\sigma'}\, \mathcal{F}\left(\sum_{\mu=0}^{3} \gamma_0 \gamma_\mu \left(a_{x,\mu} + a^+_{x,\mu} \right) \psi_{x,\sigma} c_{x,\sigma} \right)(p). \tag{4.16}$$

As a crucial improvement compared to eq. 4.4 we have replaced the double integral by a single integral, two Fourier transforms and two point-wise multiplications. This makes it significantly easier to handle H_J numerically.

To apply H_J to a wave function, we must transform the wave function from momentum to position representation, apply the interaction, transform it back, and finally store it back in momentum representation. When n denotes the number of grid points used to store the wave function, the time needed for these calculations is $\mathcal{O}(n \log n)$ for each of the two Fourier transforms and $\mathcal{O}(n)$ for each of the two point-wise multiplications, one in position representation and one in momentum representation. All of this is done in sequence, so the total complexity is $\mathcal{O}(n \log n)$, just like in chapter 2. This is in the range of customary computers.

Without the change of the basis, we would have to compute a double integral in momentum representation, which requires $\mathcal{O}(n^2)$. In that case, as of 2021, even supercomputers could only simulate very small grids.

Although we started our calculations in momentum representation, and although H_J still contains an integral over p, we ended up with the actual interaction taking place in position representation. This makes sense in view of causality. Momentum eigenstates spread over the entire space. A point-wise multiplication in momentum representation affects the particle's wave function everywhere at the same time. A point-wise multiplication in position representation means that all interaction happens locally. Any interaction over a distance needs to be mediated by something travelling that distance, which cannot happen faster than with the speed of light.

There is an important caveat to be considered when acually calculating H_J. Even while we are working in position representation, the indices σ and σ' still denote momentum eigenstates, which aren't directly accessible in position representation.

This is not a problem as long as we don't need to distinguish between these eigenstates. They are still orthogonal in position representation, so we can just perform all calculations on the spinors, knowing that we will be able to decompose them again, when needed, in momentum representation.

However particles and anti-particles are defined as momentum eigenstates with positive and negative kinetic energy. This means that we cannot easily distinguish between particles and anti-particles in position representation. This problem will be addressed in section 4.4.

The next step will be to solve the Schrödinger equation of quantum electrodynamics for the fermions.

4.2 The Impact of the Photons on the Fermions

Since H_ψ and H_J are time-independent, the solution of the fermionic many-particle Schrödinger equation

$$i\hbar \tfrac{\partial}{\partial t}\, \psi(x,t) = (H_\psi + H_J)\, \psi(x,t) \tag{4.17}$$

reads

$$\psi(t + \Delta t) = e^{-\frac{i}{\hbar}(H_\psi + H_J)\Delta t}\, \psi(x,t). \tag{4.18}$$

In chapter 2 we have developed methods, our *quantum Euler method* and its improvements, to address the problem that H_ψ and H_J do not commute. So the problem boils down to computing

$$e^{-\frac{i}{\hbar}H_\psi\,\Delta t}\,\psi(x,t) \qquad \text{and} \qquad e^{-\frac{i}{\hbar}H_J\,\Delta t}\,\psi(x,t) \tag{4.19}$$

separately.

In section 2.2 we already implemented a numerical method how to compute the time development of a free fermion, and in subsection 3.3.3 we have seen that the coefficient function of a free fermionic many-particle wave function precisely obeys the dynamics of a free fermion. So we already know how to compute $e^{-\frac{i}{\hbar}H_\psi\,\Delta t}\,\psi(x,t)$.

The remaining problem is the computation of the impact of the photons on the fermions,

$$\begin{aligned} e^{-\frac{i}{\hbar}H_J\,\Delta t}\,\psi(x,t) = \exp\Bigg(&\tfrac{i}{\hbar}\,(2\pi)^{\frac{2}{3}}\,qc\,\Delta t\int d^3p\sum_{\sigma'=0}^{3}\sum_{\sigma=0}^{3}c^+_{p,\sigma'}\psi^*_{p,\sigma'} \\ &\mathcal{F}\Bigg(\sum_{\mu=0}^{3}\gamma_0\gamma_\mu\left(a_{x,\mu}+a^+_{x,\mu}\right)\psi_{x,\sigma}c_{x,\sigma}\Bigg)(p)\Bigg)\psi(x,t). \end{aligned} \tag{4.20}$$

Although this operator features an integral over p, the actual computation takes place in position representation, inside the Fourier transform. This makes this problem very similar to the one we already solved in subsection 2.2.4, safe for the ladder operators.

As we have seen in subsection 3.3.3, the fermionic ladder operators just tell us to extract the coefficient function from the fermionic many-particle wave function before the operation, and to reinsert the result into a new fermionic many-particle wave function after the operation. This affects our interpretation of the functions involved, but it doesn't affect our calculations – safe for the distinction between fermions and anti-fermions, which will be the subject of section 4.4.

The photonic ladder operators $a_{x,\mu}+a^+_{x,\mu}$ have taken the place of the four-potential A_μ. This is not a surprise since they are the quantised version of A_μ,

$$\sqrt{\tfrac{\hbar\mu_0c^2}{\omega_k}}\left(a_{k,\mu}+a^+_{k,\mu}\right)=A_{k,\mu}+A^*_{k,\mu}, \tag{4.21}$$

but it raises the question what a product of a fermionic wave function and a photonic ladder operator even means.

Physically, this product describes the action of the photons on the fermions, so we want to treat $a_{k,\mu}+a^+_{k,\mu}$ for each μ like a normal real number, the component A_μ of an electromagnetic four-potential.

When we want to treat an operator like a number, we must do our computations in a basis of the eigenstates of the operator. $a^+_{k,\mu}$ does not have any nontrivial eigenstates, but there are eigenstates of $a_{k,\mu}$, the so-called *coherent states*, which will be discussed in section 4.3. So let's assume for now that the photons are, at the wavenumber vector k and in the component μ of the four-potential, in a coherent state $|\alpha_\mu(k)\rangle$, a normalised eigenstate of $a_{k,\mu}$ with eigenvalue $\alpha_\mu(k)$.

Then the expectation value of $a_{k,\mu}$ in the current state of the photons is the complex number

$$\begin{aligned} \langle\alpha_\mu(k)|\,a_{k,\mu}\,|\alpha_\mu(k)\rangle &= \langle\alpha_\mu(k)|\left(a_{k,\mu}\,|\alpha_\mu(k)\rangle\right) \\ &= \langle\alpha_\mu(k)|\left(\alpha_\mu(k)\,|\alpha_\mu(k)\rangle\right) \end{aligned}$$

$$= \alpha_\mu(k) \langle \alpha_\mu(k) | \alpha_\mu(k) \rangle$$
$$= \alpha_\mu(k). \tag{4.22}$$

Likewise we can compute the expectation value of $a^+_{k,\mu}$ as

$$\langle \alpha_\mu(k) | \, a^+_{k,\mu} \, | \alpha_\mu(k) \rangle = \alpha^*_\mu(k). \tag{4.23}$$

So the expectation value of $a_{k,\mu} + a^+_{k,\mu}$ is the real number $\alpha_\mu(k) + \alpha^*_\mu(k)$. Together with the prefactor it reproduces indeed a component A_μ of the electromagnetic four-potential.

So we can compute the action of the photons on the fermions just as if they were a classical electromagnetic field, provided that we succeed to describe the photons via coherent states. As we will see in section 4.3, this is not only possible, but in fact the "natural" description of the photons.

Taken together this means that we can resuse the results of subsection 2.2.4 without any modification to compute eq. 4.20. We just reinterpret the wave functions. The one-fermion wave function becomes the coefficient of a many-fermion wave function, and the classical electromagnetic four-potential becomes a field of coherent states. And as we will see in section 4.3, coherent states obey the Maxwell equations just like a classical electromagnetic field does.

This allows us to postpone the precise formulation of the dynamics of the photons and to study the impact of a field of coherent states on the fermions right away.

Figure 4.1 shows a collision between a field of fermions and a field of photons in position representation, simulated using the method developed in subsection 2.2.4. (Although we have prepared both fields as wave packets, it would we wrong to speak of a collision "between a fermion and a photon". Both wave functions are many-particle wave functions, and a coherent state does not even have a sharp number of particles.)

In the initial state, both wave packets are well-separated. The fermions are travelling right and up, the photons left and up. At about $t = 0.27$, the photons touch the fermions, and their wave functions overlap. At $t = 0.31$ the photons are leaving the fermions again, and we can already see some small parts of a different colour sticking out of the fermionic wave packet. The new colour scheme (white/magenta) indicates that these parts of the fermionic wave function have been transformed to a different momentum eigenstate ($\sigma \geq 2$ instead of $\sigma = 0$), describing anti-fermions. This is not an unexpected result. The Hamiltonian operators H_ψ and H_J of the fermions do not commute, so it is clear that the application of H_J mixes the eigenstates of H_ψ.

In the further time development we can observe anti-fermionic wave packets travelling in the opposite directon of the fermionic wave packets. While this is clearly a non-physical effect arising from the limitations of this method of simulation (which will be fixed in section 4.4), it already shows how interaction between wave packets can look like: Small parts of the original wave packet split off and take a separate path. (In particular there must not be any "leaps" in position representation which would contradict causality.)

Figure 4.2 shows the same simulation in momentum representation.

When the photons touch the fermions at $t = 0.27$, two new wave packets in white/magenta show up, representing anti-fermions. Their positions in momentum space are the mirrored position of the fermionic wave packet plus/minus the momentum of the photons they are colliding with.

Again the mirroring arises from the limitations of this method of simulation and will be fixed in section 4.4. Nevertheless we can already see some interesting effects:

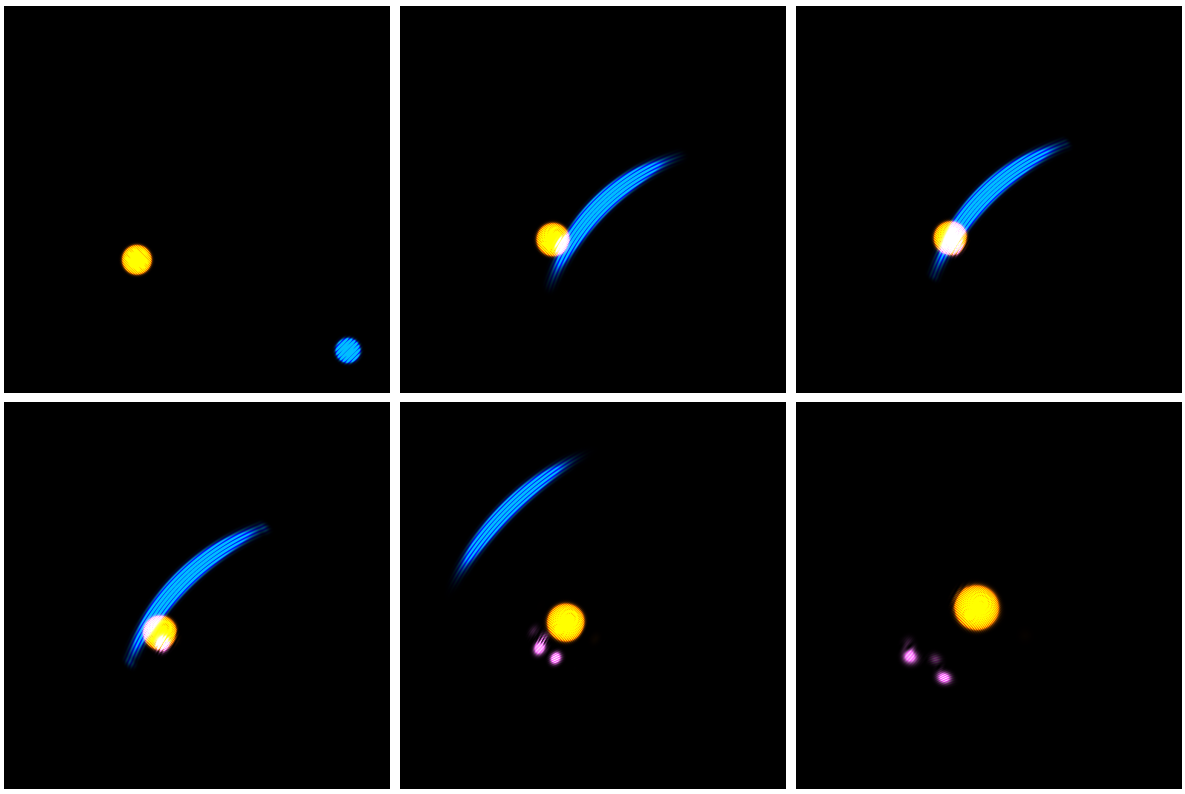

Figure 4.1: Collision between fermions and photons, position representation

From left to right and from top to bottom: $t = 0.00$, 0.27, 0.29, 0.31, 0.45, 0.65.
Numerical parameters: $\hbar = 0.01$, $c = 10$, $m = 1$, $q = 0.05$, 1024×1024 grid points, $\Delta x = 0.005$.
Initial state: fermions (yellow/red): $x = (-0.8, -0.8)$, $p = (1, 1)$, $\sigma = 0$, photons (cyan/blue): $x = (2, -2)$, $\hbar k = (-0.5, 0.5)$. The wave packets in white/magenta describe anti-fermions.
For a discussion of the units, see the subsections 2.1.5 and 4.4.3.

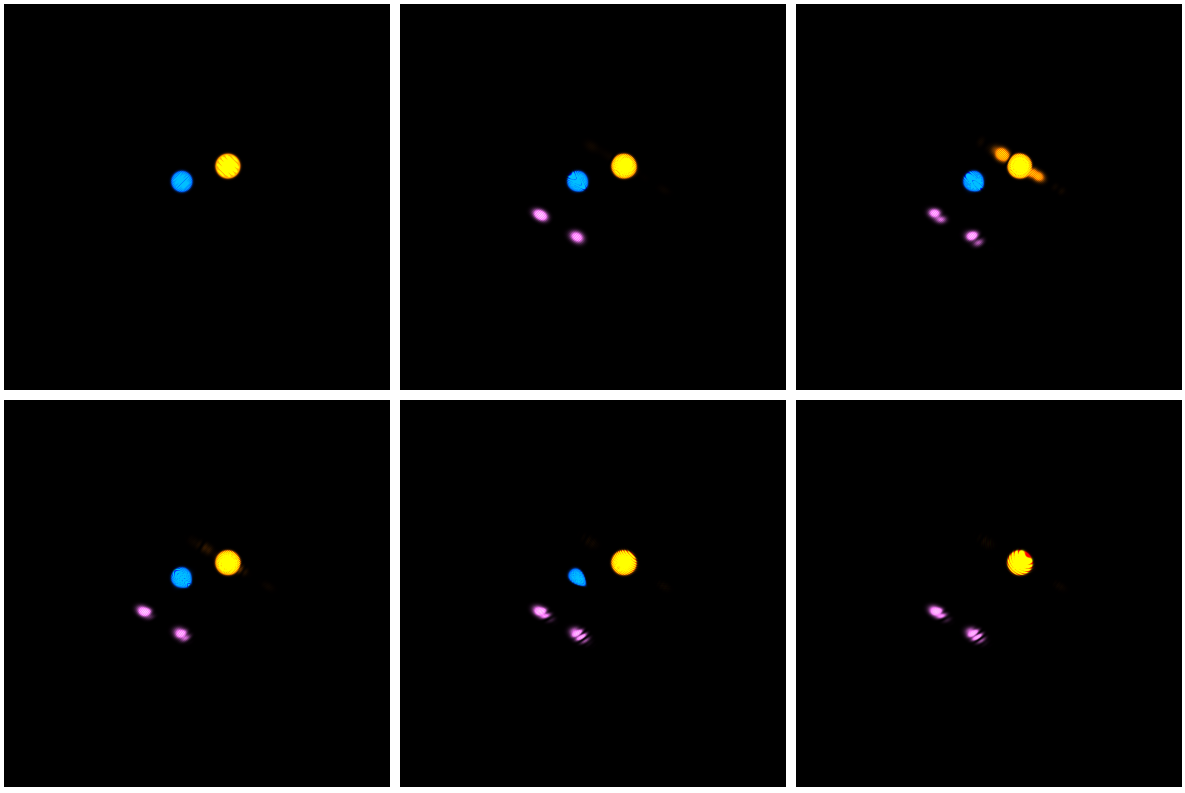

Figure 4.2: Collision between fermions and photons, momentum representation

- The photons can transform fermions into anti-fermions.
- The anti-fermions "materialise" at their new positions in momentum space. They don't travel through momentum space, but they "leap" to their new positions.
- These new positions are the (mirrored) old position plus/minus the momentum of the photons.

So we can observe, in momentum representation, the discrete momentum transfer from the photons to the fermions. This is, in the most literal sense, a *quantum leap*.

The quantum leap is discontinuous in momentum, but it is continuous in time. The "leaping" wave packets do not travel through momentum space, but they grow and shrink gradually.

At $t = 0.29$ two more wave packets have materialised. This time they are fermions rather than anti-fermions, and they show up in the vicinity of the initial momentum of the fermions, again plus/minus the momentum of the photons. And again, the momentum transfer is discrete.

At $t = 0.31$, when the photons have almost left the fermions, the two additional fermionic wave packets have vanished again. They represented a temporary transitional state. (Unlike a virtual transitional state in time-ordered perturbation theory, this transitional state is an actual physical state of the simulated system. In particular it must obey all laws of conservation such as conservation of four-momentum and, for the time being, the conservation of the norms of the wave functions.)

At $t = 0.65$ the photons have been numerically absorbed at the border of the simulated area. Since there is no further interaction, the wave functions of the fermions and the anti-fermions in momentum representation only change by their complex phases.

In summary, we can already observe a quantisation of the momentum transfer from the photons to the fermions, even though we are still using, without any modification, the method developed in subsection 2.2.4 before we introduced second quantisation.

Concerning the fermions, second quantisation only affects the interpretation of the wave function, but not the equations. This reinterpretation will be taken further (and affect the equations) in section 4.4, when we complete our model to include anti-fermions.

The photons act on the fermions via coherent states, which are many-particle states, but they behave like a classical electromagnetic field. The next section will take a closer look at the coherent states and how they are affected by the fermions.

▶ **Exercise 4.1:** Prove eq. 4.23.

Solution:

$$\begin{aligned}
\langle \alpha_\mu(k)|\, a^+_{k,\mu}\, |\alpha_\mu(k)\rangle &= \left(\langle \alpha_\mu(k)|\, a^+_{k,\mu}\right) |\alpha_\mu(k)\rangle \\
&= \left(\langle \alpha_\mu(k)|\, \alpha^*_\mu(k)\right) |\alpha_\mu(k)\rangle \\
&= \alpha^*_\mu(k)\, \langle \alpha_\mu(k)|\alpha_\mu(k)\rangle \\
&= \alpha^*_\mu(k). \quad \square
\end{aligned} \tag{4.24}$$

4.3 Coherent States

In the previous section we have described the photons as a field of coherent states, i. e. of eigenstates of the annihilation operator $a_{k,\mu}$. In this representation we can calculate the impact of the photons on the fermions without approximations. This means that for the purpose of calculating their impact on the fermions we have to decompose the quantised electromagnetic field into coherent states.

Concerning the free development of the photons, we can even stay in the representation of coherent states, since their time-development is well-known,

$$\alpha_\mu(k, t + \Delta t) = e^{-i\omega_k \Delta t} \alpha_\mu(k, t). \tag{4.25}$$

Even more, we already know this equation. As we have seen in subsection 2.3.1, the very same function $\alpha_\mu(k, t)$ is suited to describe the classical electromagnetic field in momentum representation,

$$\alpha_\mu(k, t) := \tilde{A}_\mu(k, t) + \tfrac{i}{\omega_k} \dot{\tilde{A}}_\mu(k, t). \tag{4.26}$$

This shows that an electromagnetic quantum field in a coherent state is "close to" a classical electromagnetic field.

It remains to investigate how the interaction with the fermions influences coherent states.

To find out, we let the time step operator $e^{-\frac{i}{\hbar} H_J \Delta t}$ act on a coherent state, hoping that it won't be too difficult to decompose the result back into coherent states.

For this purpose we recalculate the Hamiltonian operator H_J of the interaction from the Hamiltonian density with the field operators, eq. 4.4. This time we integrate over p' rather than k.

$$\begin{aligned} H_J = -qc \int d^3p' \sum_{\sigma'=0}^{3} \int d^3p \sum_{\sigma=0}^{3} \int d^3k \sum_{\mu=0}^{3} \\ c^+_{p',\sigma'} \psi^*_{p',\sigma'} \gamma_0 \gamma_\mu \sqrt{\tfrac{\hbar \mu_0 c^2}{2\omega_k}}\, a_{k,\mu} \psi_{p,\sigma} c_{p,\sigma}\, \delta(p' + \hbar k - p) \\ + c^+_{p',\sigma'} \psi^*_{p',\sigma'} \gamma_0 \gamma_\mu \sqrt{\tfrac{\hbar \mu_0 c^2}{2\omega_k}}\, a^+_{k,\mu} \psi_{p,\sigma} c_{p,\sigma}\, \delta(p' - \hbar k - p) \\ = -qc \int d^3k \sum_{\mu=0}^{3} \sqrt{\tfrac{\hbar \mu_0 c^2}{2\omega_k}} \int d^3p \sum_{\sigma=0}^{3} \sum_{\sigma'=0}^{3} \\ a_{k,\mu}\, c^+_{\hbar k - p,\sigma'} \psi^*_{\hbar k - p,\sigma'}\, \gamma_0 \gamma_\mu\, \psi_{p,\sigma} c_{p,\sigma} \\ + a^+_{k,\mu}\, c^+_{\hbar k + p,\sigma'} \psi^*_{\hbar k + p,\sigma'}\, \gamma_0 \gamma_\mu\, \psi_{p,\sigma} c_{p,\sigma}. \end{aligned} \tag{4.27}$$

As in subsection 3.4.1 we can identify parts of this double integral as a convolution. We abbreviate

$$\psi^+_\sigma(p) = c^+_{p,\sigma} \psi^*_{p,\sigma}, \tag{4.28}$$

$$\psi_\sigma(p) = \psi_{p,\sigma} c_{p,\sigma} \tag{4.29}$$

and obtain

$$\begin{aligned} H_J = -qc \int d^3k \sum_{\mu=0}^{3} \sqrt{\tfrac{\hbar \mu_0 c^2}{2\omega_k}} \int d^3p \sum_{\sigma'=0}^{3} \sum_{\sigma=0}^{3} a_{k,\mu}\, \psi^+_{\sigma'}(p - \hbar k)\, \gamma_0 \gamma_\mu\, \psi_\sigma(p) \\ - a^+_{k,\mu}\, \psi^+_{\sigma'}(\hbar k - p)\, \gamma_0 \gamma_\mu\, \psi_\sigma(-p) \end{aligned}$$

$$
\begin{aligned}
&= -qc \int d^3k \sum_{\mu=0}^{3} \sqrt{\tfrac{\hbar\mu_0 c^2}{2\omega_k}} \sum_{\sigma'=0}^{3} \sum_{\sigma=0}^{3} \\
&\qquad a_{k,\mu}\, (2\pi)^{\frac{3}{2}}\, \mathcal{F}^{-1}\Big(\mathcal{F}\big(\psi^+_{\sigma'}(-\hbar k)\big)(x)\, \gamma_0\gamma_\mu\, \mathcal{F}\big(\psi_\sigma(\hbar k)\big)(x)\Big)(\hbar k) \\
&\qquad - a^+_{k,\mu}\, (2\pi)^{\frac{3}{2}}\, \mathcal{F}^{-1}\Big(\mathcal{F}\big(\psi^+_{\sigma'}(\hbar k)\big)(x)\, \gamma_0\gamma_\mu\, \mathcal{F}\big(\psi_\sigma(-\hbar k)\big)(x)\Big)(\hbar k) \\
&= -qc\, (2\pi)^{\frac{3}{2}} \int d^3k \sum_{\mu=0}^{3} \sqrt{\tfrac{\hbar\mu_0 c^2}{2\omega_k}} \sum_{\sigma'=0}^{3} \sum_{\sigma=0}^{3} \\
&\qquad a_{k,\mu}\, \mathcal{F}\Big(\mathcal{F}^{-1}\big(\psi^+_{\sigma'}(\hbar k)\big)(x)\, \gamma_0\gamma_\mu\, \mathcal{F}^{-1}\big(\psi_\sigma(-\hbar k)\big)(x)\Big)(\hbar k) \\
&\qquad - a^+_{k,\mu}\, \mathcal{F}\Big(\mathcal{F}^{-1}\big(\psi^+_{\sigma'}(-\hbar k)\big)(x)\, \gamma_0\gamma_\mu\, \mathcal{F}^{-1}\big(\psi_\sigma(\hbar k)\big)(x)\Big)(\hbar k) \\
&= \int d^3k \sum_{\mu=0}^{3} \beta_\mu(k)\, a^+_{k,\mu} - \beta^*_\mu(k)\, a_{k,\mu}
\end{aligned}
\tag{4.30}
$$

with

$$
\begin{aligned}
\beta_\mu(k) = qc\, (2\pi)^{\frac{3}{2}} \sqrt{\tfrac{\hbar\mu_0 c^2}{2\omega_k}} &\sum_{\sigma'=0}^{3} \sum_{\sigma=0}^{3} \\
&\mathcal{F}\Big(\mathcal{F}^{-1}\big(\psi^+_{\sigma'}(-\hbar k)\big)(x)\, \gamma_0\gamma_\mu\, \mathcal{F}^{-1}\big(\psi_\sigma(\hbar k)\big)(x)\Big)(\hbar k)
\end{aligned}
\tag{4.31}
$$

and

$$
\begin{aligned}
\beta^*_\mu(k) = qc\, (2\pi)^{\frac{3}{2}} \sqrt{\tfrac{\hbar\mu_0 c^2}{2\omega_k}} &\sum_{\sigma'=0}^{3} \sum_{\sigma=0}^{3} \\
&\mathcal{F}\Big(\mathcal{F}^{-1}\big(\psi^+_{\sigma'}(\hbar k)\big)(x)\, \gamma_0\gamma_\mu\, \mathcal{F}^{-1}\big(\psi_\sigma(-\hbar k)\big)(x)\Big)(\hbar k).
\end{aligned}
\tag{4.32}
$$

So the interaction Hamiltonian H_J is diagonal in k and μ. To apply it to a field of coherent states, we have to apply two Fourier transforms and a point-wise multiplication to compute $\beta_\mu(k)$ and $\beta^*_\mu(k)$, which takes $\mathcal{O}(n \log n)$. After that we have just another point-wise multiplication of $\mathcal{O}(n)$, which doesn't increase the complexity. Again, H_J turns out to be computable on customary computers.

At a given wavenumber vector k and in a given component μ of the four-potential, the time development of a field $|\alpha_\mu(k,t)\rangle$ of coherent states under the influence of H_J reads

$$
|\alpha_\mu(k, t+\Delta t)\rangle = e^{-\frac{i}{\hbar} H_J \Delta t}\, |\alpha_\mu(k,t)\rangle = e^{-\frac{i}{\hbar}\Delta t \left(\beta_\mu(k)\, a^+_{k,\mu} - \beta^*_\mu(k)\, a_{k,\mu}\right)}\, |\alpha_\mu(k,t)\rangle\,. \tag{4.33}
$$

These are very good news because the operator $e^{\beta a^+ - \beta^* a}$ is a *displacement operator*. When applied to a coherent state $|\alpha\rangle$, it shifts its eigenvalue α by the complex number β,

$$
e^{\beta a^+ - \beta^* a}\, |\alpha\rangle = |\alpha + \beta\,\rangle\,. \tag{4.34}
$$

(In fact, the vacuum state $|0\rangle$ is a coherent state with eigenvalue 0, and all coherent states $|\alpha\rangle$ can be constructed by applying a displacement operator $e^{\alpha a^+ - \alpha^* a}$ to the vacuum state.)

So to compute the impact of the fermions on a field of coherent states, we simply have to compute, for each k and each μ, the parameter $\beta_\mu(k)$, and shift the coherent state by $-\frac{i}{\hbar}\Delta t\, \beta_\mu(k)$. However this is just the tip of the iceberg of good news.

There is an even more important insight provided by eq. 4.33: *A realistic quantum field of photons can be described without approximation by a field of coherent states.*

Why is this so?

- When a field of coherent states interacts with a field of fermions, it remains a field of coherent states.
- When a field of coherent states evolves freely in time, it also remains a field of coherent states.
- The vacuum state is a coherent state.
- Where do the electromagnetic fields come from? They have been produced out of the vacuum state by some interaction with fermions. But that interaction can only produce coherent states.

Apart from its theoretical implications, this property of the quantised electromagnetic field makes it significantly easier to represent it in a computer. Instead of storing one wave function for each of its infinitely many Fock states, we only need to store a single wave function for one coherent state at each k and μ. This means that the simulation of quantum electrodynamics, concerning both calculation time and memory, remains in the reach of customary computers.

So let us use a customary computer to simulate quantum electrodynamics, starting with an effect of particular interest, pair annihilation. (Spoiler: This will not work until we include an explicit distinction between fermions and anti-fermions into our model, which will be done in the next section.)

In the simulation it does not matter whether we apply eq. 4.33 completely in position representation, or whether we just calculate the parameter β in position representation and perform the actual displacement of the coherent states in momentum representation. The numerical results are the same.

Figure 4.3 shows a simulated collision of a fermionic and an anti-fermionic wave packet in a right angle in position representation. At $t = 1.5$ both wave functions overlap, causing a nonzero $\beta_\mu(k)$, which generates a (very weak) field of coherent states of photons.

At $t = 2.3$ and later we see two wave packets of photons moving vertically. Some of these photons are moving down, i. e. in the opposite direction of the fermions. This is again a limitation of the simulation, which will be fixed in the next section.

The influence of the photons on the fermions and on the anti-fermions is negligible.

Figure 4.4 shows the same simulation in momentum representation. We see that the momenta of the photons produced are the sum of the momenta of the fermions and the anti-fermions on the one hand, and the negative of that sum on the other hand. In addition there is a very small wave packet of photons with momentum zero, which correspond to outgoing spherical waves in position representation.

Again we can observe a momentum transfer in the shape of quantum leaps. (And again the negative momentum transfer is due to a limitation of the simulation.) This time the transfer is from the fermions and anti-fermions to the photons. The momentum transferred corresponds to the *difference* between the momenta of the fermionic wave packets involved. This is different from the momentum transfer in the other direction, where the "absolute" spatial momentum of the photons gets transferred to the fermions and anti-fermions. (It's not really absolute in

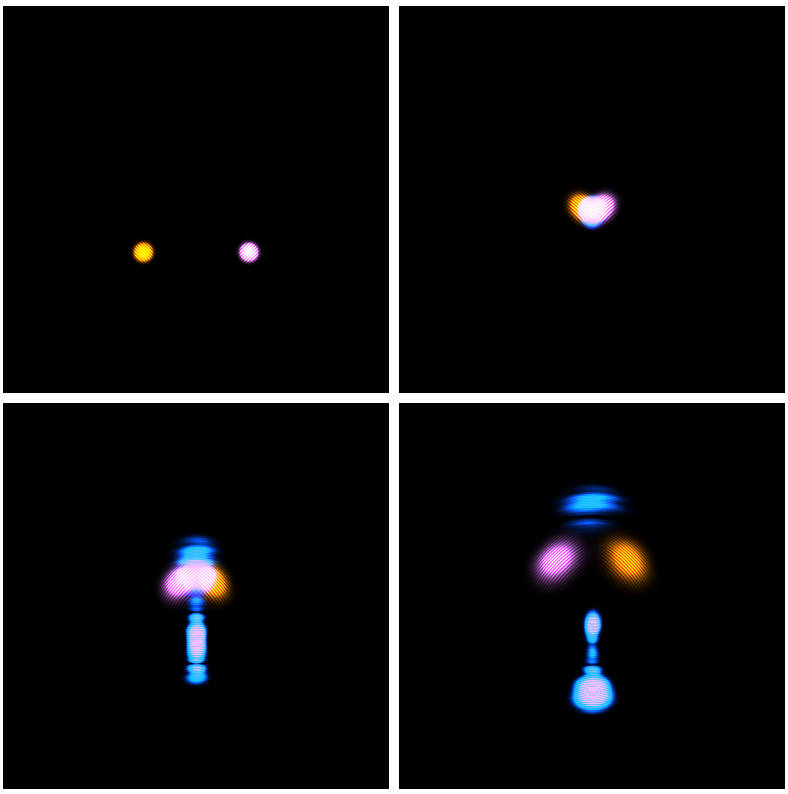

Figure 4.3: Collision between fermions and anti-fermions, position representation

From left to right and from top to bottom: $t = 0.0$, 1.5, 2.3, 3.0.
Numerical parameters: $\hbar = 0.01$, $c = 1$, $m = 1.5$, $q = 0.05$, 1024×1024 grid points, $\Delta x = 0.005$.
Initial state: fermions (yellow/red): $x = (-0.7, -0.7)$, $p = (0.7, 0.7)$, $\sigma = 0$, anti-fermions (white/magenta): $x = (0.7, -0.7)$, $p = (-0.7, 0.7)$, $\sigma = 3$.

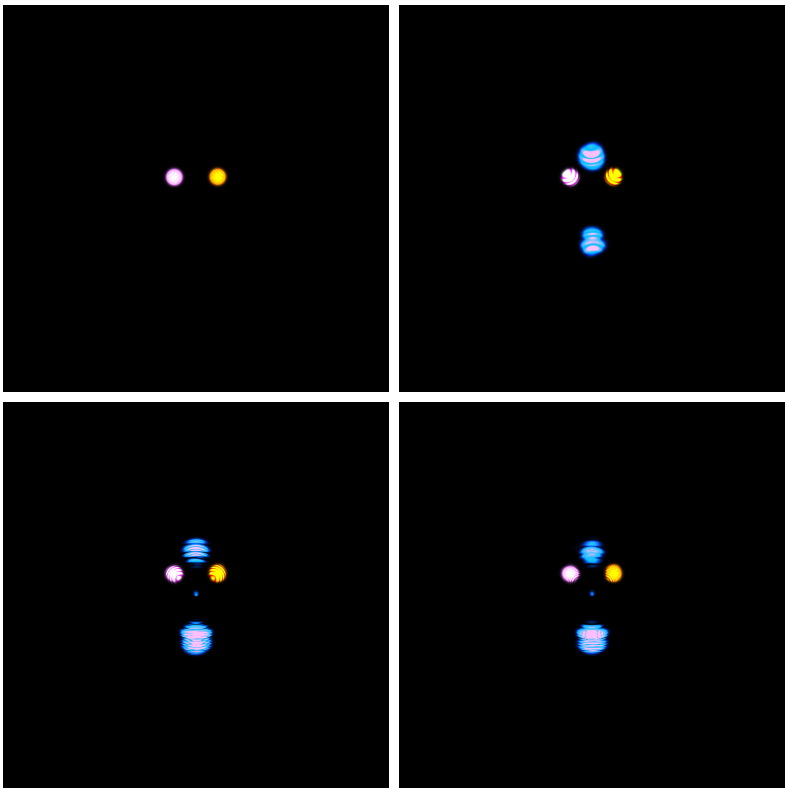

Figure 4.4: Collision between fermions and anti-fermions, momentum representation

the sense that the momentum of the photons depends on the frame of reference, although their velocity does not.)

Mathematically, this different behaviour can be ascribed to the ladder operators in H_J. At a specific momentum there is a product of two ladder operators for the fermions, but only one at a time, forming a sum, for the photons. (In the language of Feynman diagrams this corresponds to the vertex of electromagnetic interaction having two fermionic lines, but only one photonic line.)

Figure 4.5 shows the time development of the norms of the wave functions in this simulation.

The norm of the photonic wave function is extremely small. To make it visible at all, it has been scaled up by a factor of 10000. It starts to grow when the wave functions of the fermions and the anti-fermions overlap. When the overlap ends, the norm decreases again, remaining essentially constant after the interaction. For $t \gtrsim 3$ it decreases rapidly, because the photons have reached the border of the simulated area, where they get absorbed numerically.

The norms of the fermions and the anti-fermions remain essentially constant at their initial values of 1. There is a tiny norm transfer from the anti-fermions to the fermions caused by the interaction with the photons generated in the collision.

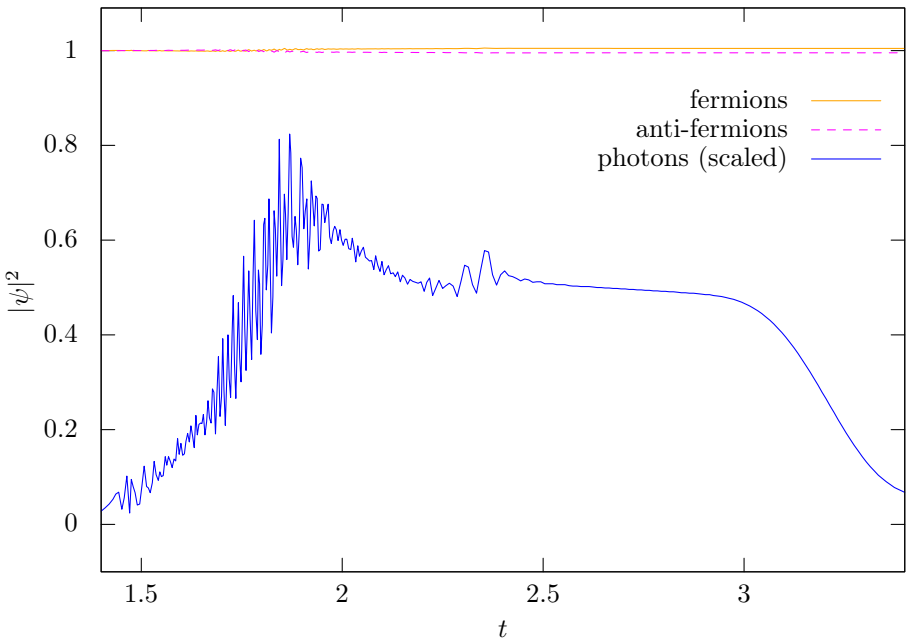

Figure 4.5: Collision between fermions and anti-fermions, norm of the wave functions

For the photons, the norm has been scaled up by a factor of 10000.

In all simulations the parameter $\beta_\mu(k)$, whose physical meaning is a current, has only been calculated for $\sigma \in \{0, 1\}$ and $\sigma' \in \{2, 3\}$ or vice versa, but it has been set to zero in the cases where both $\sigma, \sigma' \in \{0, 1\}$ or both $\sigma, \sigma' \in \{2, 3\}$. Without this, the Coulomb fields generated by the fermions and the anti-fermions blow their wave functions apart. We surmise that this problem can be solved by increasing the position window of the simulation. It might also be possible to eliminate the Coulomb field via gauge conditions.

▶ **Exercise 4.2:** Show that $\beta_\mu(k)$ and $\beta^*_\mu(k)$ are indeed the complex conjugates of each other.

Solution: All prefactors are real-valued, so we only need to prove that the terms with the Fourier transforms are the complex conjugates of each other.

$$\begin{aligned}
&\mathcal{F}\Big(\mathcal{F}^{-1}\big(\psi^+_{\sigma'}(-\hbar k)\big)(x)\,\gamma_0\gamma_\mu\,\mathcal{F}^{-1}\big(\psi_\sigma(\hbar k)\big)(x)\Big)^*(\hbar k)\\
&= \mathcal{F}\Big(\mathcal{F}^{-1}\big(\psi_\sigma(\hbar k)\big)^*(-x)\,(\gamma_0\gamma_\mu)^*\mathcal{F}^{-1}\big(\psi^+_{\sigma'}(-\hbar k)\big)^*(-x)\Big)(\hbar k)\\
&= \mathcal{F}\Big(\mathcal{F}^{-1}\big(\psi_\sigma(-\hbar k)\big)^*(x)\,\gamma_0\gamma_\mu\,\mathcal{F}^{-1}\big(\psi^+_{\sigma'}(\hbar k)\big)^*(x)\Big)(\hbar k)\\
&= \mathcal{F}\Big(\mathcal{F}^{-1}\big(\psi^+_{\sigma}(\hbar k)\big)(x)\,\gamma_0\gamma_\mu\,\mathcal{F}^{-1}\big(\psi_{\sigma'}(-\hbar k)\big)(x)\Big)(\hbar k).\quad\square
\end{aligned}\tag{4.35}$$

▶ **Exercise 4.3:** Show that the coherent state $|\alpha_\mu(k)\rangle$ with norm 1 can be expressed via the Fock states

$$|n_{k,\mu}\rangle = \frac{1}{\sqrt{n!}}\big(a^+_{k,\mu}\big)^n\,|0\rangle \tag{4.36}$$

as

$$|\alpha_\mu(k)\rangle = e^{-\frac{1}{2}|\alpha_\mu(k)|^2}\sum_{n=0}^{\infty}\frac{\alpha_\mu(k)^n}{\sqrt{n!}}\,|n_{k,\mu}\rangle\,. \tag{4.37}$$

Hint: Use the eigenvalue equation to deduce a recursive relation for the coefficients of the expansion.

Remark: This also proves, by setting $\alpha_\mu(k) = 0$, that the vacuum state is a coherent state.

▶ **Exercise 4.4:** Prove eq. 4.25.

Hint: Use the expansion into Fock states, eq. 4.37.

▶ **Exercise 4.5:** Prove eq. 4.34.

Remark: This also proves that all coherent states $|\alpha\rangle$ can be constructed by applying a displacement operator $e^{\alpha a^+ - \alpha^* a}$ to the vacuum state.

4.4 Fermions and Anti-Fermions

Although we have applied second quantisation to both the Dirac equation and the Maxwell equations, obtaining fermions and photons, the Schrödinger equation of the combined many-particle system is still the same. We are just reinterpreting its solution. For the fermions, we interpret the solution of the single-particle Dirac equation as the coefficient function of a many-particle wave function. For the photons, we don't spell out the Fock states, but we interpret the solution of the Maxwell equations as a field of photons in coherent states. And we have shown that this is not a crude approximation, but an adequate description of a realistic quantised electromagnetic field.

Nevertheless our results are still contradicting experimental observations. In a collision between fermions and photons our simulation shows outgoing anti-fermions with the negative momentum of the outgoing fermions. In a collision between fermions and anti-fermions we only see a very weak outgoing field of photons, which does not really affect the fermions and the anti-fermions. In particular, our simulation doesn't feature true many-fermion effects, pair annihilation and creation, as observed in experiments.

Mathematically, this is not a surprise. The Hamiltonian $H_\psi + H_J$ of the fermions is Hermitian, so the time evolution operator $e^{-\frac{i}{\hbar}(H_\psi+H_J)\Delta t}$ must be unitary, i. e. leave the total norm constant. Some transfer of the norm between the fermions and the anti-fermions is all we can expect, and that's what we have observed so far.

To implement pair annihilation and creation, we need an additional fermionic state where the norm can be transferred to, the vacuum state. Then the total norm of the many-fermion wave function can remain constant, and we distribute it over the one-fermion state and the vacuum state.

In fact we already have considered the fermionic vacuum state, but its Hamiltonian turned out to be steadily 0, so it doesn't play a role in the Schrödinger equation. How can we bring it back into the match?

The key is the weird behaviour of the anti-fermions. Their negative kinetic energy is the cause of the negative momentum transfer we observed in the recent simulations. To cope with it, we apply the *Feynman-Stückelberg* interpretation of anti-fermions or, equivalently, the *Dirac sea* interpretation.

4.4.1 The Feynman-Stückelberg Interpretation

The Dirac equation features eigenstates with negative energy. On the first glance this predicts an unstable universe: For every relativistic particle there are states with lower energy, so the particle will, after some time, relax to such a state. Why doesn't that happen?

Dirac's original explanation was that all eigenstates with negative energy are already occupied by fermions, making them inaccessible for fermions with positive energy [11]. This view, the so-called *Dirac sea*, implies that one can, by adding energy, convert an existing particle with negative energy to a particle with positive energy, leaving a *hole* in the "sea". After that, both the particle and the hole can travel freely, and the hole is equivalent to a particle with opposite charge. Such a particle got discovered experimentally in the cosmic rays by Anderson, four years after Dirac's prediction, and named *positron* [12].

The Dirac sea has the disadvantage that it postulates an infinite number of particles, carrying charge and mass, at each position in the universe, causing the universe to collapse due to infinite

gravity. This contradiction motivated the development of a new interpretation which doesn't have this disadvantage, the *Feynman-Stückelberg* interpretation.

According to Feynman and Stückelberg, all particles, including anti-particles, have a positive kinetic energy, but the anti-particles are mirrored in spacetime, i. e. they are mirrored in space, and their flow of time is reversed. Due to this time reversal the annihilation of a positron is, seen from the positron, a creation, and vice versa.

For our calculation this means that we have to reverse the roles of the creation and annihilation operators for anti-fermions. For eigenstates with negative kinetic energy, i. e. $\sigma \in \{2,3\}$, the annihilation operator for a fermion with momentum p becomes a creation operator for an anti-fermion with (mirrored) momentum $-p$. Likewise, the creation operator for a fermion with momentum p becomes an annihilation operator for an anti-fermion with momentum $-p$.

$$c_{p,\sigma} = b_{p,\sigma}, \qquad c^+_{p,\sigma} = b^+_{p,\sigma} \qquad \text{for } \sigma \in \{0,1\}, \tag{4.38}$$

$$c_{p,\sigma} = d^+_{-p,\sigma}, \qquad c^+_{p,\sigma} = \ d_{-p,\sigma} \qquad \text{for } \sigma \in \{2,3\}. \tag{4.39}$$

What are the effects of this reassignment on our calculations?

In the free evolution in time, described by the Hamiltonian H_ψ for free fermions, the ladder operators come in pairs. For the fermions, the pair is $b^+_{p,\sigma} b_{p,\sigma}$, i. e. the number operator for the state $\psi_{p,\sigma}$, just like before. For the anti-fermions, it is $d_{-p,\sigma}\, d^+_{-p,\sigma}$, i. e. the anti-number operator for the state $\psi_{-p,\sigma}$.

Following the traditional approach for now, we use the anticommutator relation $d\, d^+ + d^+ d = 1$ to convert the anti-number operator into a number operator. (An alternative approach will be presented in the next subsection and elaborated in section 4.5.) This has the drawback that the constant 1 in the Hamiltonian causes a constant contribution to the energy inside the infinite integral, and thus a singularity. To circumvent this singularity, we set the zero point of the energy to the infinite value $\int 1\, d^3p$, i. e. we just ignore the constant 1 in the Hamiltonian.

With this reinterpretation the operator H_ψ acts on the anti-fermions just like before. All new physics happens in the interaction Hamiltonian H_J, which can mix the ladder operators of fermions and anti-fermions.

To investigate this, we return to eq. 4.4,

$$\begin{aligned} H_J = -qc \int d^3p' \sum_{\sigma'=0}^{3} \int d^3p \sum_{\sigma=0}^{3} \sum_{\mu=0}^{3} & c^+_{p',\sigma'} \psi^*_{p',\sigma'}\, \gamma_0\gamma_\mu\, a_\mu(p-p')\, \psi_{p,\sigma} c_{p,\sigma} \\ & + c^+_{p',\sigma'} \psi^*_{p',\sigma'}\, \gamma_0\gamma_\mu\, a^+_\mu(p'-p)\, \psi_{p,\sigma} c_{p,\sigma} \end{aligned} \tag{4.40}$$

and write it as

$$H_J = -qc \int d^3p' \sum_{\sigma'=0}^{3} \int d^3p \sum_{\sigma=0}^{3} c^+_{p',\sigma'} \psi^*_{p',\sigma'}\, A(p-p')\, \psi_{p,\sigma} c_{p,\sigma} \tag{4.41}$$

with the interaction matrix

$$A(p) = \sum_{\mu=0}^{3} \gamma_0\gamma_\mu \left(a_\mu(p) + a^+_\mu(-p) \right). \tag{4.42}$$

H_J contains the operator $c^+_{p',\sigma'}\, c_{p,\sigma}$, which maps the momentum eigenstate $\psi_{p,\sigma}$ to the momentum eigenstate $\psi_{p',\sigma'}$. It also contains $c^+_{p,\sigma}\, c_{p',\sigma'}$, which does the opposite. Thus the restriction of H_J to the two-state subspace of the momentum eigenstates $\psi_{p,\sigma}$ and $\psi_{p',\sigma'}$ can be described using

$$c^+_{p',\sigma'}\, c_{p,\sigma} + c^+_{p,\sigma}\, c_{p',\sigma'} = \begin{pmatrix} 0 & 1 \\ 1 & 0 \end{pmatrix}. \tag{4.43}$$

When we denote the two components of our many-particle wave function in this subspace by $\psi(t)$ for p, σ and $\psi'(t)$ for p', σ', the interaction part of a time step of length Δt in the solution of our Schrödinger equation in this subspace reads

$$\begin{aligned} \begin{pmatrix} \psi'(t+\Delta t) \\ \psi(t+\Delta t) \end{pmatrix} &= e^{-\frac{i}{\hbar} H_J \Delta t} \psi \begin{pmatrix} \psi'(t) \\ \psi(t) \end{pmatrix} \\ &= \exp\left(iC \begin{pmatrix} 0 & 1 \\ 1 & 0 \end{pmatrix} \right) \begin{pmatrix} \psi'(t) \\ \psi(t) \end{pmatrix} \\ &= \begin{pmatrix} \cos C\, \psi'(t) + i \sin C\, \psi(t) \\ \cos C\, \psi(t) + i \sin C\, \psi'(t) \end{pmatrix}, \end{aligned} \tag{4.44}$$

where

$$C := qc^2 \sqrt{\tfrac{\mu_0}{\hbar}} \Delta t\, A(p - p'). \tag{4.45}$$

So the interaction manifests as a complex "rotation" between two fermionic eigenstates.

In the cases where both fermionic eigenstates $\psi_{p,\sigma}$ and $\psi_{p',\sigma'}$ denote particles or both denote anti-particles, eq. 4.44 describes the transition between the components of our many-particle wave function in these two states (with different spins), resulting from emission or absorption of photons with the momentum $\hbar k = p - p'$.

The interesting cases are those where one eigenstate belongs to a particle and the other one to an anti-particle.

Let $\psi_{p,\sigma}$ describe a particle and $\psi_{p',\sigma'}$ an anti-particle, i. e. $\sigma \in \{0, 1\}$ and $\sigma' \in \{2, 3\}$. Then the annihilation operator $c_{p,\sigma} = b_{p,\sigma}$ remains an annihilation operator for a particle, but the creation operator $c^+_{p',\sigma'} = d_{p',\sigma'}$ becomes another annihilation operator for a spacetime-mirrored anti-particle. Likewise, the creation operator $c^+_{p,\sigma} = b^+_{p,\sigma}$ remains a creation operator for a particle, but the annihilation operator $c_{p',\sigma} = d^+_{-p',\sigma'}$ becomes another creation operator for a spacetime-mirrored anti-particle. Their combination, the operator $c^+_{p',\sigma'}\, c_{p,\sigma} = d_{-p',\sigma'}\, b_{p,\sigma}$, maps the two-particle state, consisting of $\psi_{p,\sigma}$ and $\psi_{p',\sigma'}$, to the vacuum state.

Now we reverse the roles of p, σ and p', σ'. Then $\psi_{p,\sigma}$ describes an anti-particle and $\psi_{p',\sigma'}$ a particle, and the combined operator $c^+_{p',\sigma'}\, c_{p,\sigma} = b^+_{p',\sigma'}\, d^+_{-p,\sigma}$ maps the vacuum state to the two-particle state.

Again H_J contains both combinations. We write their sum as

$$d_{-p',\sigma'}\, b_{p,\sigma} + b^+_{p,\sigma}\, d^+_{-p',\sigma'} = \begin{pmatrix} 0 & 1 \\ 1 & 0 \end{pmatrix}. \tag{4.46}$$

Eq. 4.44 applies without change, but now it rotates between the vacuum state and the two-particle state, which consists of the particle $\psi_{p,\sigma}$ and the anti-particle $\psi_{p',\sigma'}$. Depending on which one of both states is occupied, this case describes both pair annihilation and pair creation.

So we have a Schrödinger equation which describes pair annihilation and creation. For each pair of states $\psi_{p,\sigma}$ and $\psi_{p',\sigma'}$ it acts in a four-dimensional subspace, consisting of the vacuum state, the two one-particle states, and the two-particle state.

When we try to solve this equation numerically, we face the problem that we don't have a numerical description of the vacuum state. In fact it's even worse: We *cannot* describe the vacuum state numerically.

The reason for this is that we cannot determine the amplitude of the wave function of the vacuum state, not even in the most simple case with no particles at all.

To illustrate this let's assume an empty universe. The amplitude of the wave function of the vacuum state is a constant $\mathcal{N}$ everywhere. Then we create, at some position in space, a pair of wave packets of fermions and anti-fermions, travelling in opposite directions. We make our pair generation so strong that the rotation is taken to the maximum, i. e. there are points where the amplitudes of the wave packets of the fermions and the anti-fermions are $\mathcal{N}$ and the amplitude of the vacuum state is zero.

Now we create, at some other position in space, another pair of wave packets of fermions and anti-fermions, choosing the momenta such that the fermionic wave packet will collide with the fermionic wave packet from the first pair. Then the amplitudes of the two wave packets can add up to more than $\mathcal{N}$. Since the total norm of the many-particle wave function must be constant, this implies that its total amplitude must be less than $\mathcal{N}$ somewhere else; it can even be zero. This means that there can be regions with *neither* a particle *nor* a vacuum, which does not make sense.

This contradiction arises from the assumption that we have a finite total norm $\mathcal{N}$ in the two-particle system of the fermions and the vacuum state. When we assume instead that the amplitude of the fermionic wave function remains finite, but the total norm is infinite, we don't get this contradiction, but we are left with the problem that we cannot treat the infinite amplitude of the vacuum wave function numerically.

To solve this problem, the next subsection will take us back to the Dirac sea.

▶ **Exercise 4.6:** Prove eq. 4.44 by expanding the exponential into its power series.

▶ **Exercise 4.7:** Prove eq. 4.44 by decomposing the wave function into eigenstates of $\left(\begin{smallmatrix}0&1\\1&0\end{smallmatrix}\right)$.

4.4.2 The Dirac Sea Interpretation

According to the Feynman-Stückelberg interpretation of anti-particles, an anti-particle is a mirrored particle with reversed time. As we have seen in the previous subsection, this reverses the roles of the creation and annihilator operators for the anti-particles (see eq. 4.38 and 4.39), which results in terms proportional to $b^+_{p,\sigma} b_{p,\sigma} + d_{-p,\sigma}\, d^+_{-p,\sigma}$ in the free Hamiltonian H_ψ.

From that point on we followed the traditional approach and applied the anticommutator relation $d\, d^+ + d^+ d = 1$ to convert the anti-number operator $d_{-p,\sigma}\, d^+_{-p,\sigma}$ into a number operator $d^+_{-p,\sigma} d_{-p,\sigma}$. This allows us to treat the anti-fermions as "normal" particles. The price we have to pay for this is a zero point of the energy at the infinite value $\int 1\, d^3p$.

But what happens if we just keep the anti-number operator?

At each momentum p we have a Fock space over the four single-particle momentum eigenstates labelled by σ. For each σ, this boils down to a two-dimensional space, consisting of the single-particle state $\psi_{p,\sigma}$ and the vacuum state. As we have seen in subsection 3.2.7, the anti-number

operator acts on this subspace just like the number operator, but with the roles of the one-particle state and the vacuum reversed.

This means that we can, instead of "repairing" the order of the anti-fermionic ladder operators, reinterpret the two components of the many-particle wave function for the anti-fermions: The vacuum state becomes the new one-particle state, and the one-particle state becomes the new vacuum state. (This implies a change of the structure of the fermionic Fock space, which will be discussed in detail in section 4.5.)

Then the actual physics of the anti-fermions takes place in the vacuum state, and the anti-particle state is used only temporarily for carrying out the calculations – which is just the opposite of their roles in the case of "normal" particles. We don't propagate the anti-fermions, but the vacuum state.

In other words, the anti-fermions are *holes in the Dirac sea*.

In the previous subsection we faced the problem that we could not describe the vacuum state numerically. In this new approach this is possible. However this does not yet solve the problem. The complex "rotation" in eq. 4.44 takes place between the vacuum state and the two-particle state, and now the wave function of the anti-fermions themselves has taken the place of the vacuum state, thus becoming inaccessible. Nevertheless, as we will see next, this shift of the problem is an important step towards its solution.

The reinterpretation of the ladder operators for the anti-particles is only one half of the Feynman-Stückelberg interpretation. The other half is the mirrored spacetime for the anti-particles.

The operation to reverse the roles of particles and anti-particles is named *charge conjugation* and denoted by an operator C. Likewise, we can use operators to describe the spacetime reversal. The operator P which mirrors space is called *parity*, and the *time reversal operator* is denoted by T. Using these operators, the Feynman-Stückelberg interpretation reads: *Anti-particles are CPT-reversed particles.*

This means that our holes in the Dirac sea, which we can propagate numerically, are not really the vacuum state, but *the CPT-reversed vacuum state.*

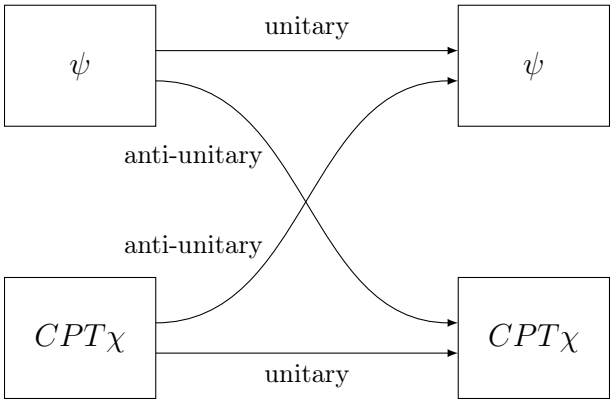

Figure 4.6: Unitary and anti-unitary mappings of $e^{-\frac{i}{\hbar}H_J\Delta t}$ between fermions and anti-fermions

The symbol ψ represents the fermionic parts of the many-particle wave function. $CPT\chi$ is the CPT-reversed vacuum state, reinterpreted to describe anti-fermions as *Dirac holes*.

As long as the fermions and the anti-fermions don't interact, this subtle difference doesn't matter. As soon as they interact, it does.

Mathematically, we are CPT-reversing one half of our Hilbert space, where "one half" means the span of two of the four eigenstates of H_ψ, those two which describe *Dirac holes*. Since H_ψ doesn't mix the states of both halves, $e^{-\frac{i}{\hbar}H_\psi \Delta t}$ remains a unitary operator. H_J, however, does map between both halves. So $e^{-\frac{i}{\hbar}H_J \Delta t}$ remains unitary only where it maps fermions to fermions or Dirac holes to Dirac holes, but it becomes anti-unitary where it maps fermions to Dirac holes or vice versa. Figure 4.6 illustrates how $e^{-\frac{i}{\hbar}H_J \Delta t}$ maps between both halves of the Hilbert space.

This implies that the interaction between fermions and Dirac holes can change the norm of their wave functions.

How can we CPT-reverse a wave function in our simulation? The operators C, P, and T, and thus their combination CPT, can be described as matrices on spinor space. In particular it is straightforward to show that when $\psi(x,t)$ is a solution of the Dirac equation, then

$$CPT\,\psi(t,x) = \gamma_0\gamma_1\gamma_2\gamma_3\,\psi(-t,-x) \tag{4.47}$$

is a solution as well.

So we can switch between a simulation of a "normal" world and a simulation of a world with mirrored spacetime by multiplying the wave function with the matrix $\gamma_0\gamma_1\gamma_2\gamma_3$, and we can prepare a wave function of Dirac holes by preparing a wave function of fermions and multiplying it by $\gamma_0\gamma_1\gamma_2\gamma_3$.

This is just one out of several possibilities to simulate Dirac holes as CPT-reversed fermions. Another one is to store the wave function of the Dirac holes directly in the momentum eigenstates with negative kinetic energy (thus applying C), to reverse the sign of Δt in the simulation in momentum representation (thus applying T), and to multiply the wave function by $i\gamma_0$ instead of $\gamma_0\gamma_1\gamma_2\gamma_3$ (thus applying P).

How does this help us to simulate the pair annihilation and creation we identified in the interaction $e^{-\frac{i}{\hbar}H_J \Delta t}$ in the previous subsection?

- In momentum representation, we store the fermionic wave function and the Dirac holes, the CPT-reversed vacuum state. That way we can use the simulation for a single relativistic particle without modification to simulate the free propagation of the system.
- Before we transform the Dirac holes to position representation, we undo their CPT reversal. That way we have access to the fermionic wave function and to the vacuum state in position representation. (And we don't have access to the anti-fermionic wave function.)
- Now we can apply the interaction operator $e^{-\frac{i}{\hbar}H_J \Delta t}$ to the fermionic wave function and to the vacuum state, which represents the anti-fermions as Dirac holes.

There are two problems left. One is that we cannot directly access momentum eigenstates, which define whether something is a fermion or an anti-fermion, in position representation. The solution is to store the fermions and the Dirac holes separately in momentum representation and to transform them separately to position representation.

The other problem is how to interpret the result of the application of $e^{-\frac{i}{\hbar}H_J \Delta t}$ to the wave functions.

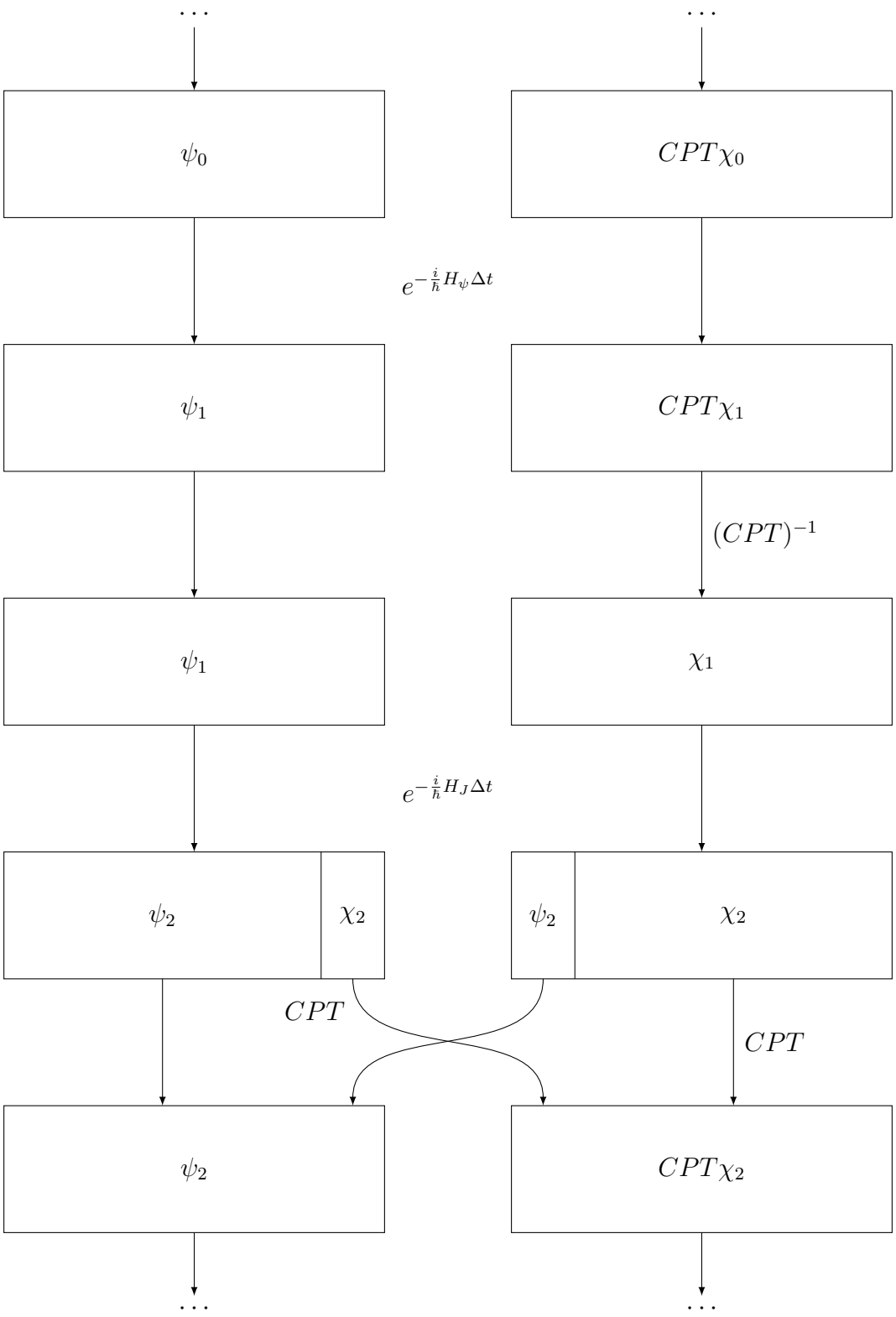

Figure 4.7: Schematic representation of the simulation

The wave functions ψ_k represent the fermions. $CPT\chi_k$ represent CPT-reversed vacuum states, reinterpreted to describe anti-fermions as *Dirac holes*. This figure shows one step of the simulation, starting with ψ_0, χ_0. After application of $e^{-\frac{i}{\hbar}H_J \Delta t}$ the wave functions are no longer momentum eigenstates, so we must decompose and recompose them. In accord with the Feynman-Stückelberg interpretation, χ_k must be stored in CPT-reversed form when we apply $e^{-\frac{i}{\hbar}H_\psi \Delta t}$. This must be taken into account during the decomposition and recomposition.

Since H_J does not commute with H_ψ, the result of the application of $e^{-\frac{i}{\hbar}H_J\Delta t}$ to a momentum eigenstate is no longer a momentum eigenstate, but there are some small parts "sticking out" to other momentum eigenstates. This includes a transfer of norm between the fermions and the Dirac holes.

When we compare this to eq. 4.44, we find that those small parts are proportional to $\sin C$, and the remaining parts are proportional to $\cos C$. This means that we have access to these components of the complex rotation by decomposing the result of the application of $e^{-\frac{i}{\hbar}H_J\Delta t}$ into momentum eigenstates. Recomposing these parts into fermions and Dirac holes makes it possible to simulate pair annihilation and creation.

During this recomposition we must take into account that in momentum representation the Dirac holes are CPT-reversed, but in position representation they are not. This means that we have to recombine the fermions directly with the parts "sticking out" from the Dirac holes, and we have to recombine the CPT-reversed Dirac holes with the CPT-reversed part "sticking out" from the fermions.

Figure 4.7 shows a schematic representation of the simulation.

In summary the steps to simulate quantum electrodynamics in the Schrödinger picture are as follows.

- The many-particle wave function of the fermions and anti-fermions is stored point-wise in momentum representation in two arrays of spinors. The first one represents the coefficient wave function of the fermions; the second one represents the *Dirac holes*, i. e. the CPT-reversed vacuum state.
- The many-particle wave function of the photons is stored point-wise in momentum representation as an array of complex four-vectors, holding the eigenvalues of coherent states.
- The free evolutions of the fermions, of the Dirac holes, and of the photons are implemented in momentum representation, where the free evolution operators $e^{-\frac{i}{\hbar}H_\psi\Delta t}$ and $e^{-\frac{i}{\hbar}H_A\Delta t}$ are diagonal.
- We undo the CPT reversal of the Dirac holes and transform all wave functions from momentum to position representation.
- In position representation we apply the time evolution operators of the interaction, eq. 4.20 for the fermions and the Dirac holes and eq. 4.33 for the photons.
- We transform all wave functions back from position to momentum representation. As the result of the interaction, the wave functions of the fermions and the Dirac holes are no longer momentum eigenstates.
- We decompose the former wave functions of the fermions and the Dirac holes into momentum eigenstates and recombine them such that they represent again the fermions and the Dirac holes.
- We CPT-reverse the wave function of the Dirac holes and iterate the simulation.

The CPT reversal is essential for turning the unitary time evolution operator of the interaction between the fermions and the Dirac holes into an anti-unitary operator, which is necessary to obtain pair annihilation and creation.

▶ **Exercise 4.8:** Show that

$$\gamma_0\gamma_1\gamma_2\gamma_3 = \begin{pmatrix} 0 & 0 & -1 & 0 \\ 0 & 0 & 0 & -1 \\ 1 & 0 & 0 & 0 \\ 0 & 1 & 0 & 0 \end{pmatrix}. \tag{4.48}$$

▶ **Exercise 4.9:** Show that when $\psi(x,t)$ is a solution of the Dirac equation, then $CPT\psi(x,t)$ as in eq. 4.47 is a solution as well.

4.4.3 Numerical Results

With the CPT reversal in place we can now simulate pair annihilation and pair creation.

Figure 4.8 shows a simulated frontal collision of two wave packets in position representation. In the initial state ($t = 0$), both are well-separated. One wave packet (yellow/red, left) describes the fermions. The other one (white/magenta, right) is the CPT-reversed vacuum state, the wave function of holes in the Dirac sea. For sake of simplicity we will refer to this wave function as anti-fermions, just like for previous simulations.

At $t = 2.26$, shortly after the collision, a field of photons (coherent states, cyan/blue) has been produced in the collision, and the fermions and the anti-fermions have started to annihilate each other.

At $t = 3.00$ the fermions and the anti-fermions have largely annihilated each other. Some small outgoing parts have been reflected rather than annihilated. The arc-shaped photonic wave functions have almost reached the border of the spatial window of the simulation, where they will get absorbed numerically.

Figure 4.9 shows the same simulation in momentum representation. At $t = 2.26$ we see that the momenta of the photons produced in the collision are rather small. The momentum uncertainty has the same order of magnitude as the mean momentum. This explains their arc-like shapes in position representation.

At $t = 3.00$ the norms of the fermionic and anti-fermionic wave functions have shrunken significantly. The remaining parts have changed their places due to reflection. This change of momentum happens as a *quantum leap*. In momentum representation the wave packets do not travel, but they vanish gradually at one momentum and simultaneously show up at another momentum.

Figure 4.10 shows the time development of the norm of the wave functions in the same simulation. During the pair annihilation the norms of the fermionic wave functions shrink to less than one quarter of their initial values, and the norm of the photonic wave function grows.

The increase of the norm of the fermions after $t \gtrsim 2.7$ and its small oscillations for $t \lesssim 2$ are due to pair creation, caused by the photons generated in the collision. The decrease of the norm of the photons after $t \gtrsim 3.2$ is due to their numerical absorption at the border of the spatial window of the simulation.

Figure 4.11 and 4.12 show a simulation of pair creation in position and momentum representation. The photonic wave packets (cyan/blue) are arc-shaped because their momenta are rather small – in the same order of magnitude as the photons produced in the previous simulation

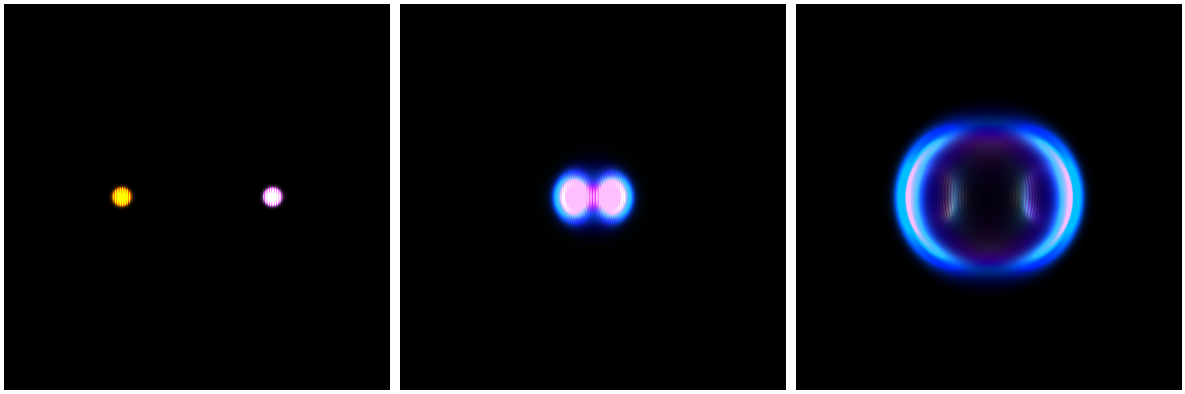

Figure 4.8: Pair annihilation, position representation

From left to right: $t = 0.00, 2.26, 3.00$.
Numerical parameters: $\hbar = 0.01$, $c = 1$, $m = 1.5$, $q = 0.05$, 1024×1024 grid points, $\Delta x = 0.005$. Initial state: fermions (yellow/red): $x = (-1, 0)$, $p = (1, 0)$, $\sigma = 0$, anti-fermions (white/magenta): $x = (1, 0)$, $p = (-1, 0)$, $\sigma = 3$.

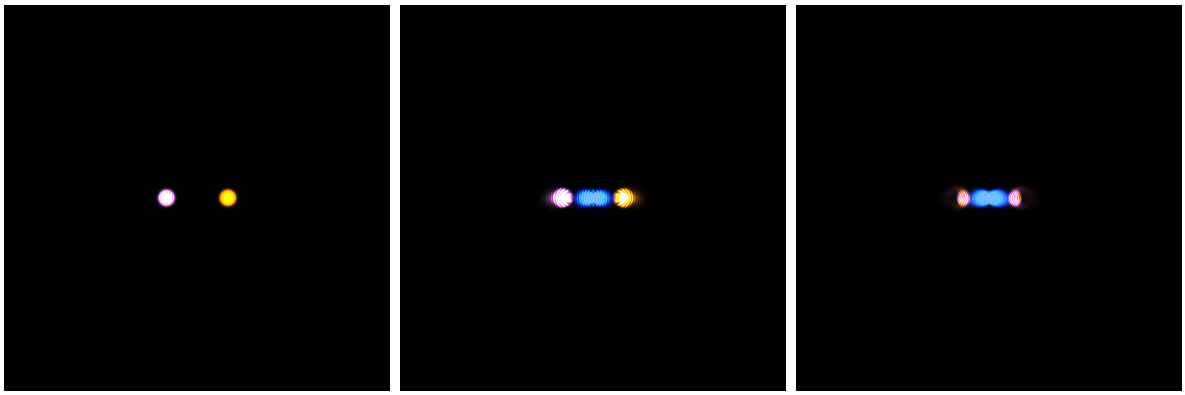

Figure 4.9: Pair annihilation, momentum representation

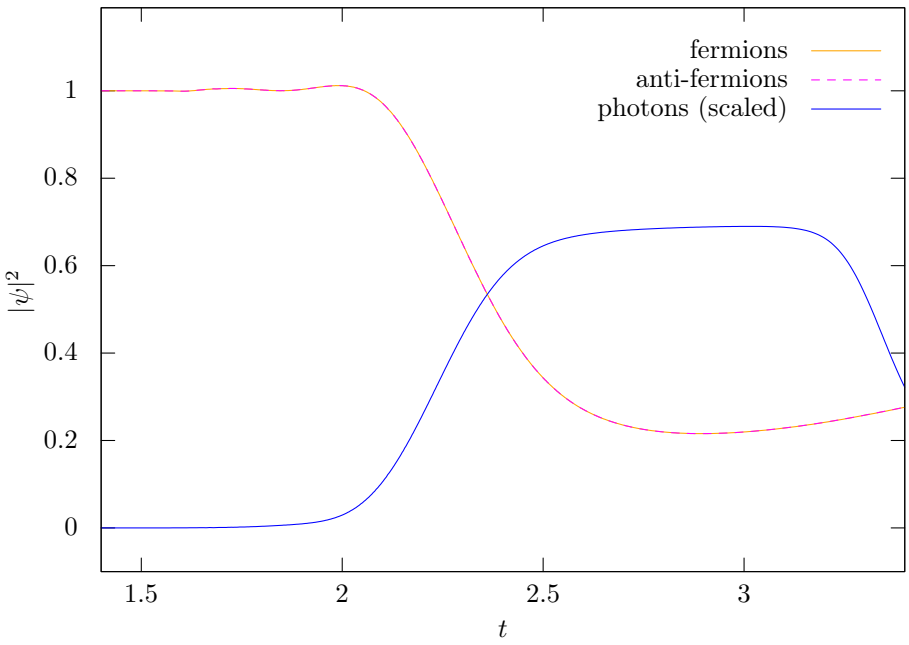

Figure 4.10: Pair annihilation, norm of the wave functions

For the photons, the norm has been scaled up by a factor of 30.

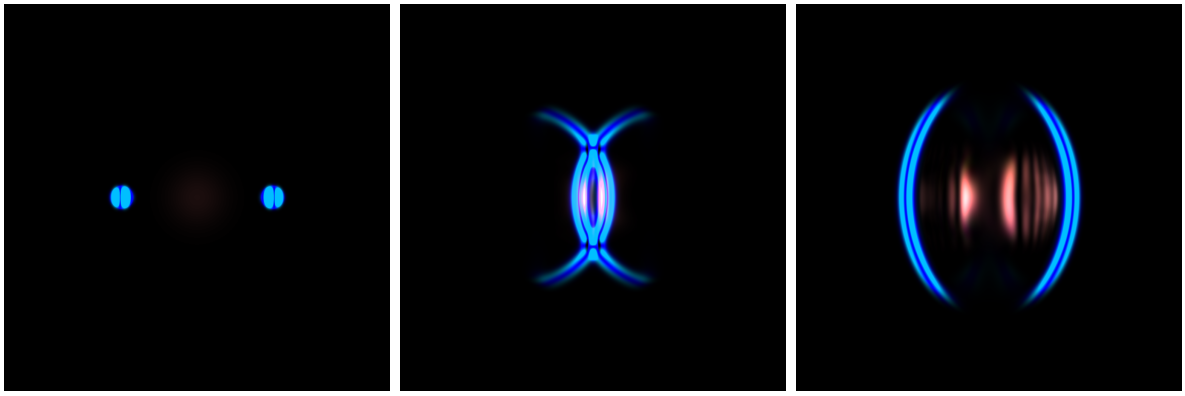

Figure 4.11: Pair creation, position representation

From left to right: $t = 0.00$, 1.17, 2.10.
Numerical parameters: $\hbar = 0.01$, $c = 1$, $m = 1.0$, $q = 0.05$, 1024×1024 grid points, $\Delta x = 0.005$. Initial state: photons (cyan/blue): $x = (\pm 1, 0)$, $\hbar k = (\pm 0.2, 0)$, $\mu = 3$. In addition the initial state contains fermions and anti-fermions with norm 0.01 and $\Delta x = 3.0$ at $x = 0$, $p = 0$.

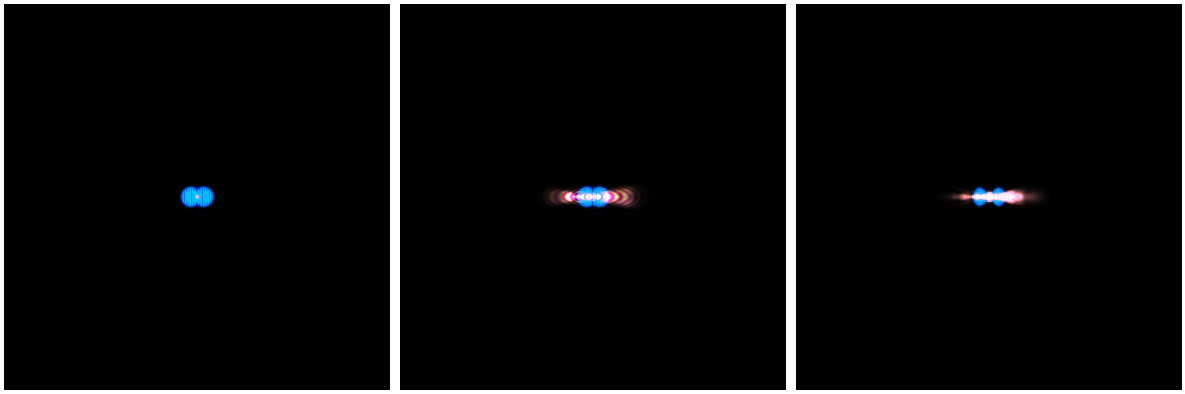

Figure 4.12: Pair creation, momentum representation

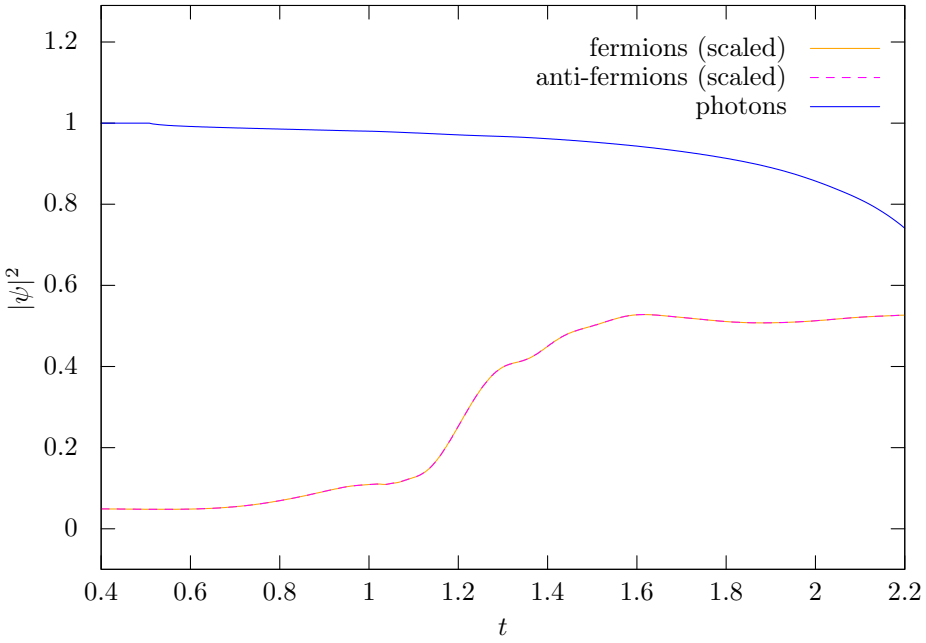

Figure 4.13: Pair creation, norm of the wave functions

For the fermions and the anti-fermions, the norm has been scaled up by a factor of 5.

of pair annihilation. Where they overlap they leave behind regions where the norm of the fermionic wave functions got increased.

Since a perfect vacuum would not allow for fermionic pairs to be produced even if the vacuum becomes unstable, the initial state contains some small contribution (with norm 0.01) of fermionic and anti-fermionic wave functions with momentum zero, spread over a large spatial area ($\Delta x = 3$). In momentum representation (fig. 4.12) they are visible as a small dot in the centre.

Figure 4.13 shows the norm of the wave functions in the case of pair creation. The small oscillations of the curve between $t \approx 0.8$ and $t \approx 1.6$ are due to interference between the two overlapping photonic wave packets, whose wavelengths are rather small compared to their sizes. The slight decrease of the fermionic wave functions after $t \gtrsim 1.6$ is due to annihilation of the newly created pairs.

In both simulations, pair annihilation and pair creation, the norms of the final states are not integer multiples of the norms of the initial states. This does not mean that fermions and anti-fermions can annihilate or get created halfway. Instead the interpretation of these results depends on the interpretation of the wave functions. According to the Copenhagen interpretation of quantum physics, an outgoing norm of about 23 % in an annihilation event means that the probability for the annihilation to take place is about 77 % in this scenario. Any further interpretation of the norms requires a mathematically precise definition of the measurement process.

Also in both simulations the initial state is perfectly symmetric with respect to both axes, x and y. Nevertheless the final states are slightly asymmetric. One possible reason for this is the proliferation of numeric errors, together with the fact that the calculations require more operations for the anti-fermions than for the fermions due to the CPT reversals.

In the simulations we are using dimensionless numerical parameters. This makes it easy to relate the results to fundamental constants. For example, in fig. 4.11 (pair creation) the photonic wave packets are located at $x = (\pm 1, 0)$, and they move with $c = 1$. So it is clear that they will meet in the centre at $t = 1$ and that the visualisation at $t = 1.17$, displaying slightly overlapping arcs, makes sense.

Since the simulations described in this subsection are close to actual physical experiments, it makes sense to translate these numerical values to actual distances and times.

Our simulation of pair annihilation uses the numerical parameters $\hbar' = 0.01$, $c' = 1$, and $m' = 1.5$. Then according to subsection 2.1.5 our units for space and time read

$$\delta t = \frac{m'\,c'^2}{\hbar'}\,\frac{\hbar}{m_e\,c^2} = \frac{1.5\cdot 1^2}{0.01}\,\frac{\hbar}{m_e\,c^2} \approx 1.932\,133\cdot 10^{-19}\,\mathrm{s} = 0.193\,213\,3\,\mathrm{as}, \tag{4.49}$$

$$\delta x = \frac{m'\,c'}{\hbar'}\,\frac{\hbar}{m_e\,c} = \frac{1.5\cdot 1}{0.01}\,\frac{\hbar}{m_e\,c} \approx 5.792\,389\cdot 10^{-11}\,\mathrm{m} = 0.579\,238\,9\,\text{Å}. \tag{4.50}$$

Since the initial positions of the fermionic wave packets are $x = (\pm 1, 0)$, this means that they are about 1.16 Å apart, which is about the size of an atom. The process of annihilation takes about 3 units of time, i. e. about 0.58 attoseconds (as), which is rather fast, even for sub-atomic processes.

Likewise, our simulation of pair creation, where the numerical parameters are $\hbar' = 0.01$, $c' = 1$, and $m' = 1$, has the units

$$\delta t = \frac{m'\,c'^2}{\hbar'}\,\frac{\hbar}{m_e\,c^2} = \frac{1\cdot 1^2}{0.01}\,\frac{\hbar}{m_e\,c^2} \approx 1.288\,089\cdot 10^{-19}\,\mathrm{s} = 0.128\,808\,9\,\mathrm{as}, \tag{4.51}$$

$$\delta x = \frac{m'\,c'}{\hbar'}\,\frac{\hbar}{m_e\,c} = \frac{1{\cdot}1}{0.01}\,\frac{\hbar}{m_e\,c} \approx 3.861\,593 \cdot 10^{-11}\,\mathrm{m} = 0.386\,159\,3\,\text{Å}. \tag{4.52}$$

The distance of the wave packets in the initial state is 0.772 Å, and the duration of the process is about 0.27 as.

All this holds when we assume that we are simulating electrons and positrons, which enter via their masses m_e. When we want to apply the results to muons and anti-muons instead, we can rescale them. Then our units for pair annihilation read

$$\delta t = \frac{m'\,c'^2}{\hbar'}\,\frac{\hbar}{m_\mu\,c^2} = \frac{1.5{\cdot}1^2}{0.01}\,\frac{\hbar}{m_\mu\,c^2} \approx 9.344\,436 \cdot 10^{-22}\,\mathrm{s} = 0.934\,443\,6\,\mathrm{zs}, \tag{4.53}$$

$$\delta x = \frac{m'\,c'}{\hbar'}\,\frac{\hbar}{m_\mu\,c} = \frac{1.5{\cdot}1}{0.01}\,\frac{\hbar}{m_\mu\,c} \approx 2.801\,391 \cdot 10^{-13}\,\mathrm{m} = 28.013\,91\,\mathrm{pm}, \tag{4.54}$$

and the units for pair creation read

$$\delta t = \frac{m'\,c'^2}{\hbar'}\,\frac{\hbar}{m_\mu\,c^2} = \frac{1{\cdot}1^2}{0.01}\,\frac{\hbar}{m_\mu\,c^2} \approx 6.229\,623 \cdot 10^{-22}\,\mathrm{s} = 0.622\,962\,3\,\mathrm{zs}, \tag{4.55}$$

$$\delta x = \frac{m'\,c'}{\hbar'}\,\frac{\hbar}{m_\mu\,c} = \frac{1{\cdot}1}{0.01}\,\frac{\hbar}{m_\mu\,c} \approx 1.867\,594 \cdot 10^{-13}\,\mathrm{m} = 18.675\,94\,\mathrm{pm}. \tag{4.56}$$

In other words, our simulations scale inversely with the masses of the fermions involved. Since a muon is about 207 times heavier than an electron, the simulations describe distances about 207 times smaller and times about 207 times faster when we apply the results to muons and anti-muons rather than to electrons and positrons.

4.5 The Structure of the Fock Space

In the previous section we reinterpreted the roles of the fermionic single-particle momentum eigenstates and the fermionic vacuum state several times. This can be a source of confusion. In view of understanding the nature of quantum electrodynamics let's re-analyse the mathematical structure we are using to model it.

Concerning the photons, we started in subsection 2.3.1 with a description of the classical electromagnetic field as a field of complex four-vectors. (Since the Maxwell equations are of second order, we can use either eight real numbers to describe the field itself and its time derivative, or we combine both in four complex numbers.)

In section 3.3 we identified a structure of harmonic oscillators in the momentum representation of this classical field. By *quantising* these harmonic oscillators and identifying their allowed energies with the energies carried by particles, the *photons*, we found a structure of a bosonic Fock space at each combination k, μ of the wavenumber vector k and the component μ of the electromagnetic four-potential. This brought us bosonic ladder operators into the Lagrangian of quantum electrodynamics and thus into the Hamiltonians H_A for the free photons and H_J for their interaction with the fermions.

Studying the Schrödinger equation obtained from H_J we found that the impact of the photons on the fermions is conveyed by coherent states, and that the impact of the fermions on the photons maps coherent states to coherent states. Thus we can, even without approximation, describe the quantised electromagnetic field by coherent states.

When we calculate the equations governing the quantised electric field, described by coherent states, they turn out to be *precisely the same equations* as those of a classical electromagnetic field.

Concerning the fermions, we started from the Dirac equation. In subsection 3.3.3 we substituted *field operators* for the wave functions, turning the Hamiltonian of a single relativistic quantum particle into a many-particle Hamiltonian. Its new feature are the fermionic ladder operators $c^+_{p,\sigma}$ and $c_{p',\sigma'}$. In the case of free fermions they combine to pairs $c^+_{p,\sigma} c_{p,\sigma}$. In the case of the interaction they combine with photonic ladder operators to products of the type $c^+_{p,\sigma} a^+_{k,\mu} c_{p',\sigma'}$ or $c^+_{p,\sigma} a_{k,\mu} c_{p',\sigma'}$, where $\hbar k = \pm(p - p')$.

In section 4.2 and 4.3 we used Fourier transforms to study the many-particle Schrödinger equation of quantum electrodynamics in position representation. We reproduced *precisely the same equations* as in the case of a single relativistic quantum particle interacting with a classical electromagnetic field. We just reinterpreted the relativistic single-particle wave function as the coefficient wave function of a many-fermion wave function and the complex classical electromagnetic field as the eigenvalues of a field of coherent states of photons.

Up to this point, second quantisation doesn't bring along any new physics. We are just reinterpreting the combination of the Maxwell equations and the Dirac equation. Nevertheless we already see effects of quantisation in the results of the numeric simulation, in particular discrete momentum transfer between the photons and the fermions.

The final step to obtain quantum electrodynamics is to reinterpret the fermionic ladder operators with positive and negative kinetic energy as the ladder operators of two types of particles, fermions and anti-fermions. By applying CPT reversal to the anti-fermions we render

their kinetic energy positive. In this *Feynman-Stückelberg interpretation*, $c^+_{p,\sigma}$ becomes $b^+_{p,\sigma}$ for $\sigma \in \{0,1\}$ or $d_{-p,\sigma}$ for $\sigma \in \{2,3\}$, and $c_{p,\sigma}$ becomes $b_{p,\sigma}$ for $\sigma \in \{0,1\}$ or $d^+_{-p,\sigma}$ for $\sigma \in \{2,3\}$.

From this point on our reinterpretations affect the structure of the Fock space itself.

In the traditional reinterpretation, we apply the fermionic anticommutator relation to "repair" the order of the anti-fermionic ladder operators in the free Hamiltonian H_ψ from $b^+b + d\,d^+$ to $b^+b + d^+d + 1$. The constant 1 in H_ψ causes an infinite contribution $\int 1\, d^3p$ to the energy, which we compensate by setting our zero point of energy to that infinite value.

Then we construct, at each momentum p, a fermionic Fock space over the four single-particle states $b^+_{p,\sigma}|0\rangle$ for $\sigma \in \{0,1\}$ and $d^+_{p,\sigma}|0\rangle$ for $\sigma \in \{2,3\}$. As we have seen in section 3.1.5, the basis states of this Fock space are

1 vacuum state,
4 single-particle states,
6 two-particle states,
4 three-particle states, and
1 four-particle state.

So our Fock space has 16 complex dimensions at each momentum p. This is the structure on which the well-established time-ordered perturbation theory is based.

This paper suggests an alternative reinterpretation. Instead of turning $d\,d^+$ into d^+d (which would give us the $\int 1\, d^3p$) we swap the roles of the single-particle state and the vacuum state for the anti-fermions. Then the anti-fermions propagate in the vacuum state, which allows us to interpret them as *holes in the Dirac sea*.

This reversal of the roles of the single-particle state and the vacuum state works for each anti-fermionic momentum eigenstate. However there are *two* anti-fermionic momentum eigenstates, $\sigma \in \{2,3\}$. Thus it does no longer make sense to assume that they occupy a common Fock space with just one vacuum state. We need separate vacuum states for both of them.

So instead of constructing, at each momentum p, one big fermionic Fock space over the four single-particle states at that momentum, we are constructing four small fermionic Fock spaces over each of the four single-particle states. Instead of one 16-dimensional Fock space we obtain four two-dimensional ones.

This would be a problem if our operators contained combinations of ladder operators like, for instance, b^+d, which map anti-fermions to fermions or vice versa. However this is not the case. In H_ψ all ladder operators come in pairs for the same state, and in H_J they either stay within the fermionic or anti-fermionic subspace (b^+b or $d\,d^+$), or they map two independent states to their respective vacuum states ($b\,d$) or vice versa (b^+d^+).

So this structure is different from the structure used in time-ordered perturbation theory, but both structures are compatible with quantum electrodynamics. The difference arises from the rearrangement of the anti-fermionic ladder operators in the traditional approach, which gives us an infinite zero point of energy. Since the choice of the zero point of energy does not change physics, both approaches must be equivalent.

In fact our simulation uses only four of the eight dimensions of the Fock space, the two fermionic single-particle states and the two anti-fermionic vacuum states. The other four states are, as explained in subsection 4.4.1, inaccessible.

To simulate these four states, the simulation uses two spinor-valued wave functions. This doubling is necessary to disentangle fermions and anti-fermions which would otherwise be inaccessible in position representation, where we apply H_J. Applying H_J in momentum representation instead would increase the calculation time from $\mathcal{O}(n)$ to $\mathcal{O}(n^2)$.

Nature itself, however, doesn't need to worry about calculation time. So it is, theoretically, possible to store the state of the whole fermionic system in a single spinor-valued wave function, where two of its momentum eigenstates denote fermions and the other two denote Dirac holes, i. e. CPT-reversed vacuum states.

So the fermionic part of quantum electrodynamics in the Schrödinger picture can be described by a single spinor-valued wave function, and its photonic part can be described by a single field of complex four-vectors, the eigenstates of coherent states. We reproduce *almost precisely the same equations* as in the case of a single relativistic quantum particle interacting with a classical electromagnetic field. The only addition is that we CPT-reverse the anti-fermionic parts of the wave function, the holes in the Dirac sea, while we let them propagate freely in momentum representation. It is this CPT reversal which makes it possible to study pair annihilation and creation in the Schrödinger picture.

In this sense we can identify the CPT reversal of the anti-fermions according to Feynman and Stückelberg as the chief ingredient of second quantisation.

Chapter 5

Conclusions and Outlook

In this paper we have redeveloped quantum electrodynamics.

The traditional approach to quantum electrodynamics is to set up the Hamiltonian in second quantisation, then switch to the interaction picture and to use time-ordered perturbation theory (Feynman diagrams) to calculate cross sections and other quantities. This well-established approach has proven extremely successful.

In this paper, after setting up the Hamiltonian in second quantisation, we develop the Schrödinger equation of quantum electrodynamics and numerical methods to solve it. When we apply these methods to simulate pair annihilation and creation, the results are qualitatively correct.

So we are replacing a well-established method which can be carried out even analytically and produces extremely accurate quantitative predictions by a new method which can only be applied numerically and has produced only qualitative results so far. What's the use?

The incompatibility between general relativity and quantum field theory consists in the difficulty to apply the traditional framework of quantum field theory, time-ordered perturbation theory, to gravity. In particular the singularities which arise from time-ordered perturbation theory can be compensated by renormalisation for all fundamental interactions except gravity, but not for gravity itself.

The new approach developed in this paper is not based on time-ordered perturbation theory, and it does not produce any singularities. Instead, it opens up the methods which are known to work for general relativity – solving a partial differential equation – for application to quantum field theory. This includes pair annihilation and creation, which are traditionally studied using Feynman diagrams and have, to our knowledge, never successfully been studied in the Schrödinger picture before.

5.1 The Standard Model

The natural next step is to generalise the methods developed in this paper from quantum electrodynamics to the full Standard Model of elementary particles, i. e. from the Lagrangian of quantum electrodynamics,

$$\mathcal{L} = i\bar{\psi}\gamma^\mu\partial_\mu\psi - m\bar{\psi}\psi - qA_\mu\bar{\psi}\gamma^\mu\psi - \tfrac{1}{4}F_{\mu\nu}F^{\mu\nu}, \tag{5.1}$$

to the Lagrangian of the full Standard Model,

$$\begin{aligned}
\mathcal{L} = {} & i\bar{e}_L^n\gamma^\mu\partial_\mu e_L^n + i\bar{e}_R^n\gamma^\mu\partial_\mu e_R^n + i\bar{\nu}_L^n\gamma^\mu\partial_\mu\nu_L^n \\
& + i\bar{u}_L^n\gamma^\mu\partial_\mu u_L^n + i\bar{u}_R^n\gamma^\mu\partial_\mu u_R^n + i\bar{d}_L^n\gamma^\mu\partial_\mu d_L^n + i\bar{d}_R^n\gamma^\mu\partial_\mu d_R^n \\
& - \lambda_e^n\varphi\bar{e}_L^n e_R^n - \lambda_u^n\varphi\bar{u}_L^n u_R^n - \lambda_d^n\varphi\bar{d}_L^n d_R^n - \bar{\lambda}_e^n\varphi e_L^n\bar{e}_R^n - \bar{\lambda}_u^n\varphi u_L^n\bar{u}_R^n - \bar{\lambda}_d^n\varphi d_L^n\bar{d}_R^n \\
& - g_1 B_\mu\left(-\bar{e}^n\gamma^\mu e^n + \tfrac{2}{3}\bar{u}^n\gamma^\mu u^n - \tfrac{1}{3}\bar{d}^n\gamma^\mu d^n\right) \\
& - g_2 W_\mu^a\left(\begin{pmatrix}\bar{\nu}_L^n\\ \bar{e}_L^n\end{pmatrix}\gamma^\mu\sigma_a\begin{pmatrix}\nu_L^n\\ e_L^n\end{pmatrix} + V^{nm}\begin{pmatrix}\bar{u}_L^n\\ \bar{d}_L^n\end{pmatrix}\gamma^\mu\sigma_a\begin{pmatrix}u_L^m\\ d_L^m\end{pmatrix}\right) \\
& - g_3 G_\mu^c\left(\bar{u}^n\gamma^\mu\lambda^c u^n + \bar{d}^n\gamma^\mu\lambda^c d^n\right) \\
& - \tfrac{1}{4}B_{\mu\nu}B^{\mu\nu} - \tfrac{1}{4}W_{\mu\nu}^a W_a^{\mu\nu} - \tfrac{1}{4}G_{\mu\nu}^c G_c^{\mu\nu} \\
& + \lambda|\varphi|^4 - \tfrac{1}{2}\mu^2|\varphi|^2 + |\partial_\mu\varphi - \tfrac{1}{2}ig_2 W_\mu^a\sigma_a\varphi - \tfrac{1}{2}ig_1 B_\mu\varphi|^2. \qquad (5.2)
\end{aligned}$$

Before we continue a few remarks seem appropriate.

- To save space we have set $\hbar = c = \mu_0 = 1$ in these Lagrangians, and we make use of the Einstein summation convention.
- This version of the Lagrangian of the Standard Model is oriented towards [2, chapter 1], but it has been composed from various sources by someone who is not deeply familiar with this field. Despite all due care, eq. 5.2 might still contain some errors.
- The fermionic wave functions e_L^n, e_R^n, ν_L^n, u_L^n, u_R^n, d_L^n, and d_R^n denote left-handed and right handed electron-like leptons, neutrinos, up-like quarks and down-like quarks of the nth generation, where $n \in \{1, 2, 3\}$. For example ν_L^2 denotes a left-handed muon neutrino and d_R^3 a right-handed bottom quark. The electron, denoted ψ in the Lagrangian of quantum electrodynamics, has been doubled to e_L^1 and e_R^1, because only its left-handed parts couple to weak interaction.
- The Yukawa parameters λ_e^n, λ_d^n, and λ_u^n (not to be confused with the Gell-Mann matrices λ^c) couple the fermions to the Higgs field φ. They replace the mass term $m\bar{\psi}\psi$ in eq. 5.1.
- Since no right-handed neutrinos have been observed yet, this version of the Lagrangian of the Standard Model does not include them. As a consequence it also does not include neutrino masses (such as Dirac mass terms $-\lambda_\nu^n\varphi\bar{\nu}_L^n\nu_R^n - \bar{\lambda}_e^n\varphi\nu_L^n\bar{\nu}_R^n$).
- This version of the Lagrangian is in the mass eigenbasis, thus the Cabibbo-Kobayashi-Masukawa (CKM) matrix V^{nm} is located in the coupling to the weak interaction.
- This Lagrangian is before electroweak symmetry breaking. After electroweak symmetry breaking – or if the Higgs boson had not been found – it would be about twice as long.

What problems can arise when we try to extend the methods developed in this paper to cover the whole Standard Model?

A key question is whether the simplification that the electromagnetic field can be described by coherent states has an analogon for the other interactions and the Higgs field. If this is not the case we have to store them as vectors of Fock states instead of complex eigenvalues of coherent states. This would significantly increase the calculation time and the memory required to carry out the simulation.

Since a finite cut-off for the number of bosons which can simultaneously occupy the same state appears to be a reasonable approximation, this problem would not rule out the applicability of this method to the full Standard Model. It would, however, make it more complicated, maybe putting it out of reach of the computing devices available at the time of this writing.

5.2 The Road to Quantum Gravity

So the extension of the method developed in this paper to the full Standard Model is expected to be intricate. On the other hand its extension to include gravity should be straightforward. That's what this method was designed for.

As of 2021, gravity is canonically described by *general relativity*.

In *special relativity*, scalar products in Minkowskian spacetime are carried out using opposed signs for spatial and temporal coordinates, for example

$$|A_\mu|^2 = \sum_{\mu=0}^{3} \sum_{\nu=0}^{3} \eta_{\mu\nu} A_\mu A_\nu = A_0^2 - A_1^2 - A_2^2 - A_3^2, \tag{5.3}$$

where

$$\eta_{\mu\nu} = \mathrm{diag}(1, -1, -1, -1) = \begin{pmatrix} 1 & 0 & 0 & 0 \\ 0 & -1 & 0 & 0 \\ 0 & 0 & -1 & 0 \\ 0 & 0 & 0 & -1 \end{pmatrix}. \tag{5.4}$$

(Using the reversed signature $\eta_{\mu\nu} = \mathrm{diag}(-1, 1, 1, 1)$ is customary, too, in particular in the context of general relativity.)

General relativity replaces $\eta_{\mu\nu}$ by a more general matrix $g_{\mu\nu}$, the *metric tensor*. It is not constant, but a dynamic variable itself. Its dynamics is described by the Einstein field equations,

$$R_{\mu\nu} - \tfrac{1}{2} R\, g_{\mu\nu} + \Lambda\, g_{\mu\nu} = \tfrac{8\pi G}{c^4}\, T_{\mu\nu}. \tag{5.5}$$

The *Ricci tensor* $R_{\mu\nu}$ and the *Ricci scalar* R describe *curvature*, and they contain derivatives of $g_{\mu\nu}$, which turn the Einstein field equations into a system of differential equations. Λ is the *cosmological constant*, G is Newton's *gravitational constant*, and $T_{\mu\nu}$ is the *stress-energy-momentum tensor*, which describes the sources of gravity in spacetime.

So the problem how to combine general relativity with quantum field theory is the problem how to combine the Einstein field equations with relativistic many-particle quantum theory. Until now, all attempts to solve this problem have failed because of the incompatibility of the Einstein equations with time-ordered perturbation theory.

The method developed in this paper treats quantum electrodynamics, a relativistic many-particle quantum theory, in the Schrödinger picture. It simulates the dynamics of a relativistic many-particle quantum system by solving, numerically, a partial differential equation over Minkowskian spacetime.

The tools to combine this method with general relativity are already in place.

- The *spin connection* describes the effects of curved spacetime on the Dirac equation.
- The stress-energy-momentum tensor can be read out from the wave functions.

The remaining task is to implement the Einstein field equations in such a way that they can be solved together with the Schrödinger equation of quantum field theory. This would allow us to simulate a quantum system where gravity and the other fundamental interactions have comparable strengths. A possible result might be a stable fermionic ground state in the centre of a black hole.

This paper does not predict gravitons or discrete spacetime. It does not give instructions how to construct a field operator to be plugged into the Einstein field equations. In some sense, however, it does the opposite.

Although we have set up the Schrödinger equation of quantum electrodynamics by inserting field operators into the Lagrangian, the final result no longer contains any ladder operators. The only thing which sets quantum electrodynamics apart from a single-particle theory is the CPT reversal of the anti-particles, which is needed to explain pair annihilation and creation. Everything else, including the discrete transfer of momentum between photons and fermions, was reproduced using precisely the same equations as in the case of a single relativistic quantum particle interacting with a classical electromagnetic field.

This suggests that this method, although it doesn't aim specifically for gravitons or discrete spacetime, is suited to reveal quantum effects of gravity.

5.3 Noncommutative Geometry

The idea to apply the methods of general relativity to quantum field theory instead of doing the opposite has in fact already been elaborated to a full-fledged theory.

In 1996, Chamseddine and Connes [13] derived the Lagrangian of the Standard Model, eq. 5.2, coupled to general relativity, eq. 5.5, from the astonishingly small input

$$\mathcal{A} = C^\infty(M) \otimes \big(\mathbb{C} \oplus \mathbb{H} \oplus M_3(\mathbb{C})\big). \tag{5.6}$$

What did they do?

The key idea behind Einstein's general relativity reads: *Gravity is geometry.* The path of particles through spacetime is always a straight line. When they appear to attract each other, it's because spacetime itself is curved.

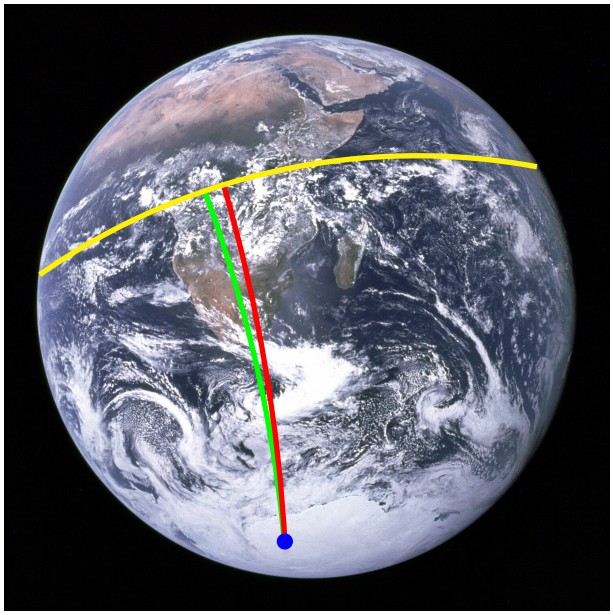

Figure 5.1: Parallel courses on the surface of a sphere

Two particles, started at the equator (yellow), moving on parallel courses straight south (green and red), will collide at the south pole (blue). (Background: *Blue Marble*, NASA, 1972, public domain, https://commons.wikimedia.org/wiki/File:The_Earth_seen_from_Apollo_17.jpg.)

As an illustration, imagine two particles moving freely, without forces, on the surface of a sphere. When we start them with equal velocity on parallel courses, they will collide. For example when they move on the surface of the Earth from the equator straight south, they will collide at the south pole (see fig. 5.1). Seen from the particles, this geometric effect, the *intrinsic curvature* of the two-dimensional surface of a three-dimensional sphere, can be interpreted as an attractive force.

This is how gravity works in general relativity. Gravity is the intrinsic curvature of the four-dimensional spacetime.

Noncommutative geometry generalises this concept from Euclidean and Minkowskian manifolds ("surfaces") to more general spaces. The "coordinates" on the *noncommutative space* $\mathcal{A}$, where the geometry happens, are not numbers, but operators on a Hilbert space, i. e. quantum observables. In particular our "quantum coordinates" are not required to be commutative.

(For a comprehensible physicist's guide to noncommutative geometry, see [14] and [15]. For the full story, see [2].)

A simple example is to take all possible wave functions in position representation as our "quantum coordinates" for Minkowskian spacetime, $\mathcal{A} = C^\infty(M)$.

Quantum observables can be continuous (like position or momentum) or discrete (like spin, charge, or weak isospin). For instance the "quantum coordinates" of a two-level system are vectors of two complex numbers, $\mathcal{A} = \mathbb{C} \oplus \mathbb{C}$. Such *discrete dimensions* can also be combined with "normal" dimensions. For example we can describe a two-level quantum system distributed over space by attaching a discrete extra dimension of two points to Minkowskian spacetime, $\mathcal{A} = C^\infty(M) \otimes (\mathbb{C} \oplus \mathbb{C})$. This type of noncommutative space can be imagined as a universe consisting of two sheets.

Noncommutative geometry then uses the Dirac equation to define distances between "points" in this noncommutative space and generalises the concepts of general relativity to this new framework.

In general relativity the Einstein field equations emerge from the description of Minkowskian spacetime using arbitrary coordinates, including moving ones which generate pseudo forces. In a similar manner, noncommutative geometry investigates transformations of the coordinates of a noncommutative space $\mathcal{A}$ and finds the structure of the (generalised) curvature allowed on that space. In a physical system on that noncommutative space this curvature manifests as a quantum interaction, described by a Lagrangian.

In other words, in noncommutative geometry, *all* interactions are intrinsic curvature.

Only very few physical scenarios can be constructed this way. The following examples are explained in detail in [15].

- In the most simple case, $\mathcal{A} = C^\infty(M)$, i. e. normal Minkowskian spacetime described by quantum coordinates, the physics arising from the allowed curvature is the Dirac equation for massless fermions, coupled to general relativity via the spin connection. An extension to quantum electrodynamics for massless fermions is possible.
- With $\mathcal{A} = C^\infty(M) \otimes (\mathbb{C} \oplus \mathbb{C})$, the allowed physics is similar to electroweak interaction, including the Higgs mechanism, again coupled to general relativity.
- With $\mathcal{A} = C^\infty(M) \otimes \big(\mathbb{C} \oplus \mathbb{H} \oplus M_3(\mathbb{C})\big)$, where $\mathbb{H}$ is the skew field of quaternions and $M_3(\mathbb{C})$ denotes the algebra of 3×3 matrices over $\mathbb{C}$, the allowed physics is the Standard Model, coupled to general relativity.

The assortment of physical systems compatible with noncommutative geometry is very limited. It does not, for instance, include quantum electrodynamics. There is no simpler way to obtain massive fermions than the Higgs mechanism. Nonwithstanding all that, one of the allowed physical scenarios is precisely the Standard Model, eq. 5.2, coupled to general relativity.

So noncommutative geometry unifies all fundamental interactions by ascribing them to gravity. This makes it a very interesting candidate for a "theory of everything". Then why doesn't it get more attention?

The main point of criticism of noncommutative geometry is that it doesn't address the incompatibility between time-ordered perturbation theory and general relativity. For this reason it is stated that no quantisation procedure compatible with this framework has been found so far. (See, for example, [16].)

This paper provides an alternative approach to quantum field theory which removes its incompatibility with general relativity and noncommutative geometry. In this sense it qualifies as a quantisation procedure which is compatible with noncommutative geometry.

So we don't predict gravitons or discrete spacetime. Does that mean that we cannot expect any physics beyond the Standard Model?

Noncommutative geometry predicts some physics beyond the Standard Model. The coupling between general relativity and the Standard Model features terms of higher-order gravity and a direct coupling between the Riemann scalar and the Higgs field [2, chapter 1, § 16.1]. Both effects can modify the laws of gravity, which might contribute to understanding the still unexplained phenomenon of dark matter. While astronomical observations suggest that dark matter cannot be a property of mass [17], it might still be possible that higher-order gravity, which becomes relevant in supermassive black holes but not in insterstellar clouds, can explain dark matter.

In addition, the coupling between gravity and quantum field theory goes, just by itself, beyond the Standard Model. For example the centre of a black hole features a gravitational singularity. Classically, this would disrupt every particle. Quantum physics, however, can deal with infinite forces. Even a quantum particle in the infinite potential $V(x) = -\delta(x)$ has a stable ground state. So it would be interesting to observe the formation of a black hole in a simulation which includes quantum effects.

5.4 Further Applications

In this paper we have developed new numerical methods to solve hyperbolical partial differential equations, the first-order *quantum Euler method* and the second-order *quantum Heun method*. Both methods are explicit single-step methods. We have applied them to quantum electrodynamics in the Schrödinger picture, but of course they can be applied to a wider range of hyperbolical partial differential equations. As stated in subsection 2.1.4 these methods can be generalised straightforwardly to higher orders. Other generalisations such as implicit methods and multi-step methods are possible, too.

Our new approach to quantum electrodynamics has been developed to study quantum gravity. However the range of its possible applications is much wider. For instance, our method to simulate the dynamics of a many-particle wave function of electrons in an external potential might be useful to study the properties of electronic configurations in solid-state physics.

5.5 Closing Remarks

So I found something. How did I get to this point?

In some sense I found something because I *didn't* search for it.

I always wanted to know how everything works, even as a little child, before I even knew the word "physics".

When I entered university I already had learned that there was a contradiction between general relativity and quantum theory, but I had no idea about the details of this contradiction, and neither my teachers nor popular science literature could tell me more about these details.

At university I studied special and general relativity, non-relativistic quantum theory, and the basics of quantum field theory. Still I didn't see the contradiction, so I asked my lecturers and got the answer: *The attempt to quantise gravity results in nonrenormaliseable divergences.*

My first idea was: *Then what about gravitising quantum field theory instead?* Noone could tell me anything about this.

In 2009, twelve years after I had left university, I decided that I really wanted to know *why* it is impossible to unify general relativity and quantum field theory, and I started to search for this systematically – as a low-priority side project in my scarce spare time. I didn't doubt that there is an incompatibility between time-ordered perturbation theory and general relativity. But I doubted that time-ordered perturbation theory is the only valid approach to quantum field theory.

One of my first ideas was to write a numeric simulation of the Dirac equation coupled to the Maxwell equations in the Schrödinger picture. This was as close as I could get to quantum field theory while staying on firm ground and while staying compatible with general relativity.

Then my plan was to try to use my approach to simulate pair annihilation and creation. I knew that this couldn't work and that I would need, at some point, to introduce "second quantisation" into my equations. Then I could observe *how* second quantisation makes everything incompatible with general relativity.

In parallel, I looked out for ongoing research on this field. The two best-known approaches, loop quantum gravity and string theory, are trying to quantise gravity. Are there really no attempts to apply, instead, the framework of general relativity to quantum field theory?

One of the first things I found was noncommutative geometry. I was deeply impressed by the elegance of the approach, which successfully derives the full Standard Model, a whole page in the book, from less than half a line of input, even coupled to general relativity. For me it was immediately clear that this is the long-sought unification of general relativity and quantum field theory. So I wondered why it wasn't widely recognised as such.

From the reactions to noncommutative geometry I found – "Noncommutative geometry lacks second quantisation." – I concluded that I was on the right track in my search for the incompatibility.

For about nine years I didn't succeed to simulate pair annihilation or creation, merely for technical reasons such as errors in my calculations and programs, and of course because I couldn't devote much time to this project.

Then in May 2018 I found the predecessor of eq. 4.44 – a hint that it might indeed be possible to plug "second quantisation" into the Schrödinger picture of quantum electrodynamics *without* destroying its compatibility with general relativity.

About one year later I succeeded to simulate pair annihilation. About another year later, pair creation worked, too, and I understood *why* it worked. (I wrote that down in section 4.4.)

So my project to find out why general relativity and quantum field theory are incompatible was a failure. Instead I found out that they *are* compatible. These things happen.

How to proceed from here? Well, this approach is far from being complete. There are no quantitative results so far, quantum electrodynamics is just a tiny part of the Standard Model, and of course its combination with general relativity still waits for being implemented. All this will take a long time, and there will be a lot of problems. It is also well possible that this method will never reach the astonishing precision of the calculations done using time-ordered perturbation theory.

Nevertheless a step towards a "theory of everthing" has been taken. Maybe noncommutative geometry *is* that theory of everything, and this tiny piece of physics was needed to make it obvious.

Thanks for your attention.

Acknowledgements

I am very grateful to (in alphabetical order) Erich, Gretel, and Markus Gerwinski, Herbert Schmidt, and Henry Schramm. Our discussions inspired me to continue this work and helped me to improve my publications.

Bibliography

[1] C. Rovelli: *Loop Quantum Gravity.*
Living Rev. Rel. **1**, 1 (1998)
arxiv:gr-qc/9710008

[2] A. Connes, M. Marcolli: *Noncommutative Geometry, Quantum Fields and Motives.*
Am. Math. Soc. Coll. Publ. **55** (2008), ISBN 978-0-8218-4210-2
https://alainconnes.org/wp-content/uploads/bookwebfinal-2.pdf

[3] M. Frigo, S. G. Johnson: *The design and implementation of FFTW3.*
Proc. IEEE **93** (2), 216–231 (2005)
http://www.fftw.org/fftw-paper-ieee.pdf

[4] P. Gerwinski: *qpendulum.cpp – Simulation of a Classical and a Quantum Pendulum.* (2020)
https://www.peter.gerwinski.de/qpendulum-1.0.tar.gz

[5] A. Co: *QPong.* (2021)
https://gitlab.cvh-server.de/aco/qpong

[6] International Bureau of Weights and Measures:
SI Brochure: The International System of Units (SI).
9th edition, 20 May 2019, ISBN 978-92-822-2272-0
https://www.bipm.org/utils/common/pdf/si-brochure/SI-Brochure-9.pdf

[7] H. Triebel: *Analysis und mathematische Physik.*
2. Auflage, Leipzig 1984, VLN 294-375/23/84

English edition:
H. Triebel: *Analysis and mathematical physics.*
Dordrecht 1986, ISBN 90-277-2077-0

[8] This analogy was coined by Fritz Haake in the 1990s in a lecture about statistical physics. The original (in German) reads:

> Elektronen sind, wie Geld, ununterscheidbar. Wenn Sie zwei Mark auf Ihrem Konto vertauschen, ändert sich nichts.

Translation:

> Electrons are, like money, indistinguishable. If you swap two [German] Marks on your bank account, nothing changes.

RIP, Fritz.

[9] В. Б. Берестецкий, Е. М. Лифшиц, Л. П. Питаевский:
Курс теоретической физики. Том IV: Квантовая электродинамика.
Издание 3-е, Москва 1989, ISBN 5-02-014422-3

English edition:
V. B. Berestetskii, E. M. Lifshitz, L. P. Pitaevskii:
Course of Theoretical Physics. Volume IV: Quantum Electrodynamics.
2nd edition, Oxford 1982, ISBN 978-0-7506-3371-0

German edition:
W. B. Berestetzki, E. M. Lifschitz, L. P. Pitajewski:
Lehrbuch der theoretischen Physik. Band IV: Quantenelektrodynamik.
6., unveränderte Auflage, Berlin 1989, ISBN 3-05-500068-4

[10] G. Breitenbach, S. Schiller, J. Mlynek:
Measurement of the quantum states of squeezed light.
Nature **387** (6632), 471–475 (1997)
http://gerdbreitenbach.de/publications/nature1997.pdf

[11] P. A. M. Dirac: *A Theory of Electrons and Protons.*
Proc. R. Soc. Lond. A **126** (801), 360–365 (1930)
doi:10.1098/rspa.1930.0013. JSTOR 95359

[12] C. D. Anderson: *The Positive Electron.*
Phys. Rev. **43** (6), 491–494 (1933)
doi:10.1103/PhysRev.43.491

[13] A. H. Chamseddine, A. Connes: *The Spectral Action Principle.*
Commun. Math. Phys. **186**, 731–750 (1997)
arxiv:hep-th/9606001

[14] T. Schücker: *Forces from Connes' Geometry.*
Lect. Notes Phys. **659**, 285–350 (2005)
arxiv:hep-th/0111236

[15] T. Schücker: *Spin Group and Almost Commutative Geometry.* (2000)
arxiv:hep-th/0007047

[16] J. Aastrup, J. Møller Grimstrup:
Intersecting Connes Noncommutative Geometry with Quantum Gravity.
Int. J. Mod. Phys. A **22**, 1589–1603 (2007)
arxiv:hep-th/0601127

[17] D. Clowe, M. Bradač, A. H. Gonzalez, M. Markevitch, S. W. Randall, C. Jones, D. Zaritsky:
A Direct Empirical Proof of the Existence of Dark Matter.
The Astrophysical Journal **648**, L109–L113 (2006)
doi:10.1086/508162